MACROPOROUS POLYMERIC AFFINITY MATRICES FOR SELECTIVE SEPARATION OF CONTAMINANTS

A THESIS

SUBMITTED TO THE

UNIVERSITY OF PUNE

FOR THE DEGREE OF

DOCTOR OF PHILOSOPHY

(IN CHEMISTRY)

BY

TARA SANKAR PATHAK

CHEMICAL ENGINEERING DIVISION

NATIONAL CHEMICAL LABORATORY

PUNE- 411008

INDIA

MARCH 2004

Dedicated

to

my parents

CERTIFICATE

Certified that the work incorporated in the thesis, **"Macroporous polymeric affinity matrices for selective separation of contaminants"** submitted by **Mr.Tara Sankar Pathak**, for the Degree of **Doctor of Philosophy**, was carried out by the candidate under my supervision in the Chemical Engineering Division, National Chemical Laboratory, Pune 411008, India. Material that has been obtained from other sources is duly acknowledged in the thesis.

Dr. S. Ponrathnam

(Research Supervisor)

Acknowledgement

First and foremost I find immense pleasure in expressing my deep sense of gratitude to my research supervisor Dr. S. Ponrathnam for his moral support, guidance and instruction throughout my research career. As a research guide, he has been a source of direction and encouragement; as a man in science, he has been an inspiration. He gave me the opportunity to independent thinking, build and experiment without any restriction. Although this eulogy is insufficient, I preserve an everlasting gratitude for him.

I specially wish to thank Dr. C. R. Rajan, for his endless support in my research career and life.

I express my immense sense of gratitude to Dr.B. D. Kulkarni, Head, Chemical Engineering Division, NCL, Pune, for his cooperation.

I am thankful to Dr. C. Ramesh and Dr. Rajmohanan, for scientific discussion during my research career.

I am grateful to all scientific and non-scientific staff members of Chemical Engineering Division for their help.

The invaluable help I received from Dr.(Mrs) A. A. Belhekar, for SEM is also appreciated.

I am also thakful to Dr. M. K. Banerjee, Dr. P. R. Chatterjee, Mr. D. V. Mohan Rao, Dr. M. M. Maiti, Dr. P. K. Chattaraj, Dr. N. C. Dey, Dr. B. Dev, Dr. T. K. Halder, Dr. A. Sannigrahi, A. Dey, S. Mahapatra, U. Mondal, N. Pathak, N. Dey and many others, for their help during my study life.

I have also had the privilege of working with our wonderful past labmates (Dr. Ramesh, Dr. Yemul, Dr. Kamal, Vikas, Rahul, Dr. Arika, Dr. Anjali, Dr. Vaishali, Dr. Varsha) and present labmates (Rajkumar, Pujari, Avinash, Ganesh, Dr. Smita, Sarika, Supriya, Pallavi, Meghana), especially each of whom accomplished a great deal. I wish all the best of luck and success in their future careers.

I am also thankful to my numerous friends: Raja, Mantri, Subho, Chitta, Annyt, Sumit, Monaj, Pradip, Rabin, Girija, Madnesh, Ajay, Amiya and Susmita, Aditya, Anamitra, Arindam, Ambarish, Bibhas,

Bikash, chanchal, debdut, Dinu, Dilip, Debasis, Gourda and Nandita boudi, Tapanda, Karunadi, Lahada, Subhas, Saptarshida, Subarnada, Tarun, Senapati, Anirban, Sukhen, Prabal, Somnath and Sujata, Ananda, Prabhas, Mohuadi, Souvikda, Divakarda, Jaychandran, Kartik and Swarnendu, for their help and company.

There are so many people to whom I am indebted for support and encourgement. I thank them all.

I also thank my friends, both close and distant, for their support, the good times, and tension-breaking moments that only good friends can provide. I gratefully acknowledge the enormous help and support I received from my friends in many ways during the Ph.D work.

I would like to thank my parents for their guidance and unwavering support throughout my life. They were behind me at every point in my life, even when I didn't really know where I was going and I am grateful for their unwavering belief in whatever I have chosen even when the "going got tough".

Words are inadequate to express the sacrifice, love and faith of my grandparents, parents and all my family members without which my dreams would have never been fulfilled.

Most of all, I thank the Lord for helping me know which path to follow.

Last but not the least I would like to thank Mr. Sathe and Mr. Giri for their help in day to day activities in the Laboratory.

I am grateful to my teachers who taught me and ushered me towards a career in Science.

Finally, my thanks are due to Council of Scientific and Industrial Research, New Delhi, India for financial support and Dr. P. Ratnasamy, former Director and Dr. S. Sivaram, Director, NCL, Pune for allowing me to carry out my research and extending all possible infrastructural facilities at NCL, and permitting me to submit the present work in the form of thesis.

(TARA SANKAR PATHAK)

TABLE OF CONTENTS

CHAPTER 1

INTRODUCTION

CHAPTER 2

SYNTHESIS AND CHARACTERISATION OF MACROPOROUS POLYMERS

CHAPTER 3

STUDY OF GUEST MOLECULE BINDING WITH CYCLODEXTRIN MODIFIED MACROPOROUS HEMA-EGDM COPOLYMERS

CHAPTER 4

STUDY OF METAL-ION BINDING WITH MODIFIED MACROPOROUS GMA-EGDM COPOLYMERS

CHAPTER 5

SUMMARY AND CONCLUSION

LIST OF FIGURES

LIST OF TABLES

LIST OF ABBREVIATIONS

HEMA	**2-Hydroxyethyl methacrylate**
GMA	**Glycidyl methacrylate**
AGE	**Allyl glycidyl ether**
EGDM	**Ethylene dimethacrylate**
DVB	**Divinyl benzene**
PVP	**Poly(vinyl pyrrolidone)**
CD	**Cyclodextrin**
HE	**Poly(2-hydroxyethyl methacrylate-co-ethylene dimethacrylate)**
GV	**Poly(glycidyl methacrylate-co-divinyl benzene)**
AG	**Poly(allyl glycidyl ether-co-ethylene dimethacrylate)**
HV	**Poly(2-hydroxyethyl methacrylate -co-divinyl benzene)**
PEI	**Polyethylenimine**
SEM	**Scanning electron microscopy**
FT-IR	**Fourier transform infrared spectroscopy**
HPLC	**High performance liquid chromatography**
rpm	**Rotations per minute**
PV	**Pore volume**
SA	**Surface area**
CLD	**Crosslink density**
NMR	**Nuclear magnetic resonance**
RT	**Room temperature**

Chapter 1

Introduction

1 Introduction

The chemistry of reactions and functionalisation of polymers has received great attention during the last two decades. Many fundamentally and industrially important reactive and functional polymers have been prepared by the reactions on linear or crosslinked polymeric reactant which introduces reactive, catalytic, or functional groups in the polymer chain. Polymers bearing reactive functional groups are polymers capable of undergoing chemical reactions. The term functional polymer has two meanings: (a) A polymer bearing functional groups like hydroxy, carboxy or amino groups etc, which makes the polymer reactive or (b) A polymer performing a specific function for which it is produced.

Macroporous crosslinked polymers are effective and efficient materials for many separation processes, and therefore they are widely used as starting material for ion exchange resins and as specific sorbents. As first reported in 1935 by Staudinger and Huseman, the copolymerisation of styrene in the presence of a small amount of divinylbenzene yielded a product that swells in good solvents but does not dissolve in them [1]. Towards the end of the 1950s, a new polymerisation technique was discovered that yielded crosslinked polystyrenes having a porous structure in the dried state [2-12].

During the past 43 years, the synthesis of macroporous copolymer networks based on the various chemical compositions has been the subject of many studies. After the development of porous networks, towards the end of the 1950s, it became necessary to distinguish these new materials from the conventional materials and the terms 'macroporous' and `macroreticular' were introduced. Functional resins are produced in two basic morphological types:

1. Gel-type (microporous) resins without an appreciable porosity in the dry state, whose interior is accessible only after swelling in the reaction environment.

2. Macroreticular (macroporous) resins with macropores stable even in the dry state, in addition to the micropores generated by the swelling of the polymer skeleton.

The term macroporous is misleading, because according to IUPAC [13], pores of diameter larger than 50 nm are macroporous, whereas macroporous networks usually have a broad pore size distribution ranging from 0.1 to 1000 nm. It is now well understood that a phase separation [14] during the formation of the network is mainly responsible for the formation of porous structures in a dried state. In order to obtain macroporous structures, a phase separation must occur during the course of the crosslinking process so that the two-phase structure is fixed by the formation of additional crosslinks. The phase separation occurs at an early stage of polymerisation, leading to the formation of microscopic globular entities that keep growing but do not coalesce because of crosslinking. Eventually, these come into contact with each other and associate to form clusters consisting of both interconnected globules and voids or pores (Figure 1.1) [15].

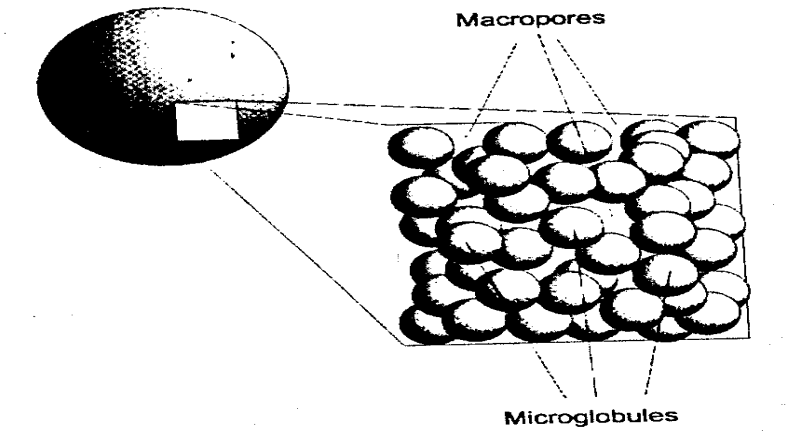

Figure 1.1: Schematic view of the morphology of macroporous polymer beads

1.1 Macroporous copolymer networks

The term macroporous resin is not intended to convey anything about the size of the pores in a resin. Instead, the expression is used simply to indicate a class of resins which have a permanent well-developed porous structure even in the dry state. Figure 1.2 represents the action of porogen in forming porous morphology in a macroporous resin.

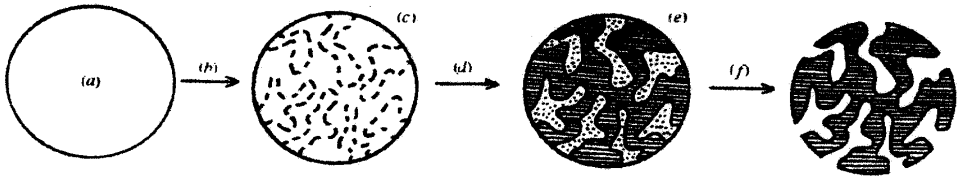

Figure 1.2: Action of porogen in forming porous morphology in a macroporous resin (a) monomer, crosslinker and porogen in isotropic solution (b) polymerisation (c) polymer network formation (d) porogen and network start to phase separate (e) porogen phase acts as a pore template (f) porogen phase removed to yield pores

The suspension polymerisation technique has generally been used for the preparation of macroporous copolymer networks in the form of beads of diameter ranging from 0.1 and 1 mm, with the majority in the range 200-600 μm. To illustrate the synthetic procedure, this technique is shown schematically in Figure 1.3. First, a monovinyl–divinyl monomer mixture containing a free-radical initiator is mixed with an inert diluent. The inert diluent must usually be soluble in the monomer mixture but insoluble in the continuous phase of the suspension polymerisation. The reaction mixture is then added into the continuous phase under agitation, so that it distributes in the form of droplets inside the continuous phase. The copolymerisation and crosslinking reactions taking place in the monomer–diluent droplets result in the formation of beads having a glassy, opaque, or milky appearance. The beads are then extracted with a good solvent to remove the soluble polymers and the diluent from the network.

Macroporous materials with pore diameters greater than 50 nm [16] have a wide range of applications in chemistry. Macroporous polymers, in particular, can be used as catalytic surfaces and supports [17-18], separation and adsorbent media [19-21], biomaterials [22-26], chromatographic materials [27-29] and thermal acoustic and electrical insulator [29-32].

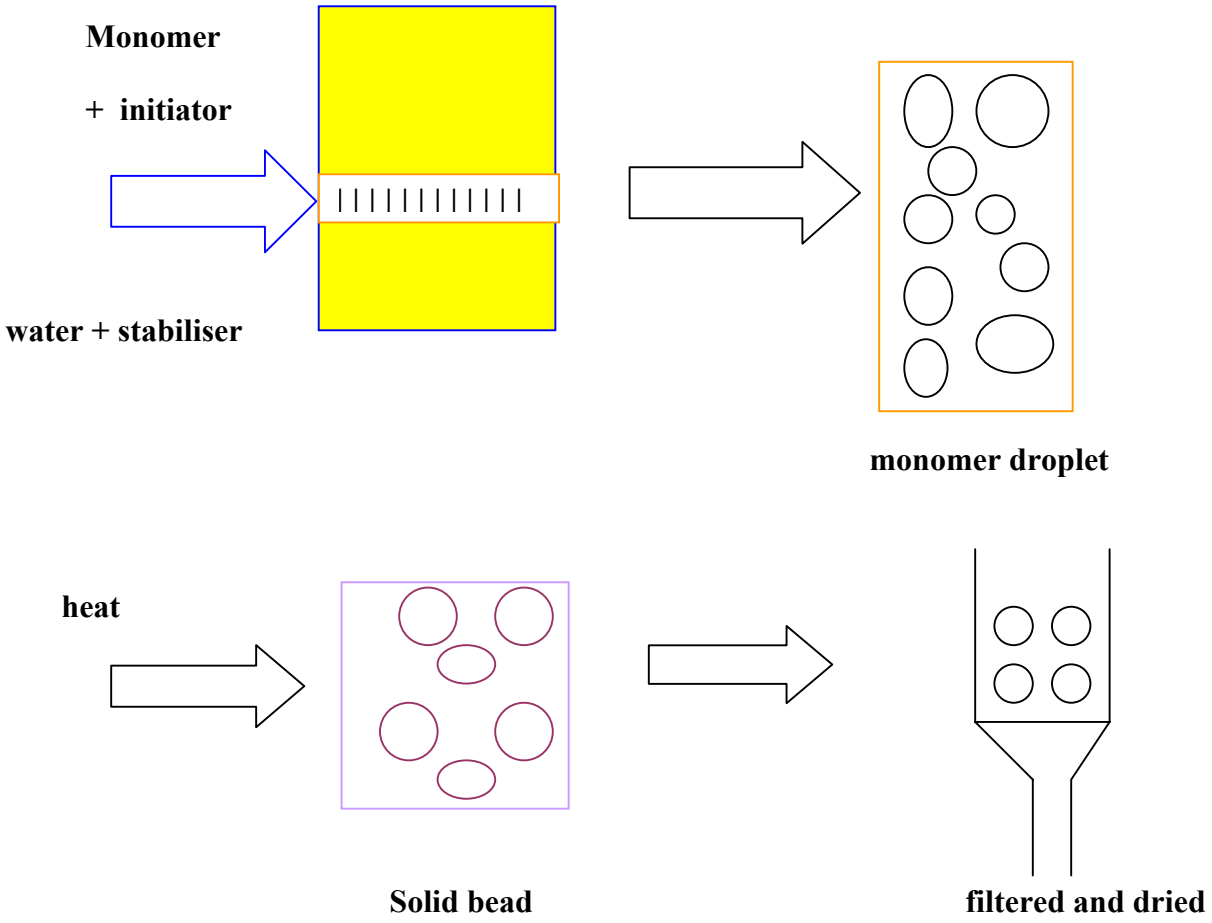

Figure 1.3: Schematic diagram of suspension polymerisation

The suspension polymerisation technique yields macroporous polymer particles with a relatively broad particle size distribution that cannot be used directly for fine chromatographic separations. Alternate procedures that afford monodisperse macroporous beads have been reported. Porous structures within the particles may be obtained upon the removal of the diluent after polymerisation [33-34]. Hydrophilic crosslinked macroporous particles have also received much interest in recent years. They can be prepared by the classical suspension polymerisation technique, in which water-insoluble derivatives of the monomers are used for the polymerisation.

Horak *et al*. used an aqueous solution of poly(vinyl pyrrolidone) as the water phase and a mixture of higher boiling alcohols as the diluent of the monomer phase for obtaining

crosslinked poly(2-hydroxyethyl methacrylate) beads [35]. They pointed out that the diluent in the monomer phase reduces the solubility of 2-hydroxyethyl methacrylate (HEMA) in water. Mueller *et al.* [36], Peppas *et al.* [37-39], Jayakrishnan *et al.* [40], Okay et al. [41] and Horak *et al.* [42] described the various techniques for the synthesis of poly(HEMA) beads in an aqueous phase containing sodium chloride and other additives. The presence of sodium chloride in the aqueous phase reduces the monomer solubility and thus allows formation of spherical, hydrophilic beads. Several diluents soluble in the monomer mixture have been tested for their suitability as inert diluents in the production of hydrophilic macroporous copolymer networks [43-45]. Coupek *et al.* first described the synthesis of macroporous polymers from HEMA and ethylene dimethacrylate (EGDM) [46]. Svec *et al.* [47-48] prepared a series of macroporous glycidyl methacrylate (GMA)/EGDM copolymer beads by classical suspension polymerisation technique using lauryl alcohol /cyclohexanol diluent mixture. The copolymers exhibited a high specific surface area, which increased markedly with increasing content of the crosslinker, EGDM. On increasing the relative volume of lauryl alcohol in the diluent mixture led to the formation of large pores and small surface areas. Synthesis of uniformly sized porous GMA/EGDM beads was described by Smigol *et al.* [49-50]. The distribution of pore sizes in a macroporous polymer can be measured by mercury intrusion porosimetry [51]. The specific surface area of the beads is measured by nitrogen adsorption isotherms. The Brunauer-Emmet-Teller equation is used to analyse the nitrogen adsorption isotherms in order to calculate the surface area of beads [52].

1.2 Suspension polymerisation

Suspension polymerisation is not a new technique, having been invented about 93 years ago. This is a case of heterogeneous polymerisation right from the beginning. The term suspension polymerisation is applied to a system in which monomers relatively insoluble in

water are suspended as liquid droplets, and the resultant polymer is obtained as a dispersed solid phase. Initiators soluble in the liquid monomer phase are used in this type of polymerisation. Terms synonymous with suspension polymerisation are pearl and bead polymerisation, especially when porosity of particle is not of critical importance. Suspension polymers are generally produced in the form of pearls or beads, which may be hard or soft in nature, depending upon the monomer composition and presence of any miscible diluent [53]. The major aim in suspension polymerisation is the formation of an uniform dispersion of monomer droplets in the aqueous phase with controlled coalescence of these droplets during the polymerisation process. The idea of using monomer droplets in an aqueous suspension seems to have been conceived as early as 1910 [54-55]. The first suspension polymerisation based on acrylic monomers leading to the formation of bead was performed by Bauer and Lauth in 1931 [56]. Several detailed and complete literature reviews on suspension polymerisation have already been published [57-61].

The interfacial tension, the degree of agitation, and the design of the stirrer/reactor system govern the dispersion of monomer droplets, typically with diameters in the range of 10 μm to 5 mm. The presence of suspending agents (stabilisers) hinder the coalescence of monomer droplets and the adhesion of partially polymerised particles during the course of polymerisation, so that the solid beads may be produced in the same spherical form in which the monomer was dispersed in the aqueous phase. The monomer phase is subjected to either turbulent pressure fluctuations or viscous shear forces, which break it into small droplets that assume a spherical shape under the influence of interfacial tension. These droplets undergo constant collisions, with some of the collisions resulting in coalescence. Eventually a dynamic equilibrium is established, leading to a stationary mean particle size. Individual drops do not retain their unique identity but instead undergo continuous break up and coalescence.

The most important issue in the practical operation of suspension polymerisation is the control of the particle size distribution. The size of the particles will depend on the monomer type, the viscosity change of the dispersed phase with time, the type and concentration of stabiliser and the agitation conditions in the reactor. In the case of large monomer droplet in the continuous phase, nucleation predominantly occurs in the droplets and each polymerising droplet behaves as an isolated batch polymerisation reactor. The notation suspension polymerisation is reserved for systems where nucleation occurs in the monomer droplet and the average number of radicals per particle is very high (10^2 to 10^6). This is usually obtained if the droplets are larger than 1 μm. In principle, in the suspension polymerisation process, large particles are obtained. But the suspension polymerisation of vinyl monomers generally also results in a small fraction of polymer particles below 1 μm as well as large beads [62]. The small particles were thought to be the result of nucleation in the aqueous phase and subsequent latex polymerisation. According to the Laplace pressure, smaller droplets are thermodynamically less stable than larger ones and undergo Ostwald ripening. The addition of hydrophobe lowers the chemical potential and prevents the diffusion of the monomer to large droplets. This leads to bimodal particle distribution with one fraction below 1 μm and the other one can be adjusted between 20 and 500 μm [63]. Beaded suspension polymers have found important applications in the immobilisation/anchoring of enzymes and other biological substrates [64-66]. In this polymerisation, agitation system design are critical to achieving the desired particle size distribution in the final product. The optimal design system balances the phenomena of coalescence/dispersion, droplet and particle suspension, and heat transfer. The initial particle size distribution achieved in the monomer/water would not necessarily be the same as that for the final polymer product even if particle coalescence could be completely prevented.

There have been a number of studies on the effect of agitation on droplet size [67-71]. The initiator is soluble in the monomer phase, which is dispersed by agitation into the dispersion medium (usually water) to form droplets (i.e. an emulsion is formed). The combination of continued agitation and the addition of a suitable stabiliser (often a surface active polymer) have a stabilising effect, hindering both the coalescence and further break-up of monomer droplets. The size of the initial emulsion droplets formed is dependent upon the balance between droplet break-up and droplet coalescence. This is in turn controlled by the type and speed of agitator used, volume fraction of the monomer phase and the type and concentration of stabiliser used.

The stabilised monomer droplets may be considered as "microreactors", with the polymerisation proceeding therein [72-75]. The type and concentration of the suspending agent plays an important role in the tendency of droplets to coalesce. As the suspension polymerisation proceeds, the viscosity of a monomer–polymer droplet increases with conversion. Hence, the physical behaviour of the droplets is not the same during the process. When dispersible material is added to the existing stabilised drops, the new material and existing drops can remain segregated for significant amounts of time [76]. The increasing viscosity of the suspended droplets, as polymerisation proceeds, makes the quantitative analysis of suspension polymerisation a complex problem [77]. It is possible to establish a number of special factors, apart from the free-radical polymerisations-that exert an important influence on particle size and particle size distribution [78-80]:

1. Geometric factors of the reactor: Profile, type of stirrer, stirrer diameter D relative to the reactor dimensions, bottom clearance of the stirrer, and internal fittings.
2. Operating parameters: Stirrer velocity N, stirring and polymerisation time, phase volume ratio φ, fill level of reactor and temperature T.
3. Substance parameters: Dynamic viscosities η_c and η_d, and densities p_c and p_d, of the continuous and discontinuous phases, and the interfacial tension σ.

The monomer must be relatively insoluble in water for the droplets to form. A typical water insoluble organic monomer has a lower surface tension than water. When such a monomer is mixed continuously as a dispersed phase in a continuous phase of water with no surfactants present, an unstable dispersion forms due to the continuous break up and coalescence of monomer droplets. Much research was done during the 1950s and 1960s on the relation of agitation to particle size. Agitation must be sufficient to prevent separation of dispersion because of the difference of specific gravity between the two phases. Agitation system design is critical to achieving the desired particle size distribution in the final product. The optimal agitation system design balances the phenomena of coalescence/dispersion, droplet and particle suspension, and heat transfer.

Advantages of suspension polymerisation process, compared to other polymerisation processes (bulk, solution and emulsion), are: (i) Easy heat removal and temperature control; (ii) Low dispersion viscosity; (iii) Low levels of impurities in the polymer product; (iv) Particle size can be controlled to a fairly narrow range; (v) The ratio of surface area to volume for small drops or particles is relatively high and local heat transfer is good and (vi) Low cost of conversion with flexibility to vary the particle properties. The disadvantages of suspension polymerisation are: (a) Polymer build up on the reactor wall, baffles, agitators and surfaces; (b) Waste water problems; (c) Difficulty in producing homogeneous copolymer composition; (d) Lower productivity for the same reactor capacity (compared to bulk) and (e) It only applies to free radical processes. Agitation is critical because as the viscosity within the bead rises, the reaction rate increases suddenly (Trommsdorff effect). This leads to a surge in heat generation, which does not usually occur in solution or emulsion polymerisation. Problems associated with continuous suspension polymerisation process are deposition of polymer on the wall of the

reactor during polymerisation (which affects the heat transfer through the reactor jacket) and difficulty in achieving high conversion.

1.3 Porous structures

As indicated earlier, resins can be classified under three categories: (a) microporous (b) macroporous and (c) macroreticular. Microporous resin are prepared from a vinyl monomer and a difunctional vinyl comonomer in the absence of any solvating media (porogen). In the dry state they are microporous, with polymer chains being separated by intermolecular distances. The preparation of macroporous resin is the same as microporous resin but with the inclusion of an inert solvent (porogen). When the solvent solvates both monomer and polymer a fully expanded network is formed with a considerable degree of porosity. Removal of solvent causes a reversible collapse of the matrix and in the dry state such matrix are called microporous resin.

When solvent employed during polymerisation is a good solvent for monomers but is a precipitant for the polymer, the term macroreticular is employed. These are highly porous and rigid which retain its overall shape and volume when the precipitant is removed. The structure of these resins are quite different from microporous and macroporous resin. They have a large and permanent pore volume and reaction sites may be regarded as being located on a permanent interior surface of the resin. Macroporous resins are prepared using large inert molecules which are subsequently washed away to create permanent voids.

1.3.1 Formation of porous structure

The free-radical crosslinking copolymerisation system for the production of macroporous copolymers includes a monovinyl monomer, a divinyl monomer (crosslinker), an initiator and inert diluent. The decomposition of the initiator produces free-radicals which initiate the polymerisation and crosslinking reactions. After a certain reaction time, a three-dimensional network of infinitely large size may start to form. The term `infinitely large size',

according to Flory [81], refers to a molecule having dimensions of an order of magnitude approaching that of the containing vessel. At this point (the gel point) the system (monomer–diluent mixture) changes from liquid to solid-like state. Continuing polymerisation and crosslinking reactions decreases the amount of soluble reaction components by increasing both the amount and the crosslinking density of the network. After complete conversion of monomers to polymer, only the network and the diluent remain in the reaction system.

Crosslinked copolymers prepared by free-radical crosslinking copolymerisation exhibit different structures and properties depending on the amounts of the crosslinker and the diluent present during the reactions as well as on the solvating power of the diluent. In free radical crosslinking copolymerisation, inhomogeneous gel formation always occur due to the fact that the crosslinker has at least two vinyl groups and therefore, if one assumes equal vinyl group reactivity, the reactivity of crosslinker is twice that of the monomer. As a consequence, the crosslinker molecules are incorporated into the growing copolymer chains much more rapidly than the monomer molecules so that final network exhibits a crosslink density distribution [82].

Dusek proposed that a phase separation occurred during gel formation, proceeding either in the form of macrosynersis or microsynersis [83]. The sensitive dependence of the properties of the porous structure on the synthesis parameters allows one to design a tailor-made macroporous material for a specific application. The main experimental parameters are the type and the amount of the diluent, the crosslinker concentration, the polymerisation temperature and the type of the initiator. Extensive study of macroporous morphology and formation of porous structure have been conducted for beaded, crosslinked styrene-divinyl benzene resins [84-85]. The internal structure of the resin beads can be controlled by different parameters in the polymerisation process, such as the amount of crosslinking monomer used,

type and volume of diluent/porogen/pore generating solvent (an inert organic solvent) added to the monomer phase.

1.3.2 Effect of the porogen on the formation of porous structure

Porous structures start to form when the amount of the diluent (porogen) and the amount of the crosslinker pass a critical value. The solvating power of the diluent has a critical effect on the porous structure of macroporous copolymers. The net solvating power of the medium (unreacted monomer mixture+diluent) changes during the course of the reaction as the monomers get consumed and this change is particularly severe where the diluent is a nonsolvent for the copolymer.

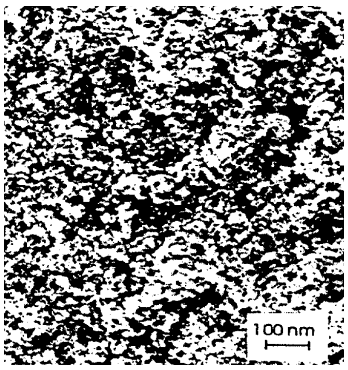

Figure 1.4: Internal structure of a macroporous copolymer bead

The preparation of macroporous copolymer beads is generally achieved as a result of the phase separation which occurs during the copolymerisation of a monomer mixture containing appropriate amounts of monomer, a crosslinking comonomer and a porogenic solvent. The internal structure of a macroporous copolymer bead (Figure 1.4) shows the wide distributions in the pore size.

The porogen is a low molar mass or polymeric substance that is miscible with the monomers but does not react during the copolymerisation and at the end of the reaction can be easily removed from the formed copolymer product [86]. The porogen may remain in the

network (gel) phase throughout the copolymerisation, resulting in the formation of expanded (swollen) particles or may separate out of the network phase resulting in the formation of porous particle. The distribution of the diluent between network and diluent phases (diluent in the pores) at the end of the copolymerisation determines the total porosity of the resulting copolymer and their swelling ratio in solvent. In presence of porogen, control of porosity, therefore the effective surface area has been extensively investigated for polystyrene, polyacrylamide, polymethacrylates etc. [87-111]. Three main classes of porogens [112-113] known are: (i) solvents for the polymer (ii) non-solvents and (iii) polymers soluble in the monomer(s).

Polymeric porogens produce only large pores. The molecular weight is then an important parameter. The pore volume is large when the molecular weight of the porogen is high [114]. The most complex and frequently investigated systems are those incorporating a nonsolvating diluent [115]. Here, as initially proposed by Kun and Kunin [116] and later observed experimentally by Jacobelli *et al*, the bead contains large agglomerates of microspheres (100-200 nm). Each microsphere consists of smaller nuclei (10-20 nm) which are more or less fused together. In between the nuclei, there is a first family of very small pores (5-15 nm) which are mainly responsible for high surface areas of these materials. In between the microspheres a second family of intermediate pores (mesopores) is observed (20-50 nm) which account for moderate surface areas (up to 100 m^2/g). A third family of pores is responsible for higher pore volumes, which can be seen when very high relative volume of diluent is used. Figure 1.5 represents the macroporous resin structure. The choice of porogen has a great influence on the shape and size of pores. The task of this porogen is to create cavities in the polymeric structure by dissolution of the monomer, while acting as a precipitant towards the growing polymer. Naturally, the total amount of porogenic solvent in the polymerisation

mixture has to be sufficiently large to ensure a porous structure and a pore volume that allows operation at reasonably low pressures in a flow through system.

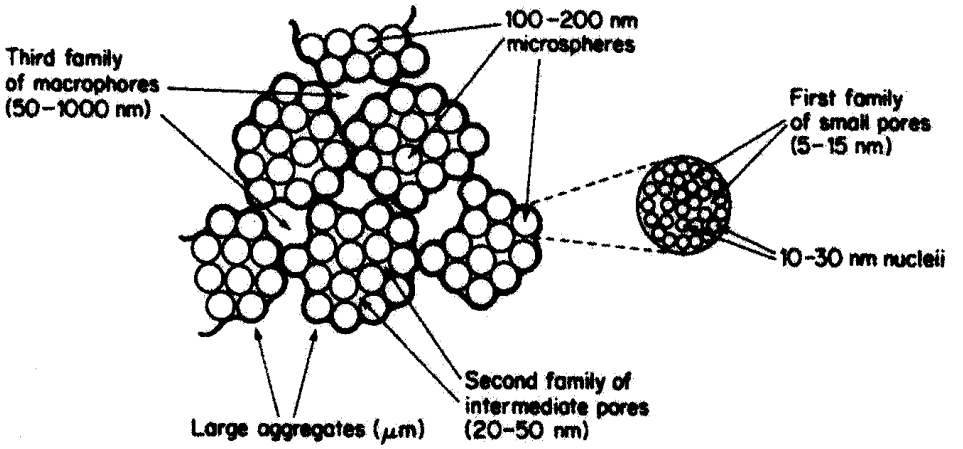

Figure 1.5: Schematic representation of the structure of macroporous domain

The polymer phase separates from the solution during polymerisation because of its limited solubility in the polymerisation mixture that results from either (or both), a molecular weight that exceeds the solubility limit of the polymer in the given solvent system or insolubility derived from cross-linking. The presence of porogen in the porogen phase is necessary if porous beads are to be obtained. In its absence, only nonporous, transparent beads are formed. However, some non-porous beads also appeared among the opaque porous beads. This was related to the phase separation occurring before the gel point when the thermodynamically poor diluent partly separates from the polymerisation mixture. Polymerisation then results in nonporous beads.

1.4 Functional polymers

As research goes on, the demand for functional polymers have increased. A functional polymer has chemically bound specific functional groups that can be used as a reagents, catalyst, protecting group etc. The polymer can be modified by active functional group introduced into the polymer chain using following processes:

(i) by direct polymerisation/copolymerisation of monomers containing the desired functional group;

(ii) by chemical modification of preformed polymer or

(iii) a combination of both of above.

A difficulty may arise in the process (i) due to considerable manipulation of co-polymerisation procedure, which is necessary to ensure a good yield of the required polymer. The second process is reliable because the functional group can be easily introduced by using standard organic synthetic procedure. The chemical modification of a resin can depend substantially on the physical properties of the resin. Functionalised polymeric support must possess a structure which permits adequate diffusion of reagent into the reactive sites, a phenomenon which depends on the extent of swelling, the effective pore size, pore volume and the chemical and mechanical properties of the resin under conditions of particular chemical reaction.

1.5 Inclusion complex formation with cyclodextrin

Cyclodextrins, cyclic oligosaccharides, were discovered by Villiers [117], about 112 years ago. The first detailed description of preparation and isolation was made in 1903 by Schardinger [118]. Hence, cyclodextrins are also known as Schardinger dextrins. The interest in cyclodextrins is seen from publications which has averaged annually above 1000 since 1996. The important parameters of α, β and γ cyclodextrins (CDs) are presented in Table 1.1.

α, β and γ-Cyclodextrins (CDs) have six, seven and eight -glucopyranose units linking through α 1-4-glycosidic linkages (Figure 1.6). The functional structural schemes of β-cyclodextrin shown in Figure 1.7 indicates the presence of a large cavity at the centre which is of great importance to the usefulness of these compounds.

The various cyclodextrins can be considered as empty capsules of molecular size. When this cavity is filled with compound, it is called an inclusion complex. Inclusion complexes are

entities comprising two or more molecules, in which one of the molecules, the host, includes, totally or in part, only by physical forces, without covalent bonding, a guest molecule [119-121]. CDs are typical host molecules and may include a great variety of molecules having the size of one or two benzene rings, or even larger ones, which have a side chain of comparable size, to form crystalline inclusion complexes. The inclusion of a guest in CD cavity is essentially a substitution by the less polar guest.

Table 1.1: Physicochemical properties of cyclodextrin

Component	*α CD*	*β CD*	*γ CD*
Appearance	white crystalline powder	white crystalline powder	White crystalline powder
No. of glucose unit	6	7	8
Mol. wt	972	1135	1297
Solubility in water, g/100 mL	14.5	1.85	23.2
Cavity diameter (Å)	4.7-5.3	6.0-6.5	7.5-8.3
Cavity height (Å)	7.9	7.9	7.9
Cavity volume (mL/mol)	174	262	427
Inner diameter (Å)	5.7	7.8	9.5
Outer diameter (Å)	13.7	15.3	16.9
Crystal water, wt%	10.2	13.2-14.4	8.13-17.7

Complex formation comprises the following elementary steps [122]:

i. The water molecules escape from the CD cavity and their energy level will correspond to that in the gaseous state. As a consequence, van der Waals interactions and the number of hydrogen bonds decrease, while the translational and three dimensional rotational degrees of freedom of the released water molecules increase.

ii. The conformation of CD ring decreases on relaxing resulting in a more stable lower energy state.

iii. The apolar guest molecule sheds its hydration shell and assumes the ideal gas state. The empty hydrate shell collapses and rearranges.

iv. The guest molecule enters the empty CD cavity and the complex is stabilised by van der Waals interactions and sometimes by hydrogen bonding.

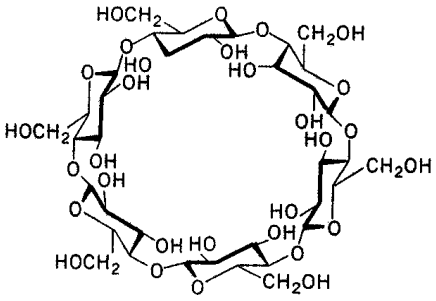

α-cyclodextrin

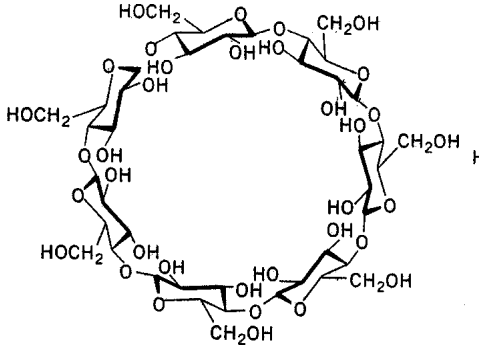

β-cyclodextrin

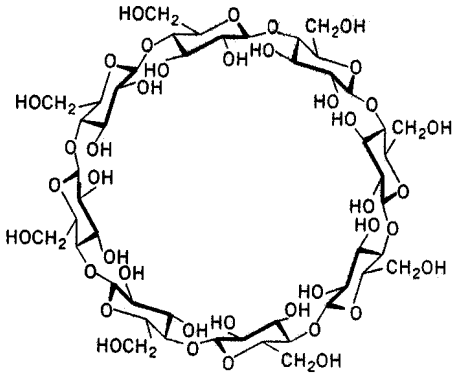

γ-cyclodextrin

Figure 1.6: Structures of α, β and γ-cyclodextrin

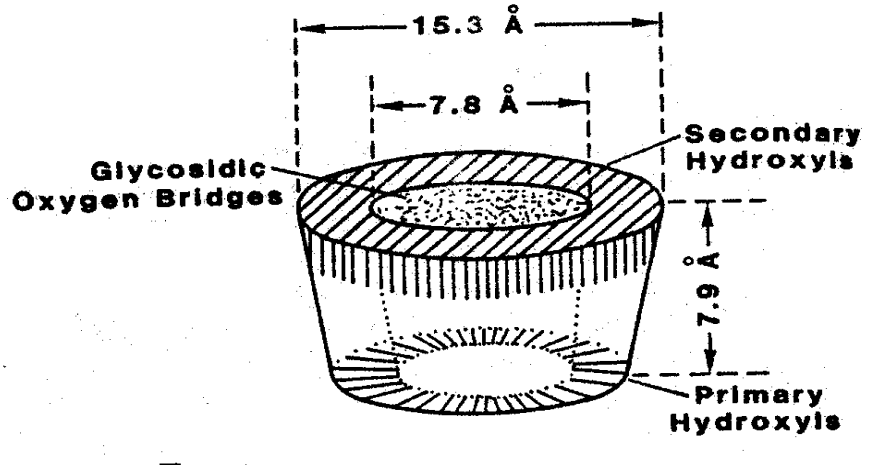

Figure 1.7: Functional structural scheme of β-cyclodextrin

v. The displaced water molecules condense from the gaseous state to the liquid state. Changes in enthalpy and entropy can be regarded as identical with those of the well known water condensation.

vi. The structure of water is restored around the exposed parts of the guest molecule, and integrated with the CD ring's hydrate shell.

$$CD + G \rightleftharpoons CD.G$$

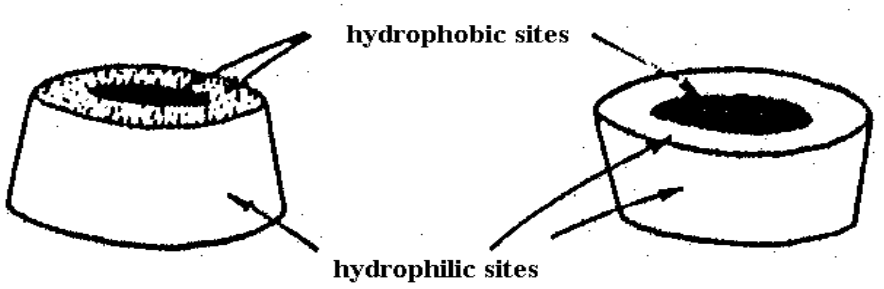

Figure 1.8: Schematic representation of the hydrophobic and hydrophilic region of cyclodextrin

Van der Waals forces, hydrophobic interactions and hydrogen bonds hold the cyclodextrin and its guest together. The extent to which these forces contribute depends on the nature of the enclosed guest molecule. The inherent ring structure is decisive, as inclusion complex are formed only if there is a tight spatial fit between the host and guest components.

The driving force is more or less independent of the guest [123], therefore thermodynamic parameters do not show great variation [124].

The conformation of the cyclodextrin molecule can be best represented by a deformed cone in which the primary hydroxyl groups (at position 6 of the α-D-glucose) are on the narrower rim while secondary hydroxyl groups (at position 2 and 3 of the α-D-glucose) crown the wider rim [125]. The cyclic nature of these molecules creates hydrophilic outer surface and a nonpolar hydrophobic cavity, which plays an important rule in the inclusion complex formation with various guest molecules [126-131], as shown in Figure. 1.8.

Complex formation is a dimensional fit between host cavity and guest molecule. Molecular dimension of cyclodextrins are shown in Figure 1.9. Covalent bonds are neither broken nor formed during inclusion complexation [132]. The binding of guest molecules within the host cyclodextrin is not fixed or permanent but is in a dynamic equilibrium. Binding strength depends on how well the `host–guest' complex fits together and on specific local interactions between surface atoms. Inclusion in cyclodextrins exerts a profound effect on the physicochemical properties of guest molecules as they are temporarily locked or caged within the host cavity giving rise to beneficial modifications of guest molecules, which are not achievable otherwise [133-134]. The potential guest list for molecular encapsulation in cyclodextrins is quite varied and includes such compounds as straight or branched chain aliphatics, aldehydes, ketones, alcohols, organic acids, fatty acids, aromatics, gases, and polar compounds such as halogens, oxyacids and amines. Due to the availability of multiple reactive hydroxyl groups, the functionality of CDs is greatly increased by chemical modification. These modifications widely enhance the applicability of cyclodextrins. Cyclodextrins are used among others in food, pharmaceuticals, cosmetics, environment protection, bioconversion, packing and textile industry [135-136].

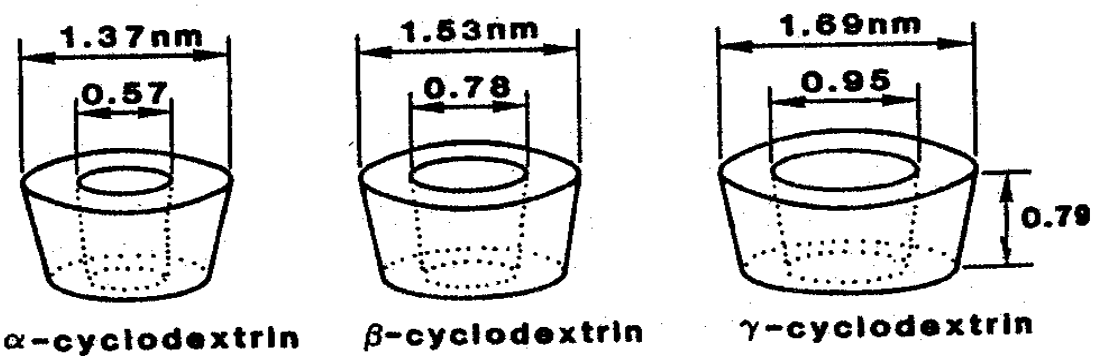

Figure 1.9: Molecular dimension of cyclodextrin

There are numerous reports and reviews describing the ability of cyclodextrins (CDs) to form inclusion complexes with many poorly water soluble molecules, such as steroids. Inclusion complex formation by cyclodextrins with steroids has triggered many pharmaceutical applications [137-138]. Breslow showed that cyclodextrin dimer can be used to selectively bind cholesterol, having an end to end dimension of 15Å [139].

1.5.1 Cyclodextrin polymers

Compounds consisting of two or more covalently linked cyclodextrin rings are called cyclodextrin polymers. The cyclodextrins fixed into polymeric structures behave differently from their monomeric derivatives.

i. Linear polymers are obtained by polymerising vinyl derivatives of cyclodextrin, when the product is insoluble.

ii. Crosslinked structure is produced when cyclodextrin reacted with bi or polyfunctional reagent.

iii. Cyclodextrin can be immobilised on synthetic and natural supports by chemical bonds resulting in products with the ability to form inclusion complexes.

iv. Polymeric products containing cyclodextrins have also been prepared by physically incorporating them into synthetic polymers.

The separation potential of a particularly interesting molecule could be enhanced several fold by incorporating cyclodextrin on to the back-bone of a polymer. Cyclodextrins can discriminate between positional isomers, functional groups, homologues and enantiomers.

Currently, chiral separation is one of the most important areas of application of CDs covalently linked to a polymeric structure. A rich variety of guest binding is successfully achieved by appropriately modifying the three CDs (partially or completely) at the hydroxyl functional group.

1.6 Removal of metal ions using macroporous polymer

Metal ions are the most perilous water pollutants due to their toxicity and carcinogenicity [140]. The presence of heavy metals in the environment is a cause of concern due to their acute and long term toxicity. Some of the metal ions are cumulative poisons capable of being adsorbed and assimilated in the tissues of the organisms causing noticeable adverse physiological effects. Hence, removal of such metal ion are necessary, even at very low concentration [141].

The necessity of removal of metal ions has led to an increasing interest in sorbents. It has been reported that the same metal ion may possess different toxicity in its different oxidation states, which are responsible for their different physico-chemical and biological activities. Pollution by arsenic in natural and industrial waste water has been monitored and controlled to avoid its high toxicity to living things. Arsenic, resulting from geochemical reactions, industrial and mining waste discharges, or from the agriculture use of arsenical pesticides, is found in many surface and ground waters. It has become a problem for water supplies in several countries such as Bangladesh, India and China.

Arsenic exists in natural systems in a variety of chemical forms, including inorganic arsenic (III) and arsenic (V), and several mono-, di- and tri -methylated arsenic compounds. Both elemental arsenic and arsenic (V) are markedly less toxic than arsenic (III). The toxicity of such compounds decreases in the order: arsine > arsenite > arsenate > alkyl arsenic acids >

arsonium compounds and metallic arsenic. Mobility of arsenic in water is highest for arsenite, so it is the most important species in fresh water where arsenate is also dominant.

1.6.1 Medical consequences of arsenic poisoning

Arsenic is an accumulative, potent and protoplasmic poison. It can damage the nervous system and is a known carcinogen, responsible for lung, skin and reportedly also intestinal cancers. It is a teratogen, meaning it can enter the metabolic system of unborn child. Its actual toxicity depends on such factors as general health and diet. It accumulates in the body and passes slowly out through hair and nails. Inhalation, ingestion and skin contact are the primary routes of human exposure to arsenic. Skin contact and inhalation are occupational hazards in the working environment with arsenic. Ingestion is a hazard for everybody. Chronic poisoning by arsenic compounds leads to loss of appetite and weight, diarrhea alternating with constipation, gastrointestinal problems, thickening and discolouration of the skin, stomach pain, nausea, vomiting, numbness in hands and feet, partial paralysis peripheral neuritis, conjunctivitis, dermatitis and sometime skin cancer.

1.6.2 Safe limit

Maximum contaminant level for safe drinking water has been 50 parts per billion (PPB). According to World Health Organization (WHO), the recommended maximum level is 10 PPB. The maximum level of arsenic found in many parts of China, India and Bangladesh in drinking water is 10000 PPB, which is 1000 times greater than the recommended limit. As indicated earlier, the toxicity of As (III) is greater than that of As(V) [142]. So the speciation of metal ions is of great importance, due to different toxicity of a particular metal ion in different oxidation state. Arsenic removal from water has been tested by chemical coagulation, ion exchange, adsorption processes and membrane filtrations.

Macroporous polymers impregnated with selective chelating ligands show advantages similar to solid-liquid and liquid-liquid extraction. Polyethylenimine (PEI) attached adsorbents

have been used heavy metal removal [143-146]. Polyethylenimine is well known for its metal chelation potentialities [147-148]. A polymeric chelating ligand, PEI, was utilised primarily in order to increase the number of sites for coordination and thus increase the capacity of the adsorbent [149]. The adsorption by polymer sorbents are reported to be the best method for the removal of metal ions at low concentration (ppm level). Presently, specific sorbents are considered as one of the most promising techniques. Specific sorbents consist of a ligand (e.g. chelating agents) that interact with the metal ions specifically and a carrier matrix (polymeric beads). Polymeric macrobeads have attracted most attention as adsorbents because they can easily be produced in different composition and modified into specific sorbents by the introduction of metal chelating groups.

1.7 References

1. H. Staudinger and E. Huseman, Berichte, **1935**, *68,* 1618.
2. K. Dusek, J. Polym. Sci., B, **1965**, *3*, 209.
3. I. M. Abrams, Ind. Eng. Chem., **1956**, *48*, 1469.
4. E. F. Meitzner and J. A. Oline, US Patent, 4,224,415 (**1980**).
5. I. M. Abrams, US Patent, 2,844,546 (**1958**).
6. W. G. Lloyd and T. Alfrey, J. Polym. Sci., **1962**, *62*, 301.
7. R. Kunin, E. F. Meitzner and N. Bortnick, J. Am. Chem. Soc., **1962**, *84*, 305.
8. R. Kunin, E. F. Meitzner, J. A. Oline, S. Fisher and N. Frish, Ind. Eng. Chem. Prod. Res. Develop., **1962**, *1*, 140.
9. K. A. Kun, J. Polym. Sci., A, **1965**, *3*, 1833.
10. J. R. Millar, D. G. Smith, W. E. Marr and T. R. E. Kressman, J. Chem. Soc., **1963**, 218.
11. J. R. Millar, D. G. Smith, W. E. Marr and T. R. E. Kressman, J. Chem. Soc., **1963**, 2779.
12. J. R. Millar, D. G. Smith, W. E. Marr and T. R. E. Kressman, J. Chem. Soc., **1964**, 2740.
13. K. S. W. Sing, D. H. Everett, R. A. W. Haul, L. Moscou, R. A. Pierotti, J. Rouquerol and T. Siemieniewska, Pure Appl. Chem., **1985**, *57,* 603.
14. H. Kuroda and Z. Osawa, Eur. Polym. J., **1995**, *31*, 1, 57.
15. F. Svec and J. M. J. Frechet, Science, **1996**, *273*, 205.
16. J. E. G. J. Wijnhoven and W. L. Vos, Science, **1998**, *281*, 802.
17. P. T. Tanev, M. Chibwe and T. J. Pinnavaia, Nature, **1994**, *368*, 321.
18. H. Deleuze, X. Schultze and D. C. Sherrington, Polymer, **1998**, *39*, 6109.
19. R. R. Bhave, Inorganic Membranes, Synthesis, Characteristic and Applications, Van Nostrand Reinhold, New York, **1991**.
20. K. Lewandowski, P. Murer, F. Svec and J. M. J. Frechet, Anal. Chem., **1998**, *70*, 1629.
21. D. B. Akolekar, A. R. Hind and S. K. Bhargava, J. Colloid. Interface Sci., **1998**, *199*, 92.
22. V. Maquet and R. Jerome, Mater. Sci. Forum, **1997**, *250,* 15.
23. M. C. Peters and D. J. Mooney, Mater. Sci. Forum, **1997**, *250*, 43.
24. S. Bancel and W. S. Hu, Biotechnology Prog., **1996**, *12,* 398.
25. C. Schugens, V. Maquet, C. Grandfils, R. Jerome and P. Teyssie, Polymer, **1996**, *37*, 1027.

26. M. B. Tennikov, N. V. Gazdina, T. B. Tennikova and F. Svec, J. Chromatography A, **1998**, *798*, 55.

27. A. Palm and M. V. Novotny, Anal. Chem., **1997**, *69*, 4499.

28. S. Xie, F. Svec and J. M. J. Frechet, J. Chromatography A, **1997**, *775*, 65.

29. E. Litovsky, M. Shapiro and A. Shavit, J. Am. Ceram. Soc., **1996**, *79*, 1366.

30. H. Seino, O. Haba, A. Mochizuki, M. Yoshioka and M. Ueda, High Perform. Polym., **1997**, *9*, 33.

31. J. J. Senkevich and S. B. Desu, Appl. Phys. Lett., **1998**, *72*, 258.

32. R. Sedev, R. Ivanova, T. Kolarov and D. Exerowa, J. Dispersion Sci. Technol., **1997**, *18*, 751.

33. C. M. Cheng, F. J. Micale, J. W. Vanderhoff and M. S. El-Aasser, J. Polym. Sci., Polym. Chem. Ed., **1992**, *30*, 235.

34. C. M. Cheng, J. W. Vanderhoff and M. S. El-Aasser, J. Polym. Sci., Polym. Chem. Ed., **1992**, *30*, 245.

35. D. Horak, F. Svec, J. Kalal, K. Gumargalieva, A. Adamyan, N. Skuba, M. Titova and N. Trostenyuk, Biomaterials, **1986**, *7*, 188.

36. K. F. Mueller, S. J. Heiber and W. L. Plankl, US Patent, 4,224,427 (**1977**).

37. C. C. R. Robert, P. A. Buri and N. A. Peppas, J. Appl. Polym. Sci., **1985**, *30*, 301.

38. B. D. Barr-Howell and N. A. Peppas, Eur. Polym. J., **1987**, *23*, 591.

39. A. B. Scranton, A. G. Mikos, L. C. Scranton and N. A. Peppas, J. Appl. Polym. Sci., **1990**, *40*, 1, 997.

40. A. Jayakrishnan, M. C. Sunny and B. C. Thanoo, Polymer, **1990**, *31*, 1339.

41. O. Okay and C. Gurun, J. Appl. Polym. Sci., **1992**, *46*, 401.

42. D. Horak, F. Lednicky and M. Bleha, Polymer, **1996**, *37*, 4243.

43. T. V. Chirila, Y. C. Chen, B. J. Griffin and I. J. Constable, Polym. Int., **1993**, *32*, 221.

44. K. J. Shea, G. J. Stoddard, D. M. Shavelle, F. Wakui and R. M. Choate, Macromolecules, **1990**, *23*, 4497.

45. S. Xie, F. Svec and J. M. J. Frechet, J. Polym. Sci. A, Polym. Chem., **1997**, *35*, 1013.

46. J. Coupek, M. Krivakova and S. Pokorny, J. Polym. Sci. C, **1973**, *42*, 185.

47. F. Svec, J. Hradil, J. Coupek and J. Kalal, Angew. Makromol. Chem., **1975**, *48*, 135.

48. F. Svec, Angew. Makromol. Chem., **1986**, *144*, 39.

49. V. Smigol and F. Svec, J. Appl. Polym. Sci., **1992**, *46*, 1439.

50. V. Smigol, F. Svec and J. M. J. Frechet, Macromolecules, **1993**, *26*, 5615.

51. S. J. Gregg and K. S. W. Sing, Adsorption, Surface Area and Porosity (2nd ed), Academic Press, New York, **1982**, p. 173.

52. S. Brunauer, P. H. Emmett and E. Teller, J. Am. Chem. Soc., **1938**, *60*, 309.

53. D. J. Peter and V. Brian, Colloids and Surfaces A, **2000**, *161*, 259.

54. F. Hofman and K. Delbruk, German Patent, 250,690 (**1909**); 254,672 (**1912**); 255,129 (**1912**).

55. K. Gottlob, US Patent, 1,149,577 (**1913**).

56. W. Bauer, H. Lauth, German Patent, 656,134 (**1931**).

57. E. Vivaldo-Lima, P. E. Wood, A. E. Hamielec and A. Penlidis, Ind. Eng. Chem. Res., **1997**, *36*, 939.

58. R. Arshady, Colloid Polym. Sci., **1992**, *270*, 717.

59. B. W. Brooks, Makromol. Chem., Macromol. Symp., **1990**, *35/36*, 121.

60. A. Geoffrey and J. C. Bevington, Eds, Comprehensive Polymer Science, Pergamon Press, Oxford, Great Britian, **1989**, Vol. *4*, Chapter 14.

61. H. G. Yuan, G. Kalfas and W. H. Ray, J. Macromol. Sci., Rev. Macromol. Chem. Phys. C, **1991**, *31,* 215.

62. K. Landfester, Macromol. Rapid. Commun., **2001**, *22,* 896.

63. A. R. M. Azad, R. M. Fitch, in: Polymer Colloids II, R. M. Fitch, Ed, Plenum Press, New York, **1980**, p. 95.

64. P. Hodge, in: P. Hodge and D. C. Sherrington (Eds), Synthesis and Separations using Functional Polymers, Wiley, Chichester, **1998**, p.43.

65. T. M. Maugh, Science, **1984**, *223*, 155.

66. A. Kotha, C. R. Rajan, S. Ponrathnam and J. G. Shewale, React. Funct. Polym., **1996**, *28*, 227.

67. F. H. Winslow and W. Matreyer, Ind. Eng. Chem., **1951**, *53*, 1108.

68. W. P. Hohenstein, Polymer Bull., **1945**, *1*, 13.

69. J. M. Church and R. Shinnar, Ind. Eng. Chem., **1961**, *53*, 479.

70. D. M. Sulvian and E .F. Lindsey, Ind. Eng. Chem. Fundam., **1962**, *1*, 87.

71. H. Hopff, H. Lussi and P. Gerspocher, Makromol. Chem., **1964**, *24*, 37, 78.

72. W. P. Hohenstein and H. Mark, J. Polym. Sci., **1946**, *1*, 127.

73. H. Hopff, H. Lussi and E. Hammer, Makromol. Chem., **1965**, *82*, 175.

74. H. Hopff, H. Lussi and E. Hammer, Makromol. Chem., **1965**, *82*, 184.

75. E. Trommsdorff, H. Kohle and P. Legally, Makromol. Chem., **1948**, *1*, 169.

76. M. Zerfa and B. W. Brooks, Chem. Eng. Sci., **1996**, *51*, 3591.

77. S. Hashim and B. W. Brooks, Chem. Eng. Sci., **2002**, *57*, 3703.

78. H. Wenning, Makromol. Chem., **1956**, *20*, 196.

79. H. Wenning, Kunstst. Plast., **1958**, *5*, 328.

80. E. Trommsdorff, Makromol. Chem., **1954**, *13*, 76.

81. P. J. Flory, J. Am. Chem. Soc., **1941**, *63*, 3083.

82. W. Funke, O. Okay and B. J. Muller, Adv. Polym. Sci., **1998**, *136*, 139.

83. K. Dusek, in: A. J. Chompff and S. Newman, Editors, Polymer Networks: Structure and Mechanical Properties, Plenum Press, New York, **1971**, p. 245.

84. P. Hodge and D. C. Sherrington, Polymer Supported Reactions in Organic Synthesis, Wiley, New York-London, **1980**.

85. H. Jacobelli, M. Bartoline and A. Guyot, J. Appl. Poly. Sci., **1979**, *23*, 927.

86. D. Horak, F. Lednicky and M. Bleha, Polymer, **1996**, *37*, 4245.

87. K. F. Muller, S. Heiber and W. Flank, US Patent, 4,224,472 (**1978**).

88. J. Seidel, J. Malinsky, K. Dusek and W. Heitz, Adv. Polym. Sci., **1967**, *5*, 113.

89. J. C. Moore, J. Polym. Sci., Part A, **1969**, *2*, 835.

90. J. Coupek, M. Krivakova and S. Pokorny, J. Polym. Sci., Polym. Symp., **1973**, *42*, 185.

91. W. Heitz, Adv. Polym. Sci., **1977**, *23*, 1.

92. J. Kalal, J. Polym. Sci., Polym. Symp. Ed., **1978**, *62*, 251.

93. D. Horak, Z. Pelzbauer, M. Bleha, M. Havsky, F. Svec and J. Kalal, J. Appl. Polym. Sci., **1980**, *26*, 411.

94. D. Horak, F. Svec, M. Bleha and J. Kalal, Angew. Makromol. Chem., **1981**, *95*, 109.

95. P. P. Wieczorek, M. Ilavsky, B. N. Kolarz and K. Dusek, J. Appl. Polym. Sci., **1982**, *27*, 277.

96. A. Guyot and M. Bartholin, Prog. Polym. Sci., **1982**, *81*, 277.

97. Y. Ohtsuka, H. Kawaguchi and Y. Yamamoto, J. Appl. Polym. Sci., **1982**, *27*, 3279.

98. H. Galina, N. B. Colaz, P. P. Wiezorek and M. Woiszynska, Br. Polym. J., **1985**, *17*, 215.

99. M. Dimonie, H. Dschell, G. Hubca, M. A. Mateescu, C. G. Oprescu, S. Todireanu, O. Maior, J. Languri and M. Iosif, J. Macromol. Sci. Chem. A, **1985**, *22*, 729.

100. C. C. R. Robert, P. A. Buri and N. A. Peppas, J. Appl. Polym. Sci., **1985**, *30*, 301.

101. D. Horak, F. Svec, J. Kalal, K. Gumaragalieve, A. Adamyan, N. Skuba, M. Titova and N. Trostenyuk, Biomaterials, **1986**, *7*, 188.

102. O. Okay, J. Appl. Polym. Sci., **1986**, *32*, 5533.

103. O. Okay, Angew. Macromol. Chem., **1986**, *143*, 209.

104. O. Okay, Angew. Macromol. Chem., **1987**, *153*, 125.

105. B. D. Barr-HoWell and N. A. Peppas, Eur. Polym. J., **1987**, *8*, 591.

106. O. Okay, Angew. Macromol. Chem., 1**988**, *157*, 1.

107. T. G. Park and A. S. Hoffman, J. Biomed. Mater. Res., **1990**, *24*, 21.

108. T. G. Park and A. S. Hoffman, Biotech. Bioeng., **1990**, *35*, 152.

109. B. N. Loraz, M. Wojaczyriska and A. W. Trochimczuk, Macromol. Chem., **1990**, *194*, 1299.

110. O. Okay and W. Funke, Makromol. Chem. Commun., **1990**, *11*, 583.

111. T. G. Park and A. S. Hoffman, J. Polym. Sci., Polym. Chem. Ed., **1992**, *30*, 505.

112. J. Seidl, J. Malinsky, K. Dusek and W. Heitz, Adv. Poly. Sci., **1967**, *5*, 113.

113. J. R. Millar, D. G. Smith, W. E. Marr and T. R. E. Kressman, J. Chem. Soc., **1963**, 218.

114. W. L. Sederel and G. J. DeJong, J. Appl. Polym. Sci., **1973**, *17*, 2835.

115. H. Hilgen, G. J. DeJong and W. L. Sederel, J. Appl. Polym. Sci., **1975**, *19*, 2647.

116. K. A. Kun and R. Kunin, J. Poly. Sci. A-1, **1968**, *6*, 2689.

117. A. C. R. Villiers, Acad. Sci., Paris, **1891**, *112*, 536.

118. F. Schardinger, Z. Unters Nahrungs-Genussmittel Gebrauchs-gegenstande **1903**, *6*, 865.

119. P. J. A. Riberiro, A. M. Amado and J. J. C. Teixeira-Dias, J. Raman Spectrosc., **1996**, *29*, 155.

120. B. Szafran and J. Pawlaczyk, J. Inc. Phenomena, **1999**, *34*, 131.

121. S. M. Han, Biomed. Chromatogr., **1997**, *11*, 259.

122. J. Szejtli, Cyclodextrin Technology, Kluwer, Dordrecht, **1988**.

123. A. Cooper and D. D MacNicol, J. Chem. Soc., Perkin Trans., **1979**, *2*, 60.

124. F. Cramer, W. Saenger and H. C. Spatz, J. Am. Chem. Soc., **1967**, *89*, 3242.

125. W. Saenger, Angew. Chem., **1980**, *92*, 344.

126. D. Duchene, Cyclodextrins and their Industrial Uses, Edition de la Sante, Paris, **1988**.

127. A. Muozdelapea, T. T. Ndou, J. B. Zung, K. L. Greene, D. H. Live and I. M. Warner, J. Am. Chem. Soc., **1991**, *113*, 1572.

128. A. Muozdalapea, I. Durán-Merás, F. Sslinas, I. M. Warner and T. T. Ndou, Anal. Chim. Acta, **1991**, *225*, 351.

129. S. Scypinski and L. J. Cline Love, Anal. Chem., **1984**, *56*, 331.

130. J. Szejtli and T. Osa, in: Comprehensive Supermolecular Chemistry, Elsevier, Oxford, **1996**, 587.

131. J. Szejtli, Cyclodextrins and their Inclusion Complexes, Akadeniai Kiado, Budapest, **1982**.

132. E. Schneiderman and A. M. Stalcup, J. Chromatogr., B, **2000**, *745*, 83.

133. J. Szetjli, Chem. Rev., **1998**, *98*, 1743.

134. G. Schmid, Trends Biotechnol., **1989**, *7*, 244.

135. R. Bhardwaj, R. T. Dorr and J. Blanchard, J. Pharm. Sci. Technol., **2000**, *54*, 233.

136. M. Lezcano, W. Ai-Soufi, M. Novo, E. Rodriguez-Nunez and J. V. Tato, J. Agric. Food Chem., **2002**, *50*, 1081.

137. J. Pitha, A. Gerloczy and A. Olivi, J. Pharm. Sci., **1994**, *83,* 833.

138. T. Loftsson, B. J. Olafsdottir and N. Bodor, Eur. J. Pharm. Biopharm., **1991**, *37,* 30.

139. R. Breslow and B. Zhang, J. Am. Chem. Soc., **1996**, *118*, 8495.

140. A. R. Clement, G. A. Eiceman and C. J. Koester, Anal. Chem., **1995**, *67*, 221.

141. S. Rapsomanikis and P. J. Craig, Anal. Chim. Acta, **1991**, *248,* 563.

142. M. Leist, R. J. Cassey and D. Caridi, J. Hazardous Mater. B, **2000**, *76*, 125.

143. M. J. Hudson and Z. Matejka, Sep. Sci. Technol., **1990**, *23*, 1417.

144. E. Duru, S. Bektas, O. Genc, S. Patir and A. Denizly, J. Appl. Polym. Sci., **2001**, *81*, 197.

145. R. R. Navarro, K. Sumi, N. Fujii and M. Matsumara, Wat. Res., **1996**, *30*, 2488.

146. A. Bahrami, A. S. Bassi and E. Yanful, Can. J. Chem. Eng., **1999**, *77*, 931.

147. S. Kobayashi, K. Hiroishi, M. Tokunoh and T. Saegusa, Macromolecules, **1987**, *20*, 1496.

148. B. L. Rivas and K. E. Geckeler, Adv. Poly. Sci., **1992**, *102*, 173.

149. R. R. Navarro, K. Sumi and M. Matsumra, Wat. Sci. Tech., **1998**, *38,* 195.

150. H. Lee, C. Neville, Handbook of Epoxy Resins, McGraw-Hill Book Co., New York, **1967**.

151. I. Dobas and J. Eichler, Chem. Prum., **1974**, *24*, 463.

Chapter 2

Synthesis and Characterisation of Macroporous Polymers

2 Introduction

Macroporous, spherical, beaded, highly crosslinked copolymers [1-8] are commercially pertinent because they possess permanent rigid porous structure that persists in swollen as well as dry states. These are usually synthesised in bead form by oil-in-water (O/W) suspension polymerisation [9-10] of a combination of vinyl and divinyl monomer in presence of inert solvent (termed as porogen), which induces pore formation in the polymer matrix.

Suspension polymerisation process can be divided in three stages. In the first stage, a liquid–liquid dispersion exists; the liquid monomer(s) containing soluble initiator is dispersed as small droplets stabilised by the combined action of stirring and stabilisers. In the second stage, also called sticky stage, a breakup-coalescence dynamic equilibrium of the monomer–polymer droplets exists which seems to determine the final particle size. The droplets breakup by the impellers' shear stress and coalesce back after colliding with each other. Finally, in the third stage, the coalescence is absent, the polymer particles are solid and they do not stick any more [11]. The porogen (organic solvent or a linear polymer), is soluble in the monomer phase, does not take part in the polymerisation process but remains within the formed beads, generating pores [12-16].

Merrifield's solid phase peptide synthesis triggered the initial interest in the use for crosslinked beaded and reactive polymers which has now been transferred to various other areas of chemistry [17]. Macroporous crosslinked polymers, having functional group in the back bone, have gained importance in many fields of scientific research as well as industrial applications, and the research activity continues to increase because several possibilities to modify their physical and chemical properties exist to tailor for specific needs such as chromatographic materials, drug delivery devices, immobilisation supports for enzymes,

catalysts, separation and adsorbent media, solid reagent and combinatorial synthesis, etc. [18-34].

Molecules diffuse freely through the pores, which form a maze of tortuous interconnected cavities differing in size. The utility of macroporous system is a sensitive function of the internal pore diameter, their distribution and morphology [35-38]. The internal structure are examined by mercury porosimetry and BET surface area measurements [39].

Svec *et al.* [40-42] were the first to synthesise and study macroporous beaded glycidyl methacrylate-ethylene dimethacrylate copolymers. The interrelation between synthesis variables and material properties have been examined for beaded 2-hydroxyethyl methacrylate–ethylene dimethacrylate (HEMA-EGDM) copolymers [43]. Kotha *et al*. reported an increase in porosity, surface area and average pore size, with the increase in crosslinker and porogen concentration for glycidyl methacrylate–divinyl benzene copolymers by suspension polymerisation [44].

In the present study, a number of copolymers of glycidyl methacrylate (GMA)-ethylene dimethacrylate (EGDM), glycidyl methacrylate (GMA)-divinyl benzene (DVB), allyl glycidyl ether (AGE)-ethylene dimethacrylate (EGDM), 2-hydroxyethyl methacrylate (HEMA)-ethylene dimethacrylate (EGDM) and 2-hydroxyethyl methacrylate (HEMA)-divinyl benzene (DVB), have been synthesised by varying the amount/type of pore generating solvent and changing the crosslink density. The effect of these synthesis variables on material characteristics such as particle size and its distribution, pore size and its distribution, pore volume, surface area, surface functional groups and surface morphology have been investigated. A selected few polymers were examined for their suitability for binding of

cyclodextrin or grafting polyethylenimine. The modified polymers were evaluated for guest-host interaction and metal sequestration.

2.1 Poly(glycidyl methacrylate-*co*-ethylene dimethacrylate)

The aim was to synthesise net-worked porous polymers in beaded form with surface epoxy groups which undergo facile transformation with a rich variety of functional groups.

2.1.1 Suspension polymerisation of GMA with EGDM

Glycidyl methacrylate (GMA): Empirical formula: $C_7H_{10}O_3$; Molecular weight: 142.16; Specific gravity: 1.042; Physical state: clear liquid; Boiling point: 195 ^oC. *Allyl glycidyl ether*: Empirical formula: $C_{10}H_{10}O_2$: Molecular weight: 130.19; Specific gravity: 0.914; Boiling point: 153.9 ^oC. *2-Hydroxyethyl methacrylate (HEMA):* Empirical formula: $C_6H_{10}O_3$; Molecular weight: 130.14; Specific gravity: 1.073; Physical state: clear liquid; Boiling point: 205 ^oC. *Ethylene dimethacrylate (EGDM):* Empirical formula: $C_{10}H_{14}O_4$; Molecular weight: 198.22; Specific gravity: 1.051; Physical state: clear liquid; Boiling point: 260 ^oC. *Divinyl benzene (DVB):* Empirical formula: $C_{10}H_{10}$; Molecular weight: 130.19; Specific gravity: 0.914; Boiling point: 197 ^oC. *Cyclohexanol:* Empirical formula: $C_6H_{12}O$; Molecular weight: 100.16; Specific gravity: 0.96; Boiling point: 161 ^oC; Physical state: white colour liquid. *Hexanol*: Empirical formula: $C_6H_{14}O$; Molecular weight: 102.18; Specific gravity: 0.814; Boiling point: 156.6 ^oC. *Octanol:* Empirical formula: $C_8H_{18}O$; Molecular weight: 130.23; Specific gravity: 0.827; Boiling point: 196 ^oC. P*oly(vinyl pyrrolidone) [PVP]:* Empirical formula: $(C_6H_9NO)_x$; Molecular weight: 3,60,000; Density: 1.1-1.3; Melting point: 100 ^oC; Physical state: off white powder. *Azobisisobutyronitrile (AIBN):* Empirical formula: $C_8H_{12}N_4$; Molecular weight: 164.21; Specific gravity: 0.96; Melting point: 103-105 ^oC; Physical state: white powder.

Glycidyl methacrylate (GMA), allyl glycidyl ether (AGE), 2-hydroxyethyl methacrylate (HEMA), divinyl benzene and ethylene dimethacrylate (EGDM) were from Sartomer, USA and used as received. Cyclohexanol, hexanol and octanol used as porogen, were from M/S Aldrich Chemical Co. (USA). Poly(vinyl pyrrolidone) [PVP] was from Polysciences, USA and used as protective colloid. Azobisisobutyronitrile [AIBN], from M/S SISCO, India was the initiator.

The suspension copolymerisation were conducted in double walled cylindrical reactor. The continuous phase was one weight percent aqueous solution of PVP. The discontinuous organic phase consisted of GMA, crosslinking divinyl monomer (EGDM), polymerisation initiator (AIBN) and cyclohexanol (porogen). The discontinuous organic phase was introduced into the aqueous phase, stirring with 8 bladed Rushton turbine was set at 300 rotations per minute and the temperature was maintained at 70 ^{o}C for 3 h. The schematic diagram is given in Figure 2.1. In a typical copolymerisation represented by experiment GE1 (Table 2.1, row 1), glycidyl methacrylate (6.1 mL; 0.0447 mol), ethylene dimethacrylate (2.1 mL; 0.0111 mol), cyclohexanol (19.9 mL) and AIBN (0.2 g) were added to 100 mL of 1 wt% aqueous PVP solution and polymerisation was continued for 3 hours. The copolymer was obtained in beaded form. It was separated by decantation, washed with water, methanol and dried to constant mass at room temperature under reduced pressure. The composition of GMA-EGDM copolymers are presented in Table 2.1. A number of experiments were conducted for each composition.

The pore generating solvent volume was varied for a given fixed monomer composition such as [GMA]:[EGDM]=1.00:0.25 so as to generate copolymers with the same composition but differing in the pore volume. Thus, copolymers GE1, GE7, GE13, GE19 and GE25 are equivalent in that all have a crosslink density of 25%. The crosslink density is defined as {[EGDM]/[GMA]} x 100. These five copolymers, of the same structural composition but of

varying porosity, were prepared by changing the volume of cyclohexanol (porogen) relative to that of the combined volumes of the two monomers as 2.43:1, 1.61:1, 0.81:1, 0.405:1 and 0:1, respectively. Similarly, six sets of copolymers, varying in their compositions, were prepared by changing the mole ratio of GMA:EGDM, termed as the crosslink density (25, 50, 75, 100, 150 and 200). Thus, 30 poly(GMA-EGDM) were synthesised for relative evaluations.

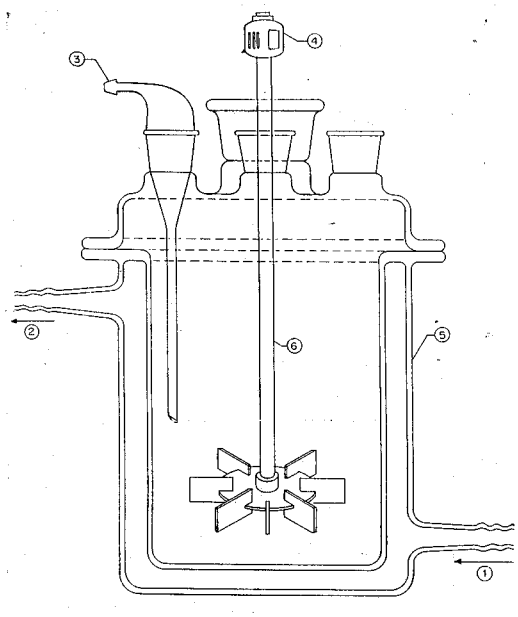

Figure 2.1: Suspension polymerisation set-up. 1. Hot water inlet, 2. Hot water outlet, 3. Nitrogen bubbler, 4. Stirrer motor, 5. Reactor flask, 6. Stirrer.

Table 2.1: Composition of glycidyl methacrylate (GMA) and ethylene dimethacrylate (EGDM) copolymers synthesised using cyclohexanol as porogen

Exp. No	GMA (mol)	EGDM (mol)	CLD %	Monomer:porogen (v/v)
GE1, GE7, GE 13, GE19, GE 25	0.0447	0.0111	25	1:2.43, 1:1.61, 1:0.81, 1:0.405, 1:0
GE2, GE8, GE14, GE20, GE26	0.0352	0.0180	50	1:2.43, 1:1.61, 1:0.81, 1:0.405, 1:0
GE3, GE9, GE15, GE21, GE27	0.0293	0.0223	75	1:2.43, 1:1.61, 1:0.81, 1:0.405, 1:0
GE4, GE10, GE16, GE22, GE28	0.0249	0.0255	100	1:2.43, 1:1.61, 1:0.81, 1:0.405, 1:0
GE5, GE11, GE17, GE23, GE29	0.0198	0.0292	150	1:2.43, 1:1.61, 1:0.81, 1:0.405, 1:0
GE6, GE12, GE18, GE24, GE30	0.0161	0.0318	200	1:2.43, 1:1.61, 1:0.81, 1:0.405, 1:0

crosslink density (CLD) is defined as the mole percent of crosslinking monomer relative to the moles of reactive functional comonomer. AIBN: 0.2 g; Water: 100 mL; PVP: 1 g.

2.1.2 Characterisation of GMA-EGDM copolymers

2.1.2.1 Mercury intrusion porosimetry

Mercury intrusion porosimetry (MIP) is used to measure pore size distribution. It spans the measurement of pores ranging from a few nanometer, to several hundred micrometers. Mercury is a non-wetting liquid for almost all substances and consequently it has to be forced into the pores of these materials. Pore size and volume quantification are accomplished by submerging the sample under a confined quantity of mercury and then hydraulically increasing the pressure of mercury. As the applied pressure is increased the radius of the pores, which can be filled with mercury, decreases and consequently the total amount of mercury intruded increases.

Porous properties were determined by mercury intrusion porosimetry in the pressure range 0-4000 kg/cm^2 with an Auto scan 60 mercury porosimeter from Quantachrome, USA. Porosity refers to the pore space in a material. Pores are classified according to size into three categories; micropores (pore diameter smaller than 2 nm), mesopores (pore diameter 2-50 nm) and macropores (pore diameter larger than 50 nm). Pore size defines an ability of the analyte molecules to penetrate inside the particle and interact with its inner surface. Mercury porosimetry is based on the Washburn equation, 2.1.

$$p.r = -2.\gamma.\cos\theta \qquad 2.1$$

Where, p is pressure, r is the radius of the pore that mercury intrudes, γ is surface tension of mercury and θ is contact angle of the mercury on the surface of the solid sample. The surface tension and contact angle of mercury are 480 mNm^{-1} and 140^o, respectively. The Washburn equation (2.1) can be derived from the equation of Yang and Dupre:

$$\gamma_{SV} = \gamma_{SL} + \gamma_{LV}.\cos\theta \qquad 2.2$$

Where, γ_{SV} is the interfacial tension between solid and vapour, γ_{SL} is interfacial tension between solid and liquid, γ_{LV} is interfacial tension between liquid and vapour and θ is the contact angle of the liquid on pore wall. The work, W, is required to move liquid up the capillary. During capillary rise, when the solid-vapour interface disappears, solid-liquid interface appears as:

$$\mathbf{W = (\gamma_{SL}-\gamma_{SV}).\ \partial A} \qquad \mathbf{2.3}$$

Where, ∂A is the area of the capillary wall covered by liquid when their level rises. According to equations 2.2 and 2.3,

$$\mathbf{W = -\ (\gamma_{LV}\ .\cos\theta).\partial A} \qquad \mathbf{2.4}$$

The work required to raise a column of liquid through a height h in a capillary with radius r is identical to work required to force the liquid out of the capillary. When a volume V of liquid is forced out of the capillary with a gas at constant pressure above ambient ∂P_{gas}, the work is presented as:

$$\mathbf{W = V\partial P_{gas}} \qquad \mathbf{2.5}$$

Equations 2.4 and 2.5 are combined to yield

$$\mathbf{\partial P_{gas}.\ V = -(\gamma.\cos\theta).\ \partial A} \qquad \mathbf{2.6}$$

When the capillary is circular in cross section, parameters V and ∂A are given by $\pi r^2 L$ and $2\pi rL$, where L is the length of the capillary.

$$\mathbf{p.\ r = -2.\gamma.\cos\theta} \qquad \mathbf{2.7}$$

This is known as Washburn equation, the operating equation in mercury porosimetry. The product pr is constant on keeping γ and θ constant. This implies that pressure is inversely proportional to radius. Thus, mercury will intrude progressively into narrower pores with increase in pressure. Using θ (140^o) and γ (0.480 N/m), the Washburn equation is p = 0.736/r.

The experimental method is dependent on the wetting or contact angle between mercury and surface of the solid. This contact angle exceeds 90^o for non-wetting liquids but is less than 90^o for wetting liquids (Figure 2.2).

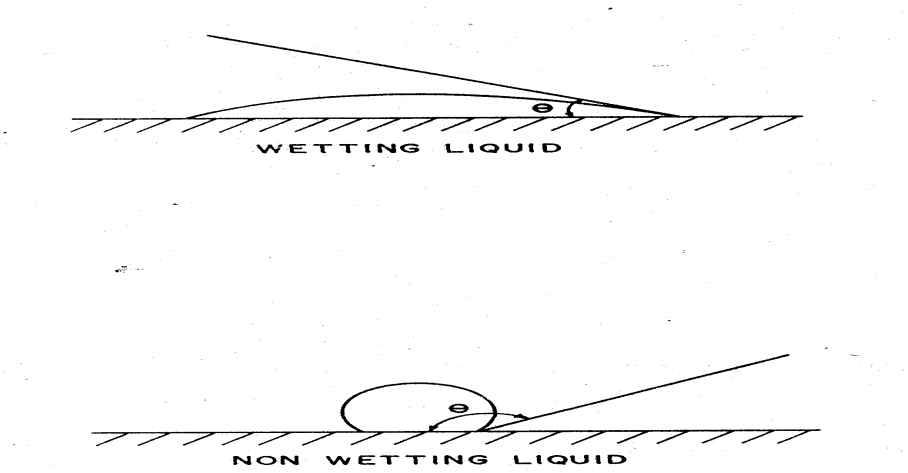

Figure 2.2: Contact angle of wetting and non-wetting liquid

In the experiment, gas was evacuated from the sample cell and mercury was transferred into the sample cell under vacuum. Pressure was applied to force mercury into the sample. During measurement, applied pressure p and intruded volume of mercury (V) were registered. As a result of analysis, an intrusion and extrusion curve was obtained.

2.1.2.2 Monosorb surface area analyser for surface area measurement

The surface area of the polymers were measured using the single point Brauner-Emmett-Teller method by measuring the adsorption of nitrogen at liquid nitrogen temperature and at the nitrogen concentration of 30 mol% (balance helium), using a monosorb surface area analyser (Quantachrome Corp., U.S.A.), based on dynamic adsorption/desorption technique. Before carrying out the surface area measurements, the instrument (analyser) was calibrated by injecting a known amount of air and the polymer (0.2-1.5 g) was pretreated *in situ* in the sample cell at 100 ^oC for 2 hour in the flow (30 cm^3 min^{-1}) of moisture free helium in order to remove the traces of moisture.

2.1.2.3 Malvern particle size analyser

Mastersizer 2000 Malvern instrument was used to obtain the particle size of synthesised polymeric beads. Mastersizer 2000 uses an integrated optical system to cover the full range from 0.02 to 2000 μm. The solid sample was dispersed in water with a stirring speed of 2350 rotations per minute. The ultrasonication was applied for 2 min at level 4.0 to make the sample well dispersed in water. The sample was added to water till the obscuration level was between 11-15%.

2.1.2.4 Scanning electron microscopy

Surface morphology of the poly(GMA-EGDM) beads were observed using scanning electron microscopy (SEM). Specimen preparation was as follows: dried poly(GMA-EGDM) beads were mounted on stubs and sputter-coated with gold. Micrographs were taken on a JEOL JSM-5200 SEM instrument.

2.1.2.5 Infra-red spectroscopy

A Shimadzu 8300-Fourier transform infrared spectrophotometer (FTIR) with a resolution of 1 cm^{-1} in the transmission mode was used to study the infra-red absorption. The sample poly(GMA-EGDM) (2 mg) was milled, mixed with potassium bromide (100 mg), and pressed into a solid disk of 1.2 cm diameter prior to the infra-red measurement.

2.1.2.6 Bead yield

The bead yield was calculated by the following expression:

$$\textbf{Bead yield} == (W_d/Wm) \times 100 \qquad \textbf{2.8}$$

Where W_d is mass of clean and dry polymer beads (g), and Wm is the mass of the monomers charged to the reactor (g).

2.1.2.7 Epoxy content

The epoxy content was determined by titration of the dried copolymer beads with a hydrochloric acid-dioxane solution at 80 ^{o}C for 6 h. Dioxane swells the beads and therefore

some of the epoxy group buried within the matrix will also react in addition to all present at the surface of the pores in the beads.

2.1.3 Results and Discussion

In suspension polymerisation, monomers, initiator and porogen are dispersed as liquid droplets, mostly in an aqueous phase, by stirring and polymerised at 70 ^{o}C for 3 hours. It was observed that in presence of porogen, the yield of the copolymer beads were in the range 90-99% but in absence of porogen, the yield of the beads were in the range 70-75%. This increase in rate of polymerisation in presence of porogen, points to influence of the porogen (cyclohexanol) on decomposition of the initiator. The porogen either chain transfers the primary radicals formed by the decomposition of AIBN and the radicals so formed are more reactive than the primary radicals or increases the rate of decomposition of AIBN, acting as a co-initiator, resulting in the greater yield. In presence of porogen, the copolymer beads obtained were opaque (white in colour) due to light scattering, an indication of porosity generated in the matrices by the porogen. Without porogen, copolymer beads obtained were transparent, indicating the absence of pores. Spherical nature and porous surface morphology of poly(GMA-EGDM) beads is seen in Figure 2.3.

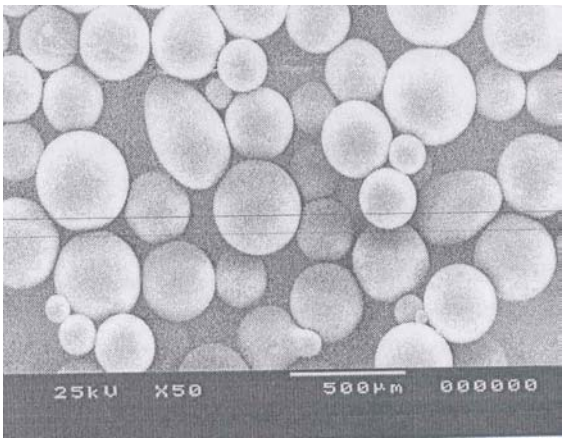

Figure 2.3: Surface morphology of poly(GMA-EGDM) beads, polymer GE10

The surface tension of GMA, EGDM and cyclohexanol in contact with water are approximately 6.9, 33.1 and 34.4 dyne/cm. Therefore GMA molecules will tend to migrate towards the surface of the droplets.

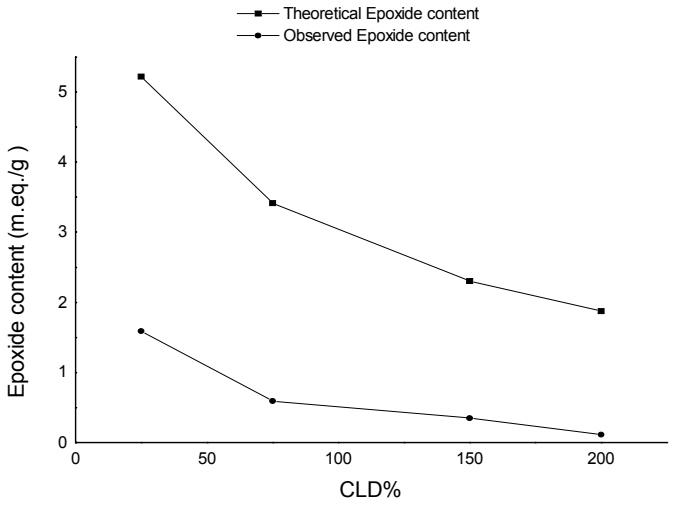

Figure 2.4: Theoretical and experimental epoxide content of poly(GMA-EGDM) beads prepared at a monomer:cyclohexanol ratio of 1:1.61

However, in actuality, the observed epoxy content is much lesser than the theoretical value because the concentration of epoxy groups present at or near the surface, which react with hydrochloric acid, is rather low. The polymerisation condition (pH=7) did not open up epoxy groups. It is clear that a majority of the epoxy groups are buried in the bulk of the matrix and are unable to react with hydrochloric acid under analytical conditions. Figure 2.4 represents the theoretical and analysed (surface) epoxy groups in poly(GMA-EGDM) relative to crosslink density at a monomer:porogen ratio of 1:1.61. This shows that surface tension issues are negated by other forces which direct most epoxy groups away from the surface.

The theoretical epoxy content decreases as GMA in the copolymer decreases, from 5.22 mmol/g at 25% CLD to 1.88 mmol/g at 200% CLD. The titratable epoxy group (Figure 2.4) decreases from 1.59 mmol/g at 25% CLD to 0.11 mmol/g at 200% CLD. Thus, while 30.4%

epoxy groups are near the surface at 25% CLD, this drops to 5.9% at 200% CLD. With increasing crosslink density, the polymer particle size increases, the swelling and diffusion rates of reagents decrease, resulting in the much lower reactable epoxy groups. The copolymers with lower CLD (25%) are suitable for chromatographic columns while those with highest CLD are suitable for enzyme immobilisation.

The typical IR spectra in Figure 2.5 shows peaks at 1722 and 1196 cm^{-1} due to C=O of ester group and C-O-C of epoxy group, respectively. It was also observed that the intensity of band at 1636 cm^{-1}, a characteristic band of C=C does not disappear but is significantly weakened. This means that epoxy group is present in the copolymer, and that beaded polymerisation traps some residual vinyl double bond within the matrix.

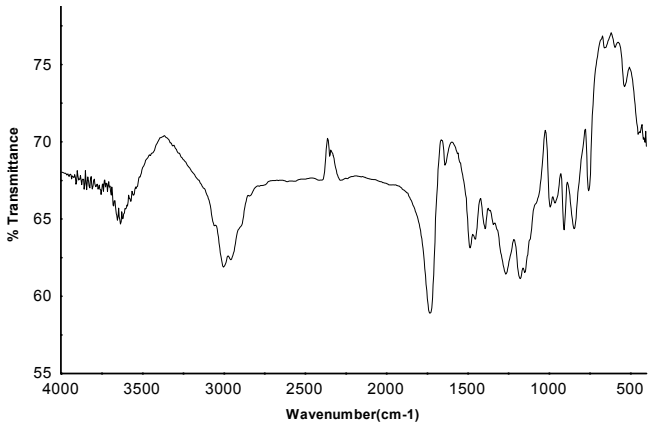

Figure 2.5: IR spectra of poly(GMA-EGDM) beads of 100% CLD at monomer:porogen ratio of 1:1.61 (GE10)

2.1.3.1 Effect of crosslink density of poly(GMA-EGDM) beads on particle size

The synthesis of poly(GMA-EGDM) beads by suspension polymerisation at 300 rpm resulted in spherical beads. Typical particle size distribution of poly(GMA-EGDM) beads as determined by particle size analyser presented in Figure 2.6 was in the 200 to 600 μm range. The particle size distribution shifts to the higher side with an increase in the relative mole ratio of the crosslinking comonomer, ethylene dimethacrylate (EGDM).

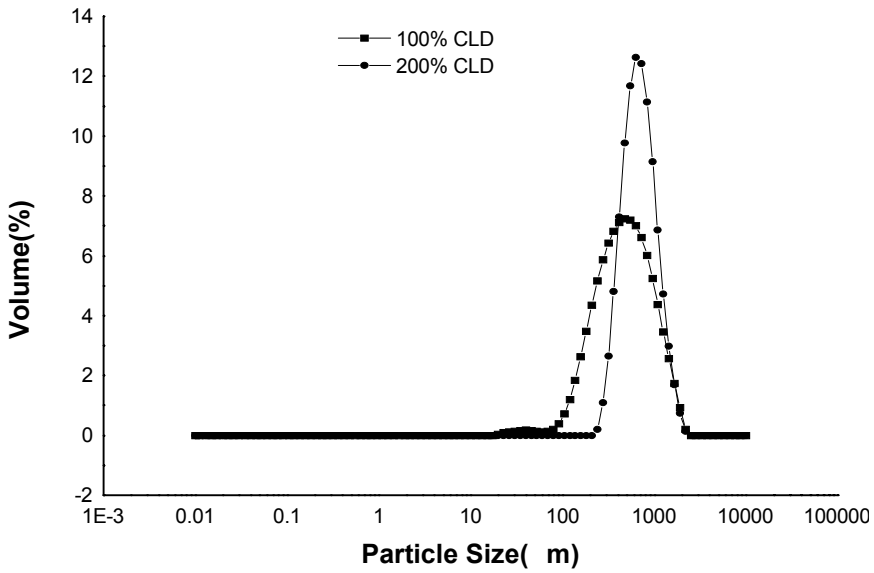

Figure 2.6: Particle size distribution in poly(GMA-EGDM) beads of 100% and 200% CLD at monomer:porogen ratio of 1:1.61 (GE10 and GE12)

With an increase of the relative mole ratio of EGDM (increasing crosslink density), the critical chain length prior to precipitation increases, resulting in larger particles. Simultaneously, the precipitation rate of copolymer chains increases with crosslink density, and particles phase separate rapidly after critical chain length, resulting in a narrower distribution. So, at lower crosslink densities particle size is smaller, with a broader distribution, compared to copolymers with higher crosslink densities.

The solubility parameter of GMA, EGDM and cyclohexanol are presented in Table 2.2 and variance in solubility parameter of copolymers with differing crosslink density are presented in Table 2.3.

Table 2.2: Solubility parameter δ of GMA, EGDM and cyclohexanol

Component	[a]δ $(cal/cm^3)^{0.5}$
GMA	8.05
EGDM	8.90
Cyclohexanol	11.40

[a]δ can be calculated using the formula d .∑G/M where G is the molar attraction constant, ∑G is the sum for all the atoms and groupings in the molecules, d is the density and M is the molecular weight.

Table 2.3: Variance in solubility parameter, $\delta^{/}$, of poly(GMA-EGDM) beads with crosslink density

CLD %	$\delta^{/}$ $(cal/cm^3)^{0.5}$
25	8.27
50	8.40
75	8.48
100	8.54
150	8.62
200	8.67

The solubility parameter of copolymer was estimated by formula $\delta^{/} = v_1\delta_1 + v_2\delta_2$, where δ_1 and δ_2 are solubility parameters of GMA and EGDM, v_1 and v_2 are the volume fraction of the monomer GMA and EGDM, respectively. An increase in the percent relative mole ratio of EGDM, crosslink density, increases the solubility parameter.

2.1.3.2 Porous properties of poly(GMA-EGDM) beads

Copolymers synthesised by suspension polymerisation have specific pore size, pore size distribution, pore volume and surface area. The macroporous morphology and formation of porous texture have been extensively investigated for beaded, crosslinked styrene-divinyl benzene resins. The internal pore structure can be controlled by several parameters such as amount of crosslinker, type and volume of porogen (also termed as diluent or pore generating solvent) added to the monomer phase. Porogen generates permanent pores in macroreticular polymers needed for chromatography. The larger pores, which are responsible for higher pore volume, are located in between agglomerates and arise when larger amount of crosslinker and porogen are used. Macroporous morphology in beaded polymers arises due to formation of gel microspheres, agglomeration of these and binding together of the agglomerates to form the beads. The appearance of gel microsphere is dependent on the crosslinker and to a smaller extent on the porogen.

During polymerisation, the polymer phase separates from the solution due to its limited solubility in the polymerisation mixture either due to build of molecular weight beyond that is soluble in the solvent (fractionation) or due to crosslinking. Phase separation generates microspheres. The task of this porogen is to create cavities in the polymeric structure by dissolution of the monomer, while acting as a precipitant towards the growing polymer.

Table 2.4: Pore volume of poly(GMA-EGDM): Effect of copolymer composition and monomer to porogen ratio

Monomer: porogen ratio	25% CLD	50% CLD	75% CLD	100% CLD	150% CLD	200% CLD
	PV (mL/g)	PV (mL/g)	PV (mL/g)	PV (mL/g)	PV (mL/g)	PV (mL/g)
1:0	0.0190 (GE 25)	0.0125 (GE 26)	0.0100 (GE 27)	0.0175 (GE 28)	0.0182 (GE 29)	0.0155 (GE 30)
1:0.405	0.0505 (GE 19)	0.0165 (GE 20)	0.0135 (GE 21)	0.0195 (GE 22)	0.0510 (GE 23)	0.0550 (GE 24)
1:0.81	0.0760 (GE 13)	0.0440 (GE 14)	0.0523 (GE 15)	0.0670 (GE 16)	0.0925 (GE 17)	0.1660 (GE 18)
1:1.61	0.1075 (GE 7)	0.5625 (GE 8)	0.5925 (GE 9)	0.7250 (GE 10)	0.7400 (GE 11)	0.8475 (GE 12)
1:2.43	0.4875 (GE 1)	0.7750 (GE 2)	0.7905 (GE 3)	0.8058 (GE 4)	0.8275 (GE 5)	0.8850 (GE 6)

Monomer codes are in parenthesis; CLD=crosslink density defined as [crosslinking monomer]:[functional monomer], which is [EGDM]:[GMA]; PV=pore volume, as estimated by mercury porosimetry.

Mercury porosimetry provides good estimates of pore size and pore size distribution in the range of importance, to the utilisation of network polymers as chromatographic materials. Copolymers prepared from monomer feed ratios low in the crosslinking comonomer (EGDM) and porogen (cyclohexanol) have low pore volume and surface area because a large number of nuclei are formed which tend to grow through each other. The data on pore volume and surface area of poly(GMA-EGDM) are presented in Tables 2.4 and 2.5. A glance at the data (Table 2.4) generated for the 30 poly(GMA-EGDM), with cyclohexanol as porogen, shows that pore

volume increases with increase in crosslink density (left to right along the table) and porogen volume (top to bottom), due to increase in the number of pores. Phase separation of copolymer from the porogen present in the monomer phase contributes to the generation of pores rather than phase separation from the monomers yet to be polymerised and linked to the growing copolymer chains. At lower crosslink density and lower volume of porogen, the inner pore volume is negligible because most porogen molecules are embedded in the network (gel) phase through out the copolymerisation. At higher crosslink density and higher volume of porogen, separation of the porogen out of the network (gel) phase results in high pore volume.

In the absence of porogen, the copolymers formed are nearly nonporous with pore volume accounting for just less than 2% on volume basis. At low crosslink density (25%), increased use of porogen increases the pore volume gradually till a monomer:porogen ratio of 1:1.61 and then increases it dramatically. At higher crosslink densities, this dramatic increase in pore volume occurs at relatively lower ratio of porogen. At the highest crosslink density studied here (200%) and at a monomer:porogen ratio of 1:2.43, the pore volume is nearly 97%, (0.885/0.909) assuming a specific gravity of 1.1 for these copolymers. Thus, copolymers with a wide variance in porosity can be synthesised by an interplay of crosslink density and porogen volume.

The data on surface area, presented in Table 2.5, were determined on copolymer particles whose diameter ranged between 150 and 450 nm. The surface area decreases initially from 5.91 to 3.12 m^2/g at a crosslink density of 25%. Similar depression is observed at all crosslink densities excepting at 150%, which is an artifact. The higher surface area of copolymers prepared without porogen originate from the unreacted monomers present when the copolymerisations were terminated after a reaction time of 3 h. It may be recalled that the

conversions (copolymer obtained at the end of 3 h) in the absence of porogen were in the range 70-75% while in the presence of porogen these were between 90-99%. On drying of the copolymers, the volume occupied by the unreacted 25-30% monomers present at the end of the reaction, in the reactions carried without porogen, generates these micropores which are observed in the surface area measurements but not in mercury porosimetry measurements, which shows up only meso and macropores.

Table 2.5: Surface area of poly(GMA-EGDM) beads: Effect of copolymer composition and monomer to porogen ratio

Monomer: porogen	25% CLD	50% CLD	75% CLD	100% CLD	150% CLD	200% CLD
	SA (m^2/g)	SA (m^2/g)	SA (m^2/g)	SA (m^2/g)	SA (m^2/g)	SA (m^2/g)
1:0	5.9126 (GE 25)	4.345 (GE 26)	5.1245 (GE 27)	5.8226 (GE28)	5.3450 (GE 29)	5.9340 (GE 30)
1:0.405	3.1234 (GE 19)	4.1236 (GE 20)	3.4846 (GE 21)	2.9525 (GE 22)	19.8794 (GE 23)	2.5782 (GE 24)
1:0.81	11.6203 (GE 13)	12.6507 (GE 14)	14.2125 (GE 15)	20.7479 (GE 16)	25.2349 (GE 17)	34.6708 (GE 18)
1:1.61	22.0768 (GE 7)	85.0631 (GE 8)	105.7812 (GE 9)	100.6911 (GE 10)	110.2543 (GE 11)	110.5787 (GE 12)
1:2.43	70.6419 (GE 1)	99.5830 (GE 2)	118.4266 (GE 3)	101.3400 (GE 4)	125.6712 (GE 5)	118.4266 (GE 6)

Monomer codes are in paranthesis; CLD=crosslink density defined as ([crosslinking monomer]/[functional monomer]) x 100, which is [EGDM]/[GMA]; SA=surface area, as estimated by BET.

Thus, surface area is very low at low crosslink density and lower amount of porogen, and it increases with crosslink density and volume of porogen, for copolymers of similar particle size distribution. In the absence of porogen, copolymer particles formed are devoid of inner pores. Surface area is entirely due to the surface of the particles. The copolymers prepared with monomer to porogen ratio 1:0.405 were found to be almost nonporous, because the polymerisation never reaches the critical point where the Flory-Huggins χ exceeds 0.5,

irrespective of a wide variance in monomer feed values and copolymer composition. At other monomer:porogen ratios, the surface area increases with relative increase in porogen volume. This increase is enhanced at higher crosslink densities. Since micropores contribute extensively to surface area and macropores contribute like-wise to pore volume it can be assumed with some certainty that both micro- and macropores increase with crosslink density and that there is a polydispersity in pore size, especially at higher crosslink densities. These pore geometries are ideally suited to anchor macromolecules such as enzymes.

The porogen present during the network (gel phase) formation may remain in the network phase through out the polymerisation, resulting in the formation of expanded network (swollen) or may separate out of the network phase, resulting in the formation of porous particle. The distribution of porogen between network and porogen phases (porogen in the pores) at the end of polymerisation determines the total porosity of the resulting polymer. While surface area increases with crosslink density, this trend is not very exact due to a concomitant decrease in the size of the microsphere.

Different applications of macroporous polymers require tailored pore size distributions. Macroporous polymer that have the same chemistry but different pore size distributions can be prepared by varying the mole ratio of monomers as well as relative volume of porogen. Tables 2.6-2.10 show pore size distribution profiles obtained for poly(GMA-EGDM) beads by mercury porosimetry.

In Table 2.6 poly(GMA-EGDM) of identical composition, 200% CLD, are compared for variances in pore structure induced by the change in the relative volume of the porogen, cyclohexanol. While cyclohexanol is not a part of the final polymer structure, it is seen to dramatically influence the formation and then distribution of the pores. When cyclohexanol is

excluded from the polymerisation recipe (GE 30), the polymer network formed is almost nonporous (pore volume=0.02 mL/g), with very low surface area (5.93 m^2/g). Table 2.6 shows that the internal pores present in this polymer network are in nano and micrometres. A comparison of Tables 2.4 and 2.5 reveals that porosity is induced within this polymer network only at a monomer:porogen ratio of 1:0.81 (GE18). The pore volume is low (0.17 mL/g) while the surface area is reasonable (34.67 m^2/g). Simultaneously, the pore size distribution broadens dramatically and pores are observed over the entire range observable by mercury porosimetry (<5 to >300 nm). The mean pore diameter lies between 5 and 15 nm. Further increase in the relative volume of the porogen (1:1.61) increases the pore volume (0.86 mL/g) and surface area (110.58 m^2/g) considerably. The study of pore size distribution indicates the presence of pores over the entire range of measurement. A further increase in the relative volume of the porogen (1:2.43) brings forth but a marginal increase in pore volume (0.89 mL/g) and surface area (118.43 m^2/g). The pore size distribution shrinks to a narrower range (,5 to 100 nm).

Table 2.6: **Effect of monomer:porogen (cyclohexanol) ratio on pore volume distribution in poly(GMA-EGDM) beads of constant composition (200%CLD)**

Code	M:P ratio (v/v)	distribution in pore radii (vol%), radius in nm								
		<5	5-10	10-15	15-20	20-30	30-50	50-100	100-300	>300
GE6	1:2.43	5.37	14.17	13.51	12.43	16.59	19.99	16.25	0.04	0.80
GE12	1:1.61	2.65	16.85	12.14	8.40	14.06	18.81	18.82	6.22	0.28
GE18	1:0.81	1.20	45.98	33.50	17.42	0.01	0.02	0.05	0.04	1.70
GE30	1:0.00	38.71	38.71	16.13	0.00	0.00	0.00	0.00	0.00	0.00

Code=polymer code number as in Tables 2.1, 2.4 and 2.5; M:P=monomer:porogen

In the absence of porogen, pore volume (Table 2.4) and surface area (Table 2.5) are negligible at all crosslink densities. Table 2.7 shows, rather interestingly, that at low crosslink density (polymer GE 25; 25% CLD) pores are distributed over the total range detectable by

mercury porosimetry. At higher CLD (100 and 200), this range shrinks. In all cases the median pores are in the 5-10 nm range.

Table 2.7: **Effect of crosslink density on pore volume distribution in poly(GMA-EGDM) beads generated without porogen**

Code	CLD	distribution in pore radii (vol%), radius in nm								
	%	<5	5-10	10-15	15-20	20-30	30-50	50-100	100-300	>300
GE25	25	26.32	50.97	9.67	0.01	0.01	0.01	0.27	0.88	11.84
GE28	100	22.86	62.43	14.70	0.00	0.00	0.00	0.00	0.00	0.00
GE30	200	38.71	38.71	16.13	0.00	0.00	0.00	0.00	0.00	0.00

CLD=crosslink density;

With the introduction of cyclohexanol (porogen) in the polymerisation droplets pores begin to form when the monomer:porogen ratio reaches 1:0.81 (Table 2.8). Simultaneously, the pore size distribution broadens while the median is still in the microporous (5-10 nm) range.

Table 2.8: **Effect of crosslink density on pore volume distribution in poly(GMA-EGDM) beads at constant monomer:porogen ratio of 1:0.81**

Code	CLD	distribution in pore radii (vol%), radius in nm								
	%	<5	5-10	10-15	15-20	20-30	30-50	50-100	100-300	>300
GE13	25	15.65	30.96	11.33	2.04	18.77	8.40	2.34	3.10	7.26
GE14	50	40.72	57.03	0.04	0.05	0.06	0.16	0.42	1.52	0.00
GE16	150	25.38	38.8	11.94	5.97	0.00	0.00	1.49	0.00	4.48
GE18	200	1.20	45.98	33.60	17.41	0.01	0.02	0.01	0.04	1.70

CLD=crosslink density;

With increase in the relative volume of the porogen (1:1.61), the pore volume and surface area are seen to increase significantly over the entire composition range. Table 2.9 shows that the pores are present over the entire range. The median pores are dependent on copolymer composition.

At still higher volume of porogen (1:2.43), increase in pore volume and surface area are marginal at all compositions. Table 2.10 shows that pores are present in the entire range. The

median pores are now in the mesoporous range (30-50 nm) and are independent of copolymer composition.

Table 2.9: **Effect of crosslink density on pore volume distribution in poly(GMA-EGDM) beads at constant monomer:porogen ratio of 1:1.61**

Code	CLD	distribution in pore radii (vol%), radius in nm								
	%	<5	5-10	10-15	15-20	20-30	30-50	50-100	100-300	>300
GE7	25	0.00	39.53	39.90	0.25	0.43	1.78	3.36	13.72	0.94
GE8	50	5.61	18.74	16.39	13.65	23.32	17.85	4.01	0.02	0.41
GE10	100	5.95	20.00	10.28	12.73	13.95	18.61	11.53	4.08	2.19
GE12	200	2.65	16.85	12.14	8.40	14.06	18.81	18.82	6.22	0.28

CLD=crosslink density;

Table 2.10: **Effect of crosslink density on pore volume distribution in poly(GMA-EGDM) beads at constant monomer:porogen ratio of 1:2.43**

Code	CLD	distribution in pore radii (vol%), radius in nm								
	%	<5	5-10	10-15	15-20	20-30	30-50	50-100	100-300	>300
GE1	25	11.28	14.87	6.84	12.14	19.49	19.66	5.98	5.64	4.10
GE2	50	6.13	14.52	12.58	11.92	14.05	17.24	11.95	4.80	4.55
GE5	150	6.64	16.72	12.39	9.90	14.85	19.58	14.74	2.55	0.28
GE6	200	5.37	14.17	13.51	12.43	16.59	19.99	16.25	0.04	0.80

CLD=crosslink density;

2.2 Poly(glycidyl methacrylate-co-divinyl benzene)

Syntheses of poly(glycidyl methacrylate-co-divinyl benzene) **[**poly(GMA-DVB)] of differing crosslink densities (CLD) were similar to poly(GMA-EGDM), presented in Section 2.1.1. The objective was to study the effect of crosslinking comonomer type on pore structure in polymer net-works. The composition of 25 poly(GMA-DVB) synthesised are presented in Table 2.11. Six sets were synthesised using cyclohexanol as porogen. The monomer:porogen ratio was varied within each set as 1:2.43, 1:1.61 and 1:0.81. The crosslink density was studied between 25% to 200%, as earlier. Hexanol was investigated as porogen at a monomer:porogen

ratio of 1:1.61 over the entire composition range while octanol was evaluated at one composition (25%) a monomer:porogen ratio of 1:1.61.

Table 2.11: Composition of glycidyl methacrylate (GMA) and divinyl benzene (DVB) copolymers synthesised using cyclohexanol, hexanol and octanol as porogens

Exp. No	GMA (mol)	DVB (mol)	CLD %	Monomer:porogen (v/v)
GV1, GV7, GV13	0.0418	0.0176	25	1:2.43, 1:1.61, 1:0.81
GV2, GV8, GV14	0.0323	0.0267	50	1:2.43, 1:1.61, 1:0.81
GV3, GV9, GV15	0.0264	0.0323	75	1:2.43, 1:1.61, 1:0.81
GV4, GV10, GV16	0.0220	0.0365	100	1:2.43, 1:1.61, 1:0.81
GV5, GV11, GV17	0.0169	0.0414	150	1:2.43, 1:1.61, 1:0.81
GV6, GV12, GV18	0.0132	0.0449	200	1:2.43, 1:1.61, 1:0.81
GV(h)1	0.0418	0.0176	25	1:1.61
GV(h)2	0.0323	0.0267	50	1:1.61
GV(h)3	0.0264	0.0323	75	1:1.61
GV(h)4	0.0220	0.0365	100	1:1.61
GV(h)5	0.0169	0.0414	150	1:1.61
GV(h)6	0.0132	0.0449	200	1:1.61
GV(o)1	0.0418	0.0176	25	1:1.61

The series GV (GV1-GV18) were synthesised using cyclohexanol as porogen; GV(h)1-GV(h)6 were synthesised using hexanol as porogen and GV(o)1 was synthesised using octanol as porogen, respectively. Crosslink density (CLD) is defined as the mole percent of crosslinking monomer relative to the moles of reactive functional comonomer. AIBN: 0.2 g; Water: 100 mL; PVP: 1 g.

The pore volume, surface area, particle size, surface morphology, infra-red spectra, bead yield and epoxy content were determined as presented in Sections 2.1.2.1 to 2.1.2.7.

2.2.1 Results and Discussion on poly(GMA-DVB) series

The characterisation of poly(GMA-EGDM) series showed that pores and inner surface area are developed only when the monomer:porogen ratio reaches 1:0.81. Hence, poly(GMA-DVB) system was studied only at monomer:porogen ratios of 1:0.81, 1:1.61 and 1:2.43. DVB is extremely hydrophobic and hence polymers in the GV series are suitable for binding hydrophobic organic molecules. The well formed pore structure by cyclohexanol were compared with those formed by equal volumes of its linear homologue, hexanol. Theoretically,

it was predicted that octanol should rapidly phase separate out of the polymerisation phase and hence the effect of this was evaluated at one composition (polymer GV(o)1).

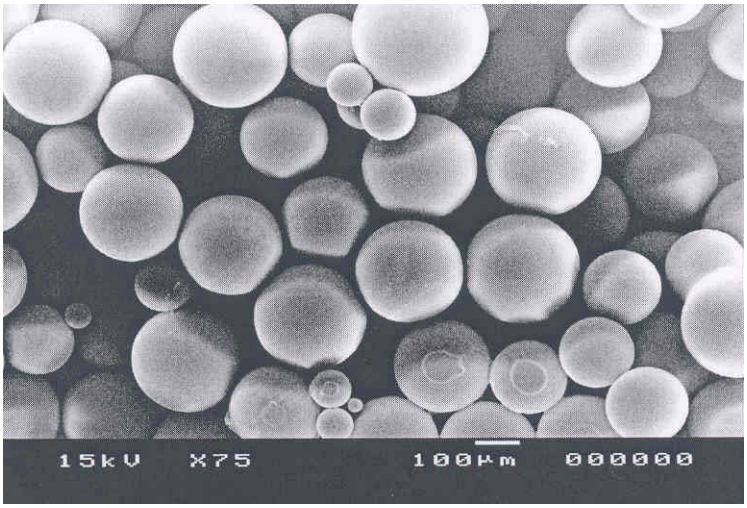

Figure 2.7: Surface morphology of poly(GMA-DVB) at 100% CLD; monomer to cyclohexanol ratio of 1:1.61 (v/v)

The yields of poly(glycidyl methacrylate-co-divinyl benzene) beads were in the range 90-99%. All dried copolymer beads were opaque, white, indicating formation of porous matrices, with all three porogens used. The SEM photograph in Figure 2.7 indicates formation of spherical beads with particle size in the range 10-600 nm, having irregular surface morphology, due to the presence of pores.

The surface state of the prepared copolymer beads is controlled by the surface tension between the dispersed phase and the continuous phase. The interfacial tension of GMA, DVB and cyclohexanol in contact with water are approximately 6.9, 16.5 and 34.4 dyne/cm. GMA, with surface tension much lower than DVB and cyclohexanol, should be enriched on the interface between the continuous phase consisting of an aqueous solution of PVP and the dispersed phase consisting of the porogen and the monomers with the polar epoxy group facing

the aqueous continuum. This should be greater than that in poly(GMA-EGDM), since the interfacial tension of EGDM, as seen in Table 2.2, is much lower (8.9) than DVB (16.5).

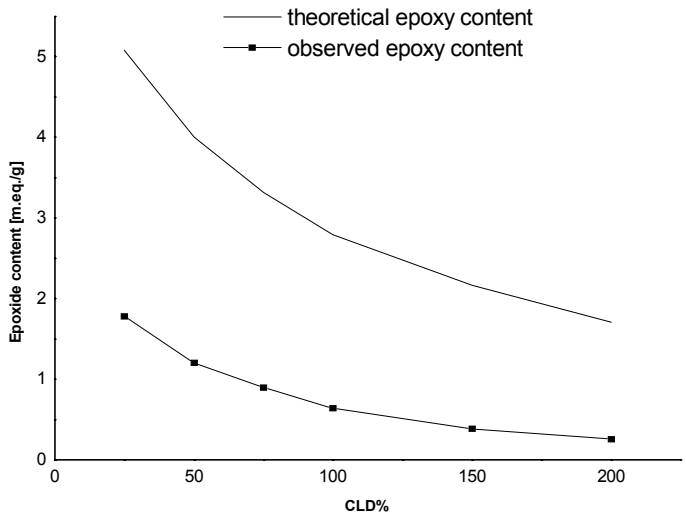

Figure 2.8: Surface epoxide group in poly(GMA-DVB) beads prepared with monomer:cyclohexanol v/v ratio of 1:1.61

The theoretical epoxy content in poly(GMA-DVB) studied here varies from 5.08 to 1.71 mmol/g (from 25 to 200% CLD). The experimentally observed epoxy content by titration was in the range 1.78 to 0.26 mmol/g (from 25 to 200% CLD). Thus, only a fraction the epoxy group in poly(GMA-DVB) beads react with hydrochloric acid, just as observed with poly(GMA-EGDM) series. A major fraction of the epoxy group in the beads are buried and are unable to react under analytical condition. However, in comparison to poly(GMA-EGDM) series, where 30.4 to 5.9% of epoxy groups were near the surface (from 25 to 200% CLD), in this series 35.0% to 14.9% were near the surface. Figure 2.8 shows the effect of crosslink density on epoxide content. Thus, substituting EGDM with a more hydrophobic comonomer (DVB) marginally reorients the epoxy group towards the surface of the pores. The other trends were along lines observed in poly(GMA-EGDM) series.

The solubility parameter of monomer, comonomer and porogen are presented in Table 2.12 and that of copolymers of differing crosslink density are presented in Table 2.13.

Table 2.12: Solubility parameter, δ, of monomers and porogens

Component	[a]δ $(cal/cm^3)^{0.5}$
GMA	8.05
DVB	9.30
Cyclohexanol	11.40
Hexanol	10.76
Octanol	10.34

[a]δ can be calculated using the formula d .∑G/M where G is the molar attraction constant, ∑G is the sum for all the atoms and groupings in the molecules, d is the density and M is the molecular weight.

Table 2.13: Variance in solubility parameter, δ′, of poly(GMA-DVB) with crosslink density

CLD%	δ′ $(cal/cm^3)^{0.5}$
25	8.43
50	8.63
75	8.75
100	8.84
150	8.95
200	9.02

The solubility parameter of poly(GMA-DVB) increases with CLD, as seen in poly(GMA-EGDM) series, indicating that phase separation will occur more gradually with increasing CLD, resulting in larger beads at higher crosslink density.

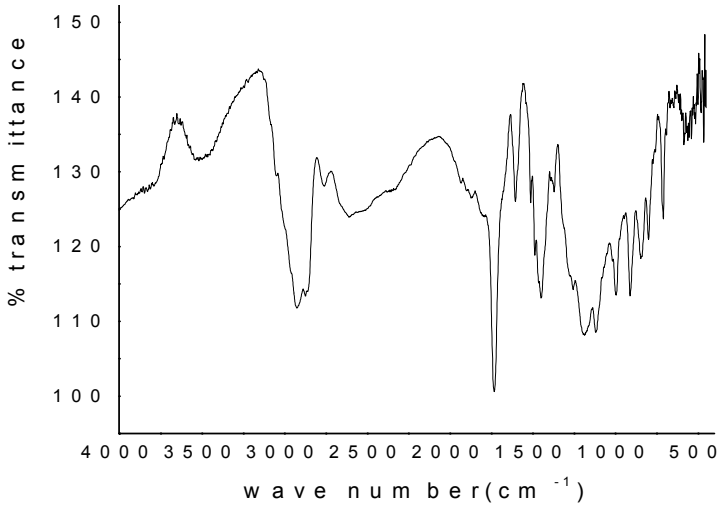

Figure 2.9: IR spectra of poly(GMA-DVB) of 100% CLD synthesised at monomer:cyclohexanol ratio of 1:1.61

IR spectra of poly(GMA-DVB) in Figure 2.9 shows peaks at 1733, 1123 cm^{-1} due to stretching vibrations of C=O of ester group and C-O-C of epoxy group, respectively. It was also observed that the band at 1636 cm^{-1}, a characteristic band of C=C stretching, disappears. This indicates that epoxy group is not consumed and that polymerisation proceeds with complete consumption of the vinyl double bond, unlike the poly(GMA-EGDM) series in which some vinyl groups are trapped in the matrix.

2.2.1.1 Porous properties of poly(GMA-DVB) beads

The pore volume and surface area of poly(GMA-DVB) beads synthesised in the presence of different porogens (cyclohexanol, hexanol and octanol), are summarised in Tables 2.14 and 2.15. The dielectric constant of cyclohexanol (ε=17.7) is higher than hexanol (ε=13.3) and octanol (ε=10.3). Thus, cyclohexanol is the best while the octanol is the worst solvent, of the three porogens. Copolymers prepared using hexanol show higher pore volume (compared to cyclohexanol) at the same monomer to porogen ratio (v/v). The solvating power of the porogen increases with polarity, resulting in a less pronounced phase separation, thereby decreasing the porosity. Copolymers prepared with lower amount of crosslinker (DVB) and porogen (cyclohexanol) are less porous, with low pore volume and surface area, because a large number of nuclei are formed which tend to grow through each other, just as observed in poly(GMA-EGDM) series. As the crosslink density increases, the pore volume increases rapidly, indicating separation of cyclohexanol out of the network (gel) phase. However, with hexanol the phase separation out of the network (gel) phase is very rapid. Pore volumes generated by cyclohexanol (Table 2.14) are marginally better compared to those for poly(GMA-EGDM) in Table 2.4 at a monomer:porogen ratio of 1:0.81. At 1:1.61 and 1:2.43 these are much better

indicating extensive phase separation here vis-à-vis poly(GMA-EGDM). This pore volume is much higher with hexanol and octanol, as predicted by solubility parameter (Table 2.12).

Table 2.14: Pore volume of poly(GMA-DVB) synthesised using cyclohexanol, hexanol and octanol: Effect of copolymer composition and monomer to porogen ratio

Monomer: porogen ratio	25% CLD	50% CLD	75% CLD	100% CLD	150% CLD	200% CLD
	PV (mL/g)	PV (mL/g)	PV (mL/g)	PV (mL/g)	PV (mL/g)	PV (mL/g)
1:0.81	0.15 (GV 13)	0.16 (GV 14)	0.19 (GV 15)	0.21 (GV 16)	0.40 (GV 17)	0.20 (GV 18)
1:1.61	0.75 (GV 7)	0.93 (GV 8)	0.97 (GV 9)	1.04 (GV 10)	1.13 (GV 11)	1.16 (GV 12)
1:2.43	0.33 (GV 1)	1.00 (GV 2)	1.15 (GV 3)	1.32 (GV 4)	1.80 (GV 5)	1.81 (GV 6)
1:1.61[a]	1.47 (GV(h)1)	1.53 (GV(h)2)	1.70 (GV(h)3)	1.88 (GV(h)4)	1.84 (GV(h)5)	1.89 (GV(h)6)
1:1.61[b]	1.36 (GV(o)1)	NS	NS	NS	NS	NS

[a] =using hexanol as porogen; [b]=using octanol as porogen; NS=not synthesised; CLD=crosslink density defined as ([crosslinking monomer]/[functional monomer])100; which is [DVB]:[GMA]; PV=pore volume, as estimated by mercury porosimetry.

Table 2.15: Surface area of poly(GMA-DVB) synthesised using cyclohexanol, hexanol and octanol: Effect of copolymer composition and monomer to porogen ratio

Monomer: porogen ratio	25% CLD	50% CLD	75% CLD	100% CLD	150% CLD	200% CLD
	SA (m^2/g)	SA (m^2/g)	SA (m^2/g)	SA (m^2/g)	SA (m^2/g)	SA (m^2/g)
1:0.81	39.16 (GV 13)	42.84 (GV 14)	42.67 (GV 15)	55.43 (GV 16)	82.98 (GV 17)	48.95 (GV 18)
1:1.61	98.10 (GV 7)	115.44 (GV 8)	113.20 (GV 9)	122.14 (GV 10)	125.43 (GV 11)	124.95 (GV 12)
1:2.43	68.20 (GV 1)	122.00 (GV 2)	117.31 (GV 3)	131.20 (GV 4)	139.21 (GV 5)	145.10 (GV 6)
1:1.61[a]	24.50 (GV(h)1)	35.40 (GV(h)2)	46.10 (GV(h)3)	48.00 (GV(h)4)	50.80 (GV(h)5)	43.90 (GV(h)6)
1:1.61[b]	11.70 (GV(o)1)	NS	NS	NS	NS	NS

[a] =using hexanol as porogen; [b]=using octanol as porogen; NS=not synthesised; CLD=crosslink density defined as ([crosslinking monomer]/[functional monomer])100; which is [DVB]/[GMA]; SA=surface area, as estimated by BET.

Surface area data presented in Table 2.15 indicates that surface area increases with crosslink density and relative porogen volume. The data for 25% CLD polymer prepared with monomer:cyclohexanol ratio of 1:1.61 is an artifact. The surface area of copolymers formed in presence of cyclohexanol were greater than those synthesised in presence of hexanol. The increase in surface area with crosslink density is due to a decrease in the size of the microsphere. This trend relative to both CLD and porogen volume is less dramatic than that for poly(GMA-EGDM) presented in Table 2.5. Comparing the two series, the surface area for poly(GMA-DVB) is consistently higher than that for equivalent poly(GMA-EGDM). Thus, micropores are generated at very low CLD and pore size distribution is broader in poly(GMA-DVB). Also, the poly(GMA-DVB) beads are extremely porous. The poly(GMA-DVB) synthesised using hexanol and octanol have lower surface area and higher pore volume, indicating that the pores are more uniformly macroporous than those prepared using cyclohexanol. These polymers are ideally suited to anchoring large molecules rather than for chromatographic separations while those prepared using cyclohexanol can be evaluated for both chromatographic and enzyme immobilization studies.

The variance in pore sizes with changes in copolymer composition at a constant monomer:porogen ratio are presented in Tables 2.16 to 2.18. Table 2.16 shows data obtained at lowest monomer:porogen (cyclohexanol) ratio of 1:0.81. The pore volume is in the range 0.15-0.40 mL/g (Table 2.14) and surface area is in the range 39.16-82.98 m^2/g (Table 2.15). These are generated by polydisperse pores in the range <5 to >300 nm. At intermediate (1:1.61) monomer:porogen ratio the pore volume (0.75-1.16 mL/g) and surface area (98.10-125.43 m^2/g) are considerably increased and the median pore radii is shifted to the higher side (30-100 nm). At the highest monomer:porogen ratio (1:2.43), the pore volume (0.33-1.80 mL/g) and

surface area (68.20-145.10 m^2/g) are further increased, unlike in the poly(GMA-EGDM) series. Also, the median pore shifts to lower value at lowest (25%) CLD while this shifts to higher value (100-300 nm) at the highest (200%) CLD.

Table 2.16: **Effect of crosslink density on pore volume distribution in poly(GMA-DVB) beads at constant monomer:porogen ratio of 1:0.81**

Code	CLD	distribution in pore radii (vol%), radius in nm								
	%	<5	5-10	10-15	15-20	20-30	30-50	50-100	100-300	>300
GV14	50	23.63	46.64	10.23	3.19	3.50	4.16	4.14	3.19	0.32
GV15	75	13.86	32.73	18.27	11.45	9.24	6.62	3.82	1.61	0.60
GV17	150	12.28	31.14	19.62	12.4	9.88	3.79	0.00	5.95	1.65

Porogen=cyclohexanol; CLD=crosslink density;

Table 2.17: **Effect of crosslink density on pore volume distribution in poly(GMA-DVB) beads at constant monomer:porogen ratio of 1:1.61**

Code	CLD	distribution in pore radii (vol%), radius in nm								
	%	<5	5-10	10-15	15-20	20-30	30-50	50-100	100-300	>300
GV7	25	5.21	14.87	12.32	10.76	18.22	21.37	10.63	4.16	1.06
GV8	50	5.27	14.05	11.28	9.79	11.82	19.69	17.51	6.12	1.97
GV10	100	4.86	15.11	9.72	8.90	10.69	17.47	20.45	6.83	0.00

Porogen=cyclohexanol; CLD=crosslink density;

Table 2.18: **Effect of crosslink density on pore volume distribution in poly(GMA-DVB) beads at constant monomer:porogen ratio of 1:2.43**

Code	CLD	distribution in pore radii (vol%), radius in nm								
	%	<5	5-10	10-15	15-20	20-30	30-50	50-100	100-300	>300
GV1	25	9.99	35.27	16.69	11.38	9.35	5.56	2.91	2.03	1.01
GV6	200	3.25	9.22	6.26	5.42	7.85	10.22	18.63	25.05	7.29

Porogen=cyclohexanol; CLD=crosslink density;

The change in pore radii distribution and median pore radii for a poly(GMA-DVB) with macroreticular pore structure (150% CLD) is shown in Table 2.19. The median pore radii increases with the porogen volume in poly(GMA-DVB) series.

Table 2.19: **Effect of monomer:porogen (cyclohexanol) ratio on pore volume distribution in poly(GMA-DVB) beads of constant composition (150%CLD)**

Code	M:P ratio (v/v)	distribution in pore radii (vol%), radius in nm								
		<5	5-10	10-15	15-20	20-30	30-50	50-100	100-300	>300
GV5	1:2.43	3.22	9.33	6.40	4.26	7.68	11.28	19.41	26.79	4.84
GV11	1:1.61	4.78	12.65	9.91	8.27	11.6	16.98	19.82	11.16	2.24
GV17	1:0.81	12.28	31.14	19.62	12.4	9.88	3.79	0.00	5.95	1.65

Code=polymer number; M:P=monomer:porogen

Pore volume and surface area are also dictated by the subtle changes in the structural features of the porogen molecule. A shift from cyclohexanol to hexanol dramatically increases the pore volume (Table 2.14) while the surface area is dramatically reduced (Table 2.15). This indicates a large shift in the median pore radii from lower to higher values, as confirmed by a look at Table 2.20. The median pore radii shifts from 30-50 nm for cyclohexanol to 100-300 nm for hexanol to >300 nm for octanol. This means that immobilization carrier (support) for enzymes of widely varying molecular sizes can be prepared by changing just the porogen type, while keeping copolymer composition and porogen volumes constant. The increased phase separation trend octanol > hexanol > cyclohexanol generates fewer pores (lower surface area) of very large size (high pore volume).

Table 2.20: **Effect of porogen type on pore volume distribution in poly(GMA-DVB) (25% CLD) at constant monomer:porogen ratio of 1:1.61**

Code	Por	distribution in pore radii (vol%), radius in nm								
		<5	5-10	10-15	15-20	20-30	30-50	50-100	100-300	>300
GV7	CHOL	5.21	14.87	12.32	10.76	18.22	21.37	10.63	4.16	1.06
GV(h)1	HOL	0.48	1.05	0.75	0.71	2.89	6.18	34.98	42.19	6.39
GV(O)1	OOL	2.59	5.64	0.23	0.89	0.52	2.40	4.65	36.87	46.19

Por=porogen; CHOL=cyclohexanol; HOL=hexanol; OOL=octanol;

The shift in pore size distribution with composition at constant monomer:porogen (hexanol) ratio (1:1.61) is clearly depicted in Figure 2.10.

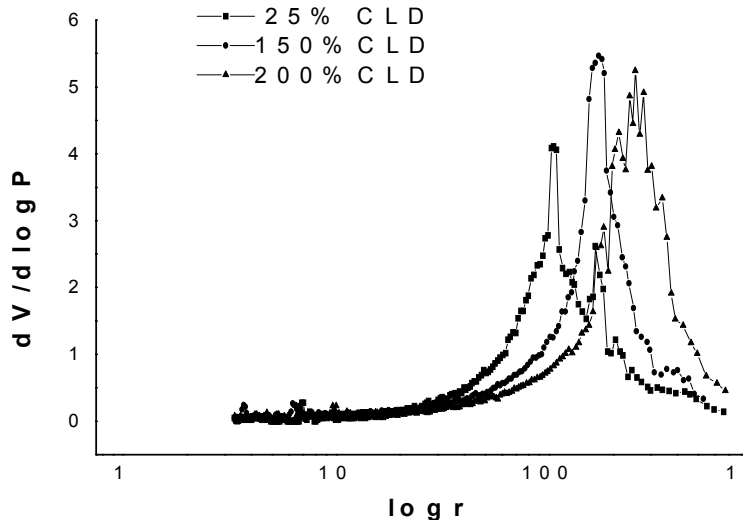

Figure 2.10: Differential pore size distribution in poly(GMA-DVB) with change in CLD at constant monomer:hexanol ratio of 1:1.61 v/v

This trend is presented in tabular form in Table 2.21.

Table 2.21: **Effect of crosslink density on pore volume distribution in poly(GMA- DVB) beads at constant monomer:porogen ratio of 1:1.61. Hexanol used as porogen**

Code	CLD	distribution in pore radii (vol%), radius in nm								
	%	<5	5-10	10-15	15-20	20-30	30-50	50-100	100-300	>300
GV(h)1	25	0.48	1.05	0.75	0.71	2.89	6.18	34.98	42.19	6.39
GV(h)5	150	0.71	2.01	1.19	1.13	1.89	4.31	14.72	64.71	9.30
GV(h)6	200	0.61	1.31	0.98	0.90	1.49	3.17	9.11	56.01	26.38

Porogen=hexanol; CLD=crosslink density;

2.3 Poly(allyl glycidyl ether-co-ethylene dimethacrylate) [poly(AGE-EGDM)]

2.3.1 Suspension polymerisation of AGE with EGDM

The aim was to investigate the effect of similar functional monomer in net-worked polymers on pore structure. GMA was replaced with AGE. The suspension copolymerisation procedure used to prepare poly(AGE-EGDM) is as presented in Section 2.1.1. The composition of synthesised AGE-EGDM co-polymers are presented in Table 2.22.

Table 2.22: Composition of Allyl glycidyl ether (AGE) and ethylene dimethacrylate (EGDM) copolymers synthesised using cyclohexanol as porogen at a monomer:porogen ratio of 1:1.61

Exp. No	AGE (mol)	EGDM (mol)	CLD %
AG1	0.0497	0.0122	25
AG2	0.0388	0.0191	50
AG3	0.0312	0.0238	75
AG4	0.0269	0.0265	100
AG5	0.0202	0.0307	150
AG6	0.0168	0.0329	200

Crosslink density (CLD) is defined as the mole percent of crosslinking monomer relative to the moles of reactive functional comonomer ([EGDM] / [AGE]) x 100. AIBN: 0.2 g; Water: 100 mL; PVP: 1 g.

2.3.2 Characterisation of poly(AGE-EGDM)

The porosity, surface area, particle size, surface morphology, infra-red spectra, bead yield and epoxy content were determined using procedures presented in Sections 2.1.2.1 to 2.1.2.7.

2.3.3 Results and Discussion on poly(AGE-EGDM) series

The data for poly(GMA-EGDM) and poly(GMA-DVB) series established that cyclohexanol provided the best option as porogen. It generated a wide distribution in pore size and optimal pore geometries were obtained at a combined monomers:porogen ratio of 1:1.61. Thus, in the poly(AGE-EGDM) series six polymers were synthesised at a constant monomer:porogen ratio of 1:1.61 by varying the CLD between 25 and 200%. Polymers with allyl units (resulting in ethene backbones, with methoxy branch point) are known to be more flexible than equivalent polymers with methacrylic units (ethene backbones with a methyl and a carboxylic branch points). Thus, it was estimated that poly(AGE-EGDM) beads will be more swellable than equivalent poly(GMA-EGDM) beads.

Poly(AGE-EGDM) beads, produced at the uniform stirring rate of 300 rpm, were in the range 200 to 600 μm. The copolymer yield was in the range 90-97%. It was observed in this series as well that the particle size increases with the crosslink density. As discussed earlier, droplet size depends on the interfacial tension. Additional factors which also govern this are density difference between the discontinuous and continuous phases and stirring rate. Greater incorporation of divinyl monomer, EGDM, will generate more crosslinked structures. This crosslinking insolubilises the growing polymer chains which thereby precipitate from the droplet solution. This precipitation rate should increase with the relative mole ratio of EGDM in the monomer feed, hence crosslink density. Rapid precipitation would lead to smaller particles. The experimental observation indicated that the governing force was the solubility parameter. The dried copolymer beads are white and not

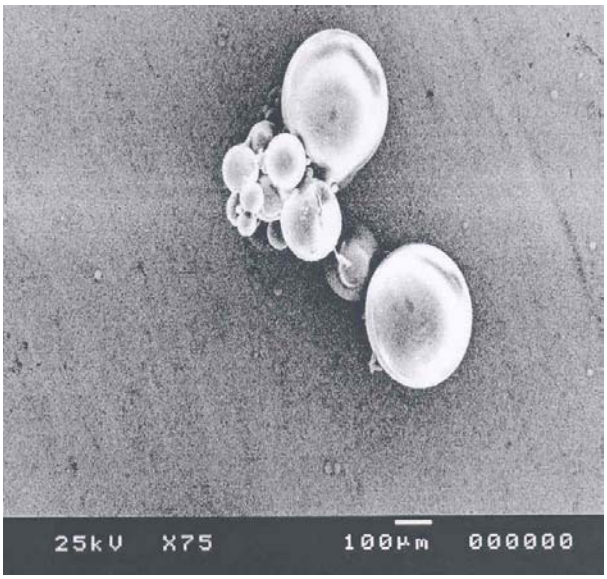

Figure 2.11: Particles of poly(AGE-EGDM), formed at 100% CLD (AG 4)

transparent indicating pore formation due to the porogen (cyclohexanol). Figure 2.11 represents the surface morphology of poly(AGE-EGDM) beads. While beads were spherical, there was considerable aggregation indicating that the protective colloid, PVP, is unable to

maintain the monomer droplets well separated as in poly(GMA-EGDM) and poly(GMA-DVB) series.

The solubility parameter of monomer, comonomer and porogen are presented in Table 2.23 and that of copolymers of differing crosslink density are presented in Table 2.24. With the increase of the relative mole ratio of EGDM (crosslink density), the solubility parameter of copolymers increase.

Table 2.23: Solubility parameter δ, of AGE, EGDM and porogen

Component	[a]δ $(cal/cm^3)^{0.5}$
AGE	7.52
EGDM	8.90
Cyclohexanol	11.40

[a]δ can be calculated using the formula d .∑G/M where G is the molar attraction constant, ∑G is the sum for all the atoms and groupings in the molecules, d is the density and M is the molecular weight.

Table 2.24: Variance in solubility parameter, δ′, of poly(AGE-EGDM) beads with crosslink density

CLD%	δ′ $(cal/cm^3)^{0.5}$
25	7.91
50	8.12
75	8.28
100	8.36
150	8.50
200	8.56

Only a fraction of epoxy groups present in (AGE-EGDM) reacted with hydrochloric acid. Since epoxy groups in allyl glycidyl ether do not react under the conditions used in the suspension polymerisation, it can be concluded that a majority of the epoxy group in the copolymer beads are buried in the bulk and are unable to react even over 6 hours at 80 ^oC, when tested in a solvent (dioxane) that swells the polymer beads. The data on variance of theoretical and analysed epoxide content with CLD is represented in Figure 2.12. A comparison

with poly(GMA-EGDM) shows that the surface epoxy group concentration is higher in poly(AGE-EGDM). In comparison to poly(GMA-EGDM) series, where 30.4 to 5.9% of epoxy groups were near the surface (from 25 to 200% CLD), in this series 32.5% to 8.9% were near the surface, indicating that poly(AGE-EGDM) are better suited to chromatographic applications.

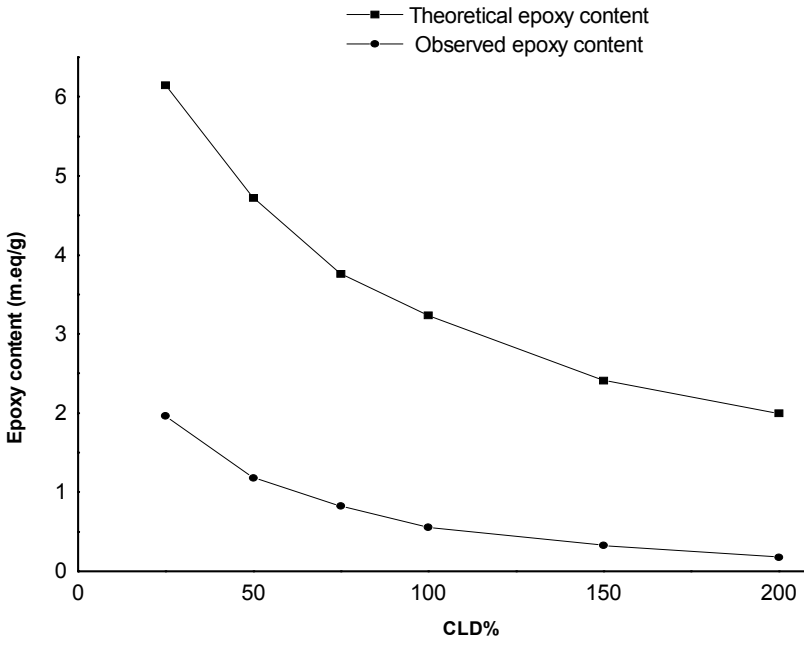

Figure 2.12: Surface epoxide group in poly(AGE-EGDM) beads prepared with monomer:cyclohexanol v/v ratio at 1:1.61

The infra-red spectra of poly(AGE-EGDM) series mirror that of the poly(GMA-DVB) series rather than the poly(GMA-EGDM) series. The typical IR spectra in Figure 2.13 shows peaks at 1731 and 1150 cm^{-1} due to stretching vibrations of C=O of ester group and C-O-C of epoxy group, respectively. It was also observed that the intensity of band at 1636 cm^{-1}, a characteristic band of C=C stretching disappears. This indicates that epoxy group are intact in the copolymer, and copolymerisation proceeds with the complete consumption of vinyl double bond.

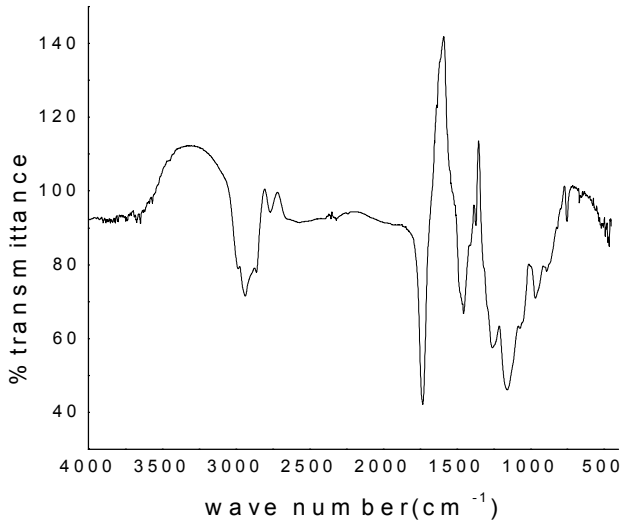

Figure 2.13: IR spectra of poly(AGE-EGDM) of 100% CLD

2.3.3.1 Pore properties of poly(AGE-EGDM) series

The data of pore volume and surface area are summarised in Table 2.25. Poly(AGE-EGDM) and poly(GMA-EGDM), with pendent epoxy groups, were synthesised with similar applications in mind. Hence, the data obtained for poly(AGE-EGDM) is compared with poly(GMA-EGDM).

Table 2.25: Pore volume and surface area of poly(AGE-EGDM) and poly(GMA-EGDM) synthesised using cyclohexanol at monomer:porogen ratio of 1:1.61

CLD %	Poly(AGE-EGDM)		Poly(GMA-EGDM)	
	Pore volume (mL/g)	Surface area (m^2/g)	Pore volume (mL/g)	Surface area (m^2/g)
25	0.83 (AG 1)	98.92 (AG 1)	0.11 (GE 7)	22.08 (GE 7)
50	1.68 (AG 2)	87.99 (AG 2)	0.56 (GE 8)	85.06 (GE 8)
75	1.28 (AG 3)	122.45 (AG 3)	0.59 (GE 9)	105.78 (GE 9)
100	1.69 (AG 4)	127.72 (AG 4)	0.73 (GE 10)	100.69 (GE 10)
150	1.56 (AG 5)	128.98 (AG 5)	0.74 (GE 11)	110.25 (GE 11)
200	1.33 (AG 6)	92.03 (AG 6)	0.85 (GE 11)	110.58 (GE 11)

In poly(AGE-EGDM) series the volume of pores, as measured by mercury porosimetry (macropores), goes through a maxima between 50 and 100% CLD (data for 75% CLD is probably an artifact). The data for surface area is inconclusive but points to a maxima between 75 and 150% CLD. It must be added that the pore volume and surface area were collected independently using two different instruments for the polymer samples generated in a single batch. A comparison with poly(GMA-EGDM) reveals that these two series differ considerably, within limits of accuracy. Pore volume is considerably higher and surface area, due to micropores, is generated at very low crosslink density in the poly(AGE-EGDM) series. This indicates that cyclohexanol phase separates rapidly from the polymerisation media in poly(AGE-EGDM) while this is more gradual in poly(GMA-EGDM). This increases the surface concentration of epoxy groups, as seen in the titration with hydrochloric acid. The pores in both series of matrices are polydisperse, ranging from micro (large surface area) to macropores (large pore volume).

From application perspectives, other issues like swellability, attrition, and elasticity are issues of importance in usage under stirred tank configuration while compressability, pressure drop are issues of concern in a column mode operation. These were not measured in the present study. In general it can be stated that poly(AGE-EGDM) series are more swellable, have less attritional loss because of greater elasticity, are more compressable relative to poly(GMA-EGDM) series at equivalent composition. Overlooking these important issues, it can be said from the studies conducted here that poly(AGE-EGDM) are better suited as chromatographic and enzyme immobilisation matrices.

Table 2.26 presents the distributions of pore size in poly(AGE-EGDM) beads of differing copolymer composition (crosslink density) at constant porogen volume (1:1.61). It is

observed that the pore size distribution is broad, especially at higher crosslink density. The median pore radii lies between 50-300 nm, excepting for polymer with 25% CLD (30-50 nm).

Table 2.26: **Effect of crosslink density on pore volume distribution in poly(AGE-EGDM) beads at constant monomer:porogen ratio of 1:1.61. Porogen is cyclohexanol**

Code	CLD	distribution in pore radii (vol%), radius in nm								
	%	<5	5-10	10-15	15-20	20-30	30-50	50-100	100-300	>300
AG 1	25	4.53	13.53	11.66	8.21	14.25	19.51	15.76	5.92	1.45
AG 2	50	0.50	6.45	6.19	4.88	7.58	11.87	20.43	32.59	9.47
AG 3	75	4.43	12.02	8.72	7.33	10.46	15.79	22.53	18.70	0.00
AG 4	100	3.05	8.23	5.95	5.27	7.63	11.85	19.95	26.32	9.08
AG 5	150	3.18	9.73	6.71	4.56	8.28	14.47	20.47	25.64	5.36
AG 6	200	0.00	8.66	7.66	6.40	10.05	13.05	22.13	24.55	3.12

CLD=crosslink density;

2.4 Poly(2-hydroxyethyl methacrylate-co-ethylene dimethacrylate) [poly(HEMA-EGDM)]

2.4.1 Suspension polymerisation of HEMA with EGDM

The objective was to synthesise porous networked polymer beads with hydroxy functional groups. Synthesis of poly(HEMA-EGDM) were as that presented in Section 2.1.1. Composition of synthesised copolymers are presented in Table 2.27. As in poly(GMA-EGDM) series, synthesis was conducted under a variety of conditions and pore structure were evaluated to establish the optimal ones. This polymerisation series was aimed at generating macroporous beaded polymer with particle size in the range 150-450 nm, having pore volume between 0.5 and 1 mL/g, with surface area between 50 and 100 m^2/g with hydroxy functional groups, which could be derivatised using acids (ester), isocyanates (urethane) and halides (ethers).

The pore generating solvent volume was varied for a given fixed monomer composition, such as [HEMA]:[EGDM]=1.00:0.25, so as to generate copolymers with the same composition but differing in the pore volume. Thus, copolymers HE1, HE7, HE13, HE19 and HE25 have a crosslink density of 25% but are of varying porosity, due to the changing volume

of cyclohexanol (porogen) relative to that of the combined volumes of the two monomers as 2.43:1, 1.61:1, 0.81:1, 0.405:1 and 0:1, respectively. Similarly, six sets of copolymers, varying in their compositions, were prepared by changing the mole ratio of HEMA:EGDM (25, 50, 75, 100, 150 and 200 CLD). Thus, 30 poly(HEMA-EGDM) were synthesised using cyclohexanol as porogen.

Table 2.27: Compositions of poly(HEMA-EGDM) synthesised using cyclohexanol as porogen, at varying monomer:porogen ratio

Exp. No	HEMA (mol)	EGDM (mol)	CLD %	Monomer:porogen (v/v)
HE1, HE7, HE 13, HE19, HE 25	0.0486	0.0122	25	1:2.43, 1:1.61, 1:0.81, 1:0.405, 1:0
HE2, HE8, HE14, HE20, HE26	0.0379	0.0191	50	1:2.43, 1:1.61, 1:0.81, 1:0.405, 1:0
HE3, HE9, HE15, HE21, HE27	0.0313	0.0233	75	1:2.43, 1:1.61, 1:0.81, 1:0.405, 1:0
HE4, HE10, HE16, HE22, HE28	0.0264	0.0265	100	1:2.43, 1:1.61, 1:0.81, 1:0.405, 1:0
HE5, HE11, HE17, HE23, HE29	0.0206	0.0302	150	1:2.43, 1:1.61, 1:0.81, 1:0.405, 1:0
HE6, HE12, HE18, HE24, HE30	0.0165	0.0329	200	1:2.43, 1:1.61, 1:0.81, 1:0.405, 1:0

crosslink density (CLD) is defined as the mole percent of crosslinking monomer relative to the moles of reactive functional comonomer. AIBN: 0.2 g; Water: 100 mL; PVP: 1 g.

Poly(HEMA-EGDM) formed were porous at the monomer:porogen ratio of 1:1.61. However, the pore volumes were quite low, as seen in Section 2.4.3. Hence, at this fixed monomer:porogen ratio, the effectiveness of a number of solvent combinations as porogens were examined over the entire copolymerisation composition range (25-200% CLD). These were: (i) 50/50 v/v cyclohexanol/paraffin oil; (ii) 75/25 v/v cyclohexanol/lauryl alcohol (dodecanol); (iii) 50/50 v/v cyclohexanol/lauryl alcohol and (iv) hexanol. In this lot 24 poly(HEMA-EGDM) were synthesised and characterised.

2.4.2 Characterisation

The pore volume, surface area, particle size, surface morphology, infra-red spectra, and bead yield were determined as presented in Sections 2.1.2.1 to 2.1.2.6.

2.4.3 Results and discussion on poly(HEMA-EGDM) series

Suspension polymerisation of a monomer such as HEMA is a problem due to its solubility in the continuous aqueous phase. Addition of higher alcohols such as cyclohexanol solubilised HEMA in the organic phase. Thus, suspension polymerisation conditions suitable for water insoluble monomers such as GMA could be used for HEMA-EGDM series.

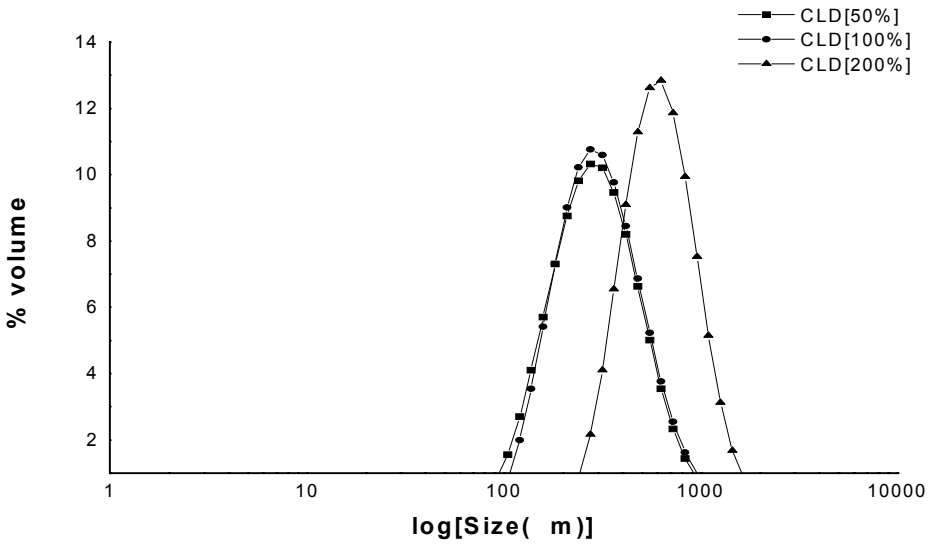

Figure 2.14: Particle size distribution in poly(HEMA-EGDM) beads of 50, 100 and 200% CLD at monomer:porogen ratio of 1:1.61 (HE8, HE10 and HE12)

The polymer conversions were above 99% in all cases, unlike in the poly(GMA-EGDM) series. Figure 2.14 shows typically particle size distribution of poly(HEMA-EGDM) beads as determined by particle size analyser. The particle sizes were in the range 200 to 600 μm. The particle size distribution shifted towards the higher size with an increase in the relative mole ratio of the crosslinking comonomer in a manner akin to poly(GMA-EGDM) series. The solubility parameter of HEMA, EGDM and cyclohexanol (monomer, comonomer and porogen) are presented in Table 2.28 and that for poly(HEMA-EGDM) of differing crosslink density are presented in Table 2.29.

Table 2.28: Solubility parameter δ of HEMA, EGDM and cyclohexanol

Component	[a]δ $(cal/cm^3)^{0.5}$
HEMA	11.4
EGDM	8.9
Cyclohexanol	11.4

[a]δ can be calculated using the formula d .∑G/M where G is the molar attraction constant, ∑G is the sum for all the atoms and groupings in the molecules, d is the density and M is the molecular weight.

Table 2.29: Variance in solubility parameter, δ/, of poly(HEMA-EGDM) beads with crosslink density

CLD %	δ/ $(cal/cm^3)^{0.5}$
25	10.7
50	10.3
75	10.1
100	9.9
150	9.7
200	9.5

With the increase of the relative mole ratio of EGDM (and hence crosslink density), the solubility parameter of copolymer decreases. Unlike in the poly(GMA-EGDM) series, with decreasing solubility parameter of copolymer, the critical chain length prior to precipitation increases, resulting in larger particles. Simultaneously, the precipitation rate of copolymer chain decreases with crosslink density, and particles phase separate rapidly, resulting in a narrower distribution. So copolymer with lower crosslink densities are formed as small particles with a narrower distribution, as compared to copolymers with higher crosslink densities.

The typical IR spectra in Figure 2.15 shows peaks at 3421.5, 1718.5 and 1072 cm^{-1} due to stretching vibrations of -OH group, C=O of ester group and C-O of -COH group, respectively. It was also observed that the intensity of band at 1637.5 cm^{-1}, a characteristic band of C=C stretching, does not disappear but is significantly weakened indicating that it is not

completely consumed, but that there are still some residual vinyl double bonds buried inside the network structure, as in the poly(GMA-EGDM) series.

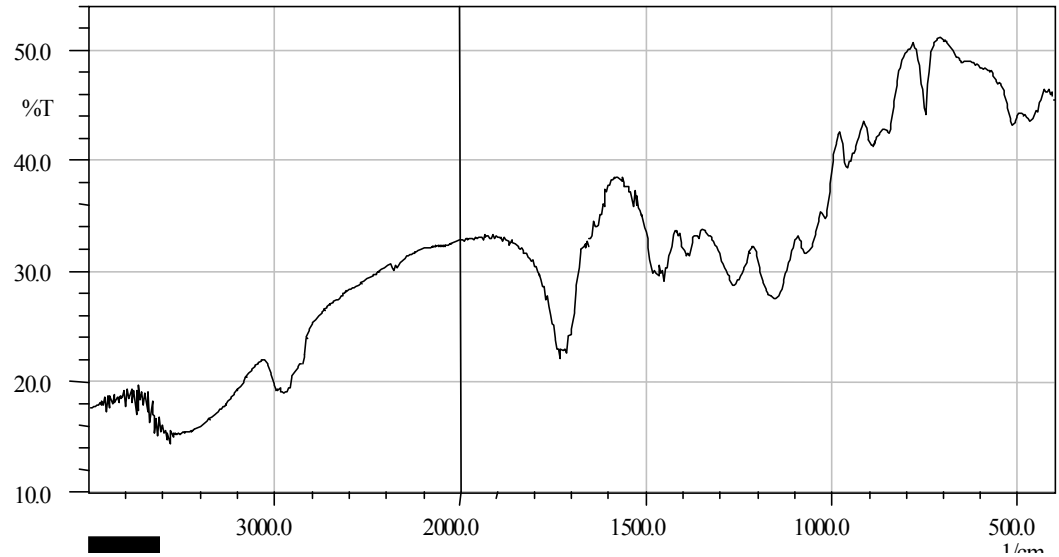

Figure 2.15: IR spectra of poly(HEMA-EGDM) beads of 100% CLD at monomer:porogen ratio of 1:1.61 (HE10)

2.4.3.1 Porous properties of poly(HEMA-EGDM) beads

The data of pore volume and surface area for poly(HEMA-EGDM) are presented in Tables 2.30 to 2 33. Cyclohexanol is a marginal porogen for the poly(HEMA-EGDM) series. The pore volumes (Table 2.30) are extremely low except at higher crosslink densities and porogen volumes. Thus, cyclohexanol increases the solubility of 2-hydroxyethyl methacrylate in the organic phase but becomes a poorer porogen because it does not efficiently phase separate from the growing polymer particles. In comparison, in poly(GMA-EGDM) series (Table 2.4) higher pore volumes are obtained at lower crosslink densities and monomer:porogen volumes.

When cyclohexanol is replaced with others as porogens (Table 2.31), the pore volumes obtained are consistently higher. Volume increase is marginal on partial (50%) replacement of cyclohexanol with paraffin oil (long chain alkane).

Table 2.30: Pore volume of poly(HEMA-EGDM) beads: Effect of copolymer composition and monomer to porogen ratio

Monomer: porogen rato	25% CLD	50% CLD	75% CLD	100% CLD	150% CLD	200% CLD
	PV (mL/g)	PV (mL/g)	PV (mL/g)	PV (mL/g)	PV (mL/g)	PV (mL/g)
1:0	0.0017 (HE 25)	0.0075 (HE 26)	0.0049 (HE 27)	0.0545 (HE 28)	0.0329 (HE 29)	0.0130 (HE 30)
1:0.405	0.0029 (HE 19)	0.0097 (HE 20)	0.0245 (HE 21)	0.0613 (HE 22)	0.0456 (HE 23)	0.0373 (HE 24)
1:0.81	0.0080 (HE 13)	0.0110 (HE 14)	0.0540 (HE 15)	0.0630 (HE 16)	0.1380 (HE 17)	0.1780 (HE 18)
1:1.61	0.0300 (HE 7)	0.0460 (HE 8)	0.2350 (HE 9)	0.2645 (HE 10)	0.4070 (HE 11)	0.6740 (HE 12)
1:2.43	0.1850 (HE 1)	0.3837 (HE 2)	0.3952 (HE 3)	0.4229 (HE 4)	0.4510 (HE 5)	0.8020 (HE 6)

CLD=crosslink density defined as ([crosslinking monomer]/[functional monomer]) x 100, which is [EGDM]/[HEMA]; PV=pore volume, as estimated by mercury porosimetry.

Table 2.31: Pore volume of poly(HEMA-EGDM) beads: Effect of porogen type

porogen type v/v	25% CLD	50% CLD	75% CLD	100% CLD	150% CLD	200% CLD
	PV (mL/g)	PV (mL/g)	PV (mL/g)	PV (mL/g)	PV (mL/g)	PV (mL/g)
CHOL 100	0.03 (HE 7)	0.05 (HE 8)	0.24 (HE 9)	0.26 (HE 10)	0.41 (HE 11)	0.67 (HE 12)
CHOL/PO 50/50	0.08 (HE 31)	0.40 (HE 32)	0.32 (HE 33)	0.11 (HE 34)	0.18 (HE 35)	0.22 (HE 36)
CHOL/LA 75/25	0.57 (HE 43)	0.83 (HE 44)	0.73 (HE 45)	0.80 (HE 46)	0.73 (HE 47)	0.91 (HE 48)
CHOL/LA 50/50	0.96 (HE 37)	0.96 (HE 38)	0.78 (HE 39)	1.03 (HE 40)	0.91 (HE 41)	1.07 (HE 42)
HOL 100	0.87 (HE 49)	0.92 (HE 50)	0.93 (HE 51)	0.85 (HE 52)	1.07 (HE 53)	0.95 (HE 54)

CHOL=cyclohexanol; PO=paraffin oil; LA=lauryl alcohol (dodecanol); HOL=hexanol; CLD=crosslink density defined as ([crosslinking monomer]/[functional monomer]) x 100, which is [EGDM]/[HEMA]; PV=pore volume, as estimated by mercury porosimetry.

When a long chain alkane with terminal hydroxy group (lauryl alcohol) is used in place of paraffin oil, the pore volume increases more appreciably, with the increase dependent on the

relative volume of the lauryl alcohol. When cyclohexanol is replaced with hexanol, its linear analogue, the pore volume increases appreciably.

Table 2.32: Surface area of poly(HEMA-EGDM) beads: Effect of copolymer composition and monomer to porogen ratio

Monomer: porogen ratio	25% CLD	50% CLD	75% CLD	100% CLD	150 % CLD	200 % CLD
	SA (m^2/g)	SA (m^2/g)	SA (m^2/g)	SA (m^2/g)	SA (m^2/g)	SA (m^2/g)
1:0	0.0984 (HE 25)	1.2976 (HE 26)	1.3478 (HE 27)	12.6519 (HE 28)	4.5853 (HE 29)	2.8745 (HE 30)
1:0.405	0.1094 (HE 19)	0.0987 (HE 20)	8.6472 (HE 21)	16.7574 (HE 22)	12.7658 (HE 23)	14.8769 (HE 24)
1:0.81	3.1395 (HE 13)	5.2061 (HE 14)	5.9236 (HE 15)	22.2156 (HE 16)	44.4315 (HE 17)	52.7755 (HE 18)
1:1.61	7.2447 (HE 7)	10.0716 (HE 8)	83.3474 (HE 9)	66.9399 (HE 10)	77.7053 (HE 11)	112.9446 (HE 12)
1:2.43	6.1501 (HE 1)	77.2704 (HE 2)	48.0534 (HE 3)	65.0785 (HE 4)	93.9843 (HE 5)	76.1570 (HE 6)

CLD=crosslink density defined as ([crosslinking monomer]/[functional monomer]) x 100, which is [EGDM]/[HEMA]; SA=surface area, as estimated by BET.

The surface area measurements, shown in Table 2.32 for polymers synthesised with cyclohexanol as porogen, indicate lower values compared to an exact equivalent poly(GMA-EGDM) composition. In the absence of cyclohexanol, copolymer particles formed are devoid of inner pores. Surface area is entirely due to the surface of the particles. While the data is scattered, some trends are noted. In the absence of porogen, the surface areas are lower than at a monomer:porogen ratio of 1:0.405, unlike in the poly(GMA-EGDM) series, because polymerisation is nearly (>99%) complete and hence the beads are free from unreacted monomers which contribute to surface area. While surface area seems to go through a maxima with crosslink density, in the absence of cyclohexanol, it tends to increase with cyclohexanol

volume and crosslink density. Surface area are high only at high crosslink density (100% CLD) and porogen volume (1:1.61 and above).

In Table 2.33 the surface area of the porous polymers are compared. In the 75-200% CLD range, surface area obtained with other porogens are lower indicating that pores are in the meso and macroporous range. While the pore volumes of copolymers synthesised with cyclohexanol and cyclohexanol/paraffin oil 50/50 v/v are nearly comparable, the surface area of the latter series are much lower, indicating that pores formed are of larger size. With partial replacement with lauryl alcohol, pore volumes are much higher and at the same time surface area are much lower indicating rapid phase separation of lauryl alcohol from the growing polymer phase and thereby generating macropores. With hexanol both pore volume and surface area are increased indicating that the pores formed are of all (micro, meso and macro) dimensions.

Table 2.33: Surface area of poly(HEMA-EGDM) beads: Effect of porogen type

porogen type v/v	**25% CLD**	**50% CLD**	**75% CLD**	**100% CLD**	**150% CLD**	**200% CLD**
	SA (m^2/g)	**SA (m^2/g)**	**SA (m^2/g)**	**SA (m^2/g)**	**SA (m^2/g)**	**SA (m^2/g)**
CHOL 100	7.24 (HE 7)	10.02 (HE 8)	83.35 (HE 9)	69.94 (HE 10)	71.71 (HE 11)	112.94 (HE 12)
CHOL/PO 50/50	11.39 (HE 31)	93.18 (HE 32)	25.77 (HE 33)	17.21 (HE 34)	20.78 (HE 35)	24.72 (HE 36)
CHOL/LA 75/25	15.86 (HE 43)	15.32 (HE 44)	30.84 (HE 45)	60.92 (HE 46)	55.32 (HE 47)	31.76 (HE 48)
CHOL/LA 50/50	14.88 (HE 37)	32.28 (HE 38)	38.26 (HE 39)	29.49 (HE 40)	47.53 (HE 41)	30.06 (HE 42)
HOL 100	80.72 (HE 49)	77.82 (HE 50)	49.29 (HE 51)	34.74 (HE 52)	55.79 (HE 53)	72.55 (HE 54)

CHOL=cyclohexanol; PO=paraffin oil; LA=lauryl alcohol (dodecanol); HOL=hexanol; CLD=crosslink density defined as ([crosslinking monomer]/[functional monomer]) x 100, which is [EGDM]/[HEMA]; PV=pore volume, as estimated by mercury porosimetry.

Table 2.34: Effect of crosslink density on pore volume distribution in poly(HEMA-EGDM) beads without porogen

Code	CLD	distribution in pore radii (vol%), radius in nm								
	%	<5	5 -10	10 -15	15 -20	20 -30	30 -50	50 -100	100 -300	>300
HE26	50	48.2	31.53	0.01	0.01	0.02	0.03	0.31	0.95	18.93
HE28	100	20.19	34.86	2.75	7.34	3.67	2.75	25.69	0.00	0.00
HE30	200	18.46	26.92	18.46	13.08	10.77	7.69	2.31	0.00	0.00

Porogen=cyclohexanol; CLD=crosslink density;

The copolymers formed in the poly(HEMA-EGDM) series are almost nonporous in the absence of porogen., as seen in Tables 2.30 and 2.31. The pore size distribution data, in Table 2.34, indicates that the pores are in the micro range at low (25%) CLD and spread with increase in CLD to 100 nm, though most are still in the micro-range.

In the poly(GMA-EGDM) series, at a monomer:porogen ratio of 1:1.61, pore volume and surface area are in the range 0.11 to 0.85 mL/g (25-200%CLD, Table 2.4). The poly(HEMA-EGDM) series differs from the above series only in that the epoxy group is replaced by a hydroxymethylene unit. This apparently marginal variance depresses the pore volume considerably. Pore volume, under similar conditions, is in the range 0.03 to 0.67 mL/g (Table 2.30).

Table 2.35: Effect of crosslink density on pore volume distribution in poly(HEMA-EGDM) beads at constant monomer:porogen ratio of 1:1.61

Code	CLD	distribution in pore radii (vol%), radius in nm								
	%	<5	5 -10	10 -15	15 -20	20 -30	30 -50	50 -100	100 -300	>300
HE7	25	44.99	42.49	2.50	0.00	0.00	0.00	0.00	0.00	10.00
HE10	100	15.69	40.45	17.58	8.13	8.51	3.97	2.65	0.94	0.19
HE12	200	7.64	21.29	15.65	13.51	19.43	12.24	6.53	1.93	0.00

Porogen=cyclohexanol; CLD=crosslink density;

The pore size distribution presented in Table 2.35 indicates that median continues to be in the micro and mesoporous range, unlike that in the poly(GMA-EGDM) series. Thus, cyclohexanol is a poor porogen for the poly(HEMA-EGDM) series.

Table 2.36: **Effect of crosslink density on pore volume distribution in poly(HEMA-EGDM) beads at constant monomer:porogen ratio of 1:2.43**

Code	CLD	distribution in pore radii (vol%), radius in nm								
	%	<5	5 -10	10 -15	15 -20	20 -30	30 -50	50 -100	100 -300	>300
HE1	25	0.00	0.00	0.00	0.00	0.00	50.00	50.00	0.00	0.00
HE4	100	24.83	42.81	3.60	2.29	0.00	0.98	0.00	23.20	0.00
HE6	200	2.88	3.59	2.69	2.33	3.66	6.73	18.20	52.60	3.21

Porogen=cyclohexanol; CLD=crosslink density;

At higher relative volume of porogen (1:2.43), the pore volume increases to 0.19 to 0.80 mL/g (Table 2.30). As compared to copolymers synthesised at monomer:porogen ratio of 1:1.61, the pore size distribution shifts to meso and macroporous range. This shift decreases the surface area of copolymers (Table 2.32), indicating that the number of pores probably decreases with the relative increase in porogen volume.

From Figure 2.16 it is indicated that, the nature of the beads is spherical.

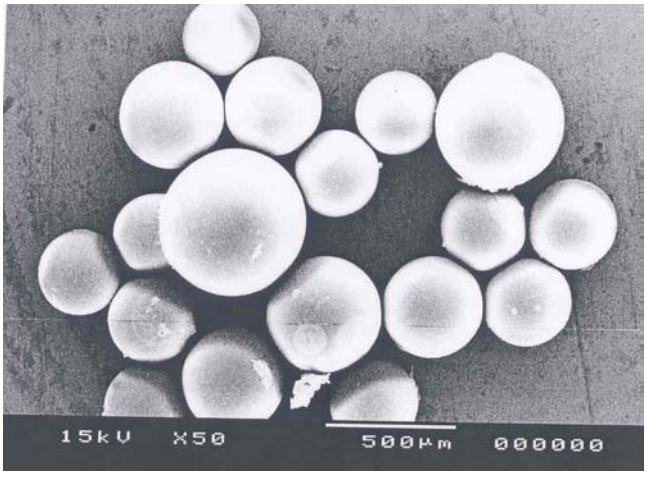

Figure 2.16: Surface morphology of poly(2-hydroxyethyl methacrylate-co-ethylene dimethacrylate) beads

These copolymers will be evaluated for their suitability as base supports for anchoring chiral ligands.

2.5 Poly(2-hydroxyethyl methacrylate-co-divinyl benzene)

The objective was to study the effect of crosslinking comonomer on the pore structure.

2.5.1 Experimental

The chemicals used are given in Section 2.2.1. The synthesis procedure for poly(2-hydroxyethyl methacrylate-co-divinyl benzene) [poly(HEMA-DVB)] was as presented in Section 2.1.1. The compositions of poly(HEMA-DVB) synthesised are presented in Table 2.37.

Table 2.37: Synthesis of poly(HEMA-DVB) using cyclohexanol at a monomer:porogen ratio of 1:1.61

Exp. No	HEMA (mol)	DVB (mol)	CLD %
HV1	0.0453	0.0189	25
HV2	0.0338	0.0287	50
HV3	0.0272	0.0344	75
HV4	0.0231	0.0379	100
HV5	0.0173	0.0428	150
HV6	0.0141	0.0456	200

Crosslink density (CLD) is defined as the mole percent of crosslinking monomer relative to the moles of reactive functional comonomer ([DVB] / [HEMA]). AIBN: 0.2 g; Water: 100 mL; PVP: 1 g.

2.5.2 Characterisation

The pore volume, surface area, particle size, surface morphology, infra-red spectra, and bead yield were determined as presented in Sections 2.1.2.1 to 2.1.2.6.

2.5.3 Results and Discussion on poly(HEMA-DVB) series

Poly(HEMA-DVB) beads produced by suspension polymerisation were spherical and in the size range 0.2-0.6 mm. The particle size increases with increase in crosslink density. The yield was in the range 90-97%. The bulk density of copolymer beads decreases with increasing crosslink density (Figure 2 17), indicating that the polymers become increasingly porous. This decrease in bulk density is very sharp initially and then tends to level off at higher CLD.

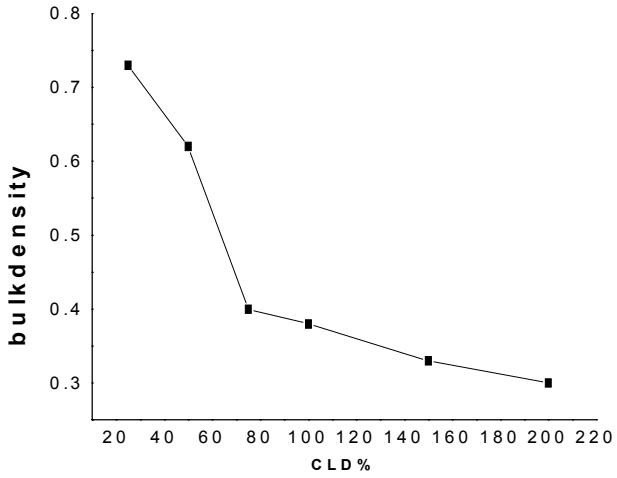

Figure 2.17: Variance in bulk density with composition for poly(HEMA-DVB) series

The typical IR spectra in Figure 2.18 shows peaks at 3567.5, 1721.8 and 1082.2 cm^{-1} due to stretching vibrations of -OH group, C=O of ester group and C-O of -COH group, respectively. It was also observed that the intensity of band at 1637.5 cm^{-1}, a characteristic band of C=C stretching disappears indicating that C=C double bond is completely consumed.

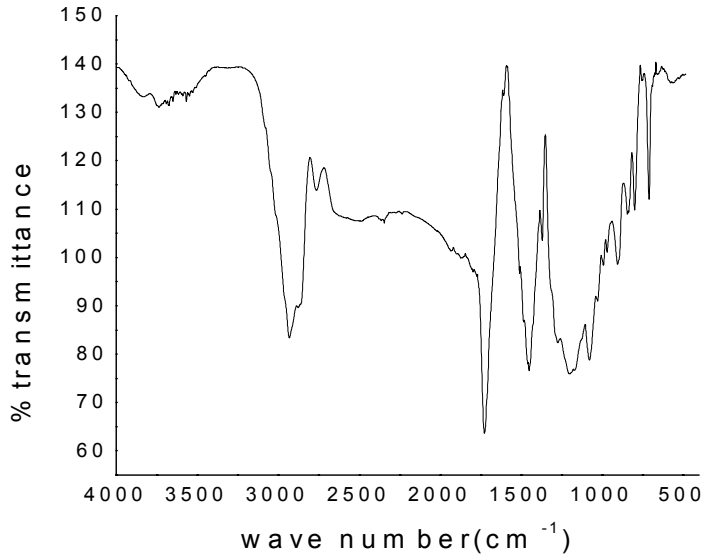

Figure 2.18: IR spectra of poly(HEMA-DVB) beads of 100% CLD at monomer:porogen ratio of 1:1.61

2.5.4 Porous properties of poly(HEMA-DVB) beads

The data of pore volume and surface area for poly(HEMA-DVB) determined by mercury porosimetry and BET are presented in Table 2.38 and compared with that observed for poly(HEMA-EGDM) series of similar composition and porogen volume.

Table 2.38: Pore volume and surface area of poly(HEMA-DVB) and poly(HEMA-EGDM) synthesised using cyclohexanol at monomer:porogen ratio of 1:1.61

CLD %	Poly(HEMA-DVB)		Poly(HEMA-EGDM)	
	Pore volume (mL/g)	Surface area (m^2/g)	Pore volume (mL/g)	Surface area (m^2/g)
25	0.05 (HV 1)	8.02 (HV 1)	0.03 (HE 7)	7.24 (HE 7)
50	0.13 (HV 2)	18.10 (HV 2)	0.05 (HE 8)	10.07 (HE 8)
75	0.50 (HV 3)	97.26 (HV 3)	0.24 (HE 9)	83.35 (HE 9)
100	0.73 (HV 4)	108.48 (HV 4)	0.26 (HE 10)	66.94 (HE 10)
150	0.95 (HV 5)	127.01 (HV 5)	0.41 (HE 11)	77.71 (HE 11)
200	1.01 (HV 6)	120.21 (HV 6)	0.67 (HE 12)	112.94 (HE 12)

From Table 2.38, it is seen that at lower crosslink density, the inner pore volume in poly(HEMA-DVB) series is low. This continues to increase with increase in crosslink density, due to an increase in the number of pores. Phase separation of copolymer from the porogen present in the monomer phase contributes to the generation of pores rather than phase separation from the monomers yet to be linked to the copolymer chains. Similarly, surface area is low at low crosslink density, and increases with crosslink density for particles of similar size distribution. In comparison, polymers of similar composition in the poly(HEMA-EGDM) series are consistently less porous, both in terms of pore volume and surface area. Thus, cyclohexanol acts as a suitable porogen in presence of more hydrophobic DVB, even though it is a solvent for HEMA.

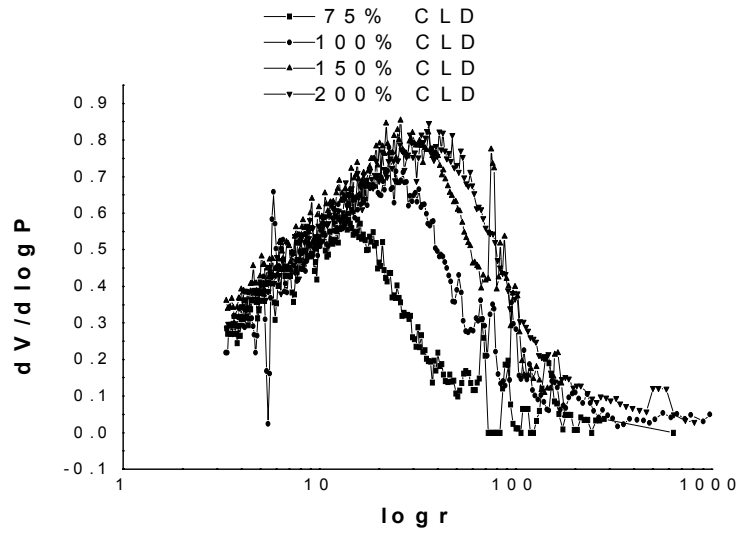

Figure 2.19: Differential pore size distribution curves of the poly(hydroxyethyl methacrylate-co-divinyl benzene) beads using cyclohexanol as a porogen with different cross-link density

Figure 2.19 presents the differential pore size distributions in poly(HEMA-DVB) beads of differing copolymer composition (crosslink density) at constant porogen volume which were prepared by varying crosslink density keeping monomer and porogen ratio (1:1.61) constant. It is seen that at higher crosslink density, the pore size distribution is broad.

The copolymer formed at high crosslink density possesses a very broad pore size distribution because of the formation of macropores in the copolymer matrix. This makes these matrices suitable to immobilize variety of enzymes and also to anchor chiral ligands, for used in stereoselective resolution.

2.6 References

1. A. Guyot and M. Bartholin, Prog. Polym. Sci., **1992**, *8*, 277.
2. P. Hodge, in P. Hodge and D. C. Sherrington, Eds., Syntheses and Separations using Functional Polymers, Wiley, New York, **1989**.
3. J. E. G. J. Wijnhoven and W. L. Vos, Science, **1998**, *281*, 802.
4. P. T. Tanev, M. Chibwe and T. J. Pinnavaia, Nature, 1**994**, *368*, 321.
5. V. Maquet and R. Jerome, Mater. Sci. Forum, **1997**, *250*, 15.
6. M. C. Peters and D. J. Mooney, Mater. Sci. Forum, **1997**, *250*, 43.
7. S. Bancel and W. S. Hu, Biotechnol. Prog., **1996**, *12*, 398.
8. C. Viklund, F. Svec and J. M. J. Frechet, Chem. Mater., **1996**, *8*, 744.
9. H. G Yuan, G. Kalfas, and W. H. Ray, J. Macromol. Sci., Rev. Macromol. Chem. Phys. C, **1991**, *31*, 215.
10. E. Vivaldo-Lima, P. E. Wood, A. E. Hamielec and A. Penlidis, Ind. Eng. Chem. Res., **1997**, *36*, 939.
11. D. S. S. Nunes and F. M. B. Coutinho, Eur. Polym. J., **2001**, *36*, 547.
12. M. A. Hamid, R. Naheed, M. Fuzail and E. Rehman, Eur. Polym. J, **1999**, *35*, 1799.
13. K. Lewandowski, F. Svec and J. M. J. Frechet, J. Appl. Polym. Sci., **1998**, *67*, 597.
14. D. Horak, F. Svec, M. Ilavsky, M. Bleha, J. Baldrian and J. Kalal, Angew Makromol. Chem., **1981**, *95*, 117.
15. D. Horak, F. Svec, M. Ilavsky, M. Bleha, J. Baldrian and J. Kalal, Angew Makromol. Chem., **1981**, *95*, 109.
16. Y. C. Liang, F. Svec and J. M. J. Frechet, J. Polym. Sci. Polym. Chem., **1997**, *35*, 2631.
17. R. B. Merrifield, J. Am Chem. Soc., **1963**, *85*, 2149.
18. E. C. Riqueza, A. P. Aguiar, L. C. S. Maria and M. R. M. P. Aguiar, Polym. Bull., **2002**, *48*, 407.
19. M. B. Tennikov, N. V. Gazdina, T. B. Tennikova and F. Svec, J. Chromatogr., A. **1998**, *798*, 55.
20. A. Palm and M. V. Novotny, Anal. Chem., **1997**, *69*, 4499.
21. S. Xie, F. Svec and J. M. J. Frechet, J. Chromatogr., A, **1997**, *775*, 65.
22. T. M. Maugh, Science, **1984**, *223*, 474.
23. S. P. Fulton, N. B. Afeyan and F. E. Regnier, J. Chromatogr., **1991**, *547*, 452.
24. P. T. Tanev, M. Chibwe and T. J. Pinnavaia, Nature, 1**994**, *368*, 321.
25. H. Deleuze, X. Schultze and D. C. Sherrington, Polymer, **1998**, *39*, 6109.

26. R. R. Bhave, Inorganic Membranes: Synthesis, Characteristics and Application, Van Nostrand Reinhold, New York, **1991.**

27. K. Lewandowski, P. Murer, F. Svec and J. M. J. Fretchet, Anal.Chem., **1998,** *70*, 1629.

28. P. Hodge and D. C. Sherrington, Polymer Supported Reactions in Organic Synthesis, Wiley, New York, London, **1980.**

29. D. C. Sherrington, Chem. Commun., **1998,** 2275.

30. E. Glass, Hydrophilic Polymers, Adv. Chem. Series 248, American Chemical Society, Washington, **1996**; p. 61.

31. M. Fishman, R. Friedman and S. Huang, Polymers from Agricultural Coproducts, ACS Symposium Series 575, American Chemical Society, Washington DC, **1994**; Ch. 12.

32. P. Jhonson and G. Lloyd-Jones, Drug Delivery Systems: Fundamentals and Techniques, (Ellis Horwood Serires in Biomedicine), VCH Verlagsgesellschaft, Weinheim, Germany, **1987**.

33. E. Kenawy and D. C. Sherrington, Eur. Polym. J., **1992**, *28*, 841.

34. M. Galia, F. Svec and J. M J. Frechet, J. Polym. Sci., Polym. Chem. Ed, **1994**, *32*, 2169.

35. A. Imhof and D. J. Pine, Nature, **1997**, *389*, 948.

36. A. Imhof and D. J. Pine, Adv. Mater., **1998**, *10*, 697.

37. P. Perrin, Langmuir, **1998**, *14*, 5977.

38. G. Widawski, M. Rawiso and B. Francois, Nature, **1994**, *369*, 387.

39. S. Lowell and J. E. Shields, Powder Surface Area and Porosity, Chapman and Hall Ltd., London, New York, p. 97-120.

40. F. Svec, J. Hradil, J. Coupek and J. Kalal, Angew. Macromole. Chem., **1975**, *48*, 135.

41. F. Svec, D. Horak and J. Kalal, Angew. Macromole. Chem., **1977**, *63*, 37.

42. F. Svec, J. Labsky, L. Lanyova, J. Hradil, S. Pokorny, and J. Kalal, Angew. Macromole. Chem., **1980**, *90*, 47.

43. D. Horak, F. Lednicky and M. Bleha, Polymer J., **1996,** *37*, 4245.

44. A. Kotha, C. R. Rajan, S. Ponrathnam, and J. G. Shewale, Reactive and Functional Polymers, **1996**, *28*, 227.

Chapter 3

Study of Guest Molecule Binding with Cyclodextrin Modified Macroporous HEMA-EGDM Copolymers

3.1 Introduction

Cyclodextrins are mesmeric, highly potent and promising molecules, with wide range of action and activity, beckoning investigators from all domains of chemistry [1]. These are cyclic molecules, consisting of six to eight glucose units linked through α 1-4-glycosidic linkage, which form inclusion complexes with a variety of components [2-11]. The separation potential of particular interesting molecule could be enhanced several fold by incorporating cyclodextrin on to a polymer backbone [12]. The cavity of cyclodextrin is hydrophobic while external faces are hydrophilic. Cyclodextrins are usually capable of forming inclusion complexes with hydrophobic compounds by taking up a whole molecule, or some part of it [13-15]. The great interest of binding cyclodextrin on to the backbone of macroporous crosslinked beaded polymer [16-19] can offer a highly selective system for chromatographic separation.

The hydrophobicity and the shape of the guest molecules mainly affect the inclusion complex formation. Due to size and hydrophobicity, steroids can form non-covalent host–guest complexes with cyclodextrins. This phenomenon has initiated many pharmaceutical applications [20-22]. High guest binding is successfully achieved by placing appropriate functional residues at the required sites.

In this investigation, a number of macroporous, beaded, crosslinked copolymers of 2-hydroxyethyl methacrylate and ethylene dimethacrylate were synthesised and used as matrices. Diisocyanates were used as coupling agents in the preparation of affinity chromatography matrices. The derivatisation and coupling procedure depends on the nature of the functional group present on the model matrix as well as on the ligand.

Here α, β and γ-cyclodextrin were used as ligands and cholesterol acts as guest. This is host-guest interaction chemistry.

3.2 Experimental

3.2.1 Materials

α-Cyclodextrin (α-CD): Empirical formula: $C_{36}H_{60}O_{30}$; Molecular weight: 972.86; Melting point: 278°C; Physical state: white crystalline powder. *β-Cyclodextrin (β-CD):* Empirical formula: $C_{42}H_{70}O_{35}$; Molecular weight: 1135.01; Melting point: 260°C; Physical state: white crystalline powder. *γ -Cyclodextrin (γ -CD):* Empirical formula: $C_{48}H_{80}O_{40}$; Molecular weight: 1297; Melting point: 267°C; Physical state: white crystalline powder. *Toluene-2,4-diisocyanate (TDI):* Empirical formula: $C_9H_6N_2O_2$; Molecular weight: 174.16; Specific gravity: 1.214. *Cholesterol:* Empirical formula: $C_{26}H_{42}O$; Molecular weight: 386.66; Melting point: 148-150°C; Physical state: white powder.

The details of hydroxyethyl methacrylate and other materials are given in Chapter 2. α, β and γ-cyclodextrin were obtained from Cerester (USA), 2,4-toluene diisocyanate was procured from Sigma (USA). 1,4-Dioxane, and N,N-dimethyl acetamide were procured from SD Fine Chemicals Boisor, India. Cholesterol was obtained from Aldrich Chemicals and HPLC grade methanol was obtained from E-Merck.

3.2.2 Synthesis of poly(HEMA-EGDM) of different crosslink densities

The synthesis is presented in Section 2.1.1.2. The composition of synthesised HEMA-EGDM copolymers are presented in Table 3.1. The continuous phase comprised

1% (wt/v) PVP in water. The discontinuous phase composed of 8.2 mL of HEMA and EGDM with 0.2 g of AIBN. Monomer: porogen (cyclohexanol) ratio was 1: 1.61 (v/v).

Table 3.1: Monomer feed ratio of 2-hydroxyethyl methacrylate with ethylene dimethacrylate

Polymer No.	HEMA (mol)	EGDM (mol)	CLD (%)
HE7	0.0486	0.0122	25
HE8	0.0379	0.0191	50
HE9	0.0313	0.0233	75
HE10	0.0264	0.0265	100
HE11	0.0206	0.0302	150
HE12	0.0165	0.0329	200

3.2.3 Synthesis of affinity matrix (HE-TDI-CD)

Poly(hydroxyethyl methacrylate-co-ethylene dimethacrylate) [HE] beads [23] were coupled to α, β and γ-cyclodextrin in two sequential steps through urethane linkage using urethane spacer based on toluene diisocyanate (TDI). The activation step was carried out with 1:1 molar quantities of –NCO group (present in diisocyanate) with respect to –OH group in the HE beads. The first activation step is the reaction of –NCO group of TDI in molar quantities with respect to specific mole of –OH group in the HE matrix. This step was conducted in a stoppered test tube in a suitable aprotic solvent [24] without stirring at room temperature under argon atmosphere, for one week. After completion of the activation step, the matrices were washed 5-6 times with anhydrous 1,4-dioxane. The second step was the coupling of cyclodextrin to the activated matrices. Cyclodextrin solution was made in anhydrous N,N-dimethyl acetamide. The solution of cyclodextrin was added to the activated matrices. This coupling reaction was also conducted in the same stoppered test tube in a suitable aprotic solvent at room temperature under argon atmosphere, for one week. After completion of the reaction,

the matrices were washed 5-6 times with dry acetone and kept in oven at 60^{o}C. The composition of cyclodextrin modified affinity matrix are given in Tables 3.2, 3.3 and 3.4. The reaction Scheme for the synthesis of HE-TDI-CD, are given in steps 1-3.

Table 3.2: Modification of poly(HEMA-EGDM) through urethane linkage to covalently bind α-cyclodextrin

Polymer No.	CLD (%)	Polymer (g)	TDI (mL)	α-CD (mmol)
HE7a	25	2.5	1.99	2.318
HE8a	50	2.5	1.58	1.818
HE9a	75	2.5	1.28	1.493
HE10a	100	2.5	1.09	1.268
HE11a	150	2.5	0.84	0.975
HE12a	200	2.5	0.68	0.792

CLD = Crosslink density; TDI = 2,4-toluene diisocyanate; α-CD = α-cyclodextrin

Table 3.3: Modification of poly(HEMA-EGDM) through urethane linkage to covalently bind β-cyclodextrin

Polymer No.	CLD (%)	Polymer (g)	TDI (mL)	β-CD (mmol)
HE7b	25	2.5	1.99	1.987
HE8b	50	2.5	1.58	1.558
HE9b	75	2.5	1.28	1.280
HE10b	100	2.5	1.09	1.087
HE11b	150	2.5	0.84	0.835
HE12b	200	2.5	0.68	0.678

Table 3.4: Modification of poly(HEMA-EGDM) through urethane linkage to covalently bind γ-cyclodextrin

Polymer No.	CLD (%)	Polymer (g)	TDI (mL)	γ-CD (mmol)
HE7c	25	2.5	1.99	1.738
HE8c	50	2.5	1.58	1.363
HE9c	75	2.5	1.28	1.120
HE10c	100	2.5	1.09	0.951
HE11c	150	2.5	0.84	0.731
HE12c	200	2.5	0.68	0.593

Step 1

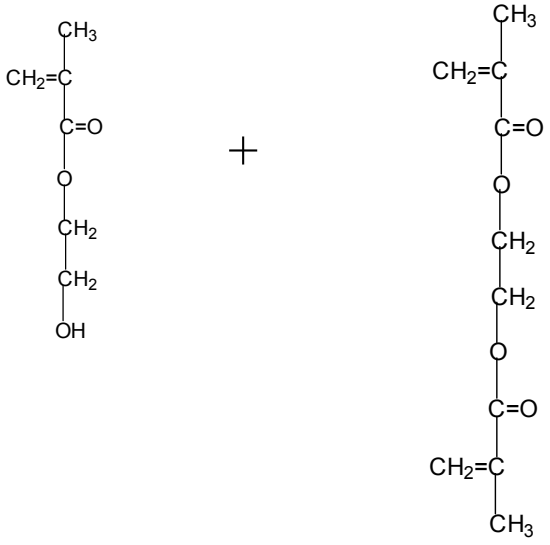

[A] [B]

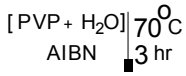

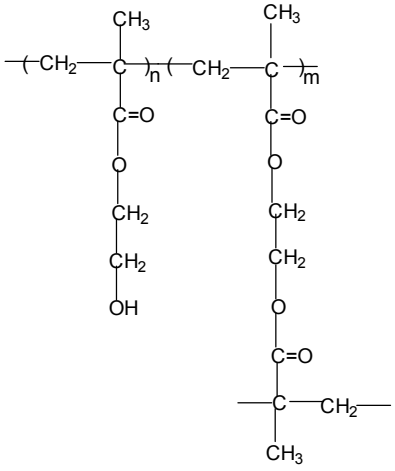

[C]

Step 2

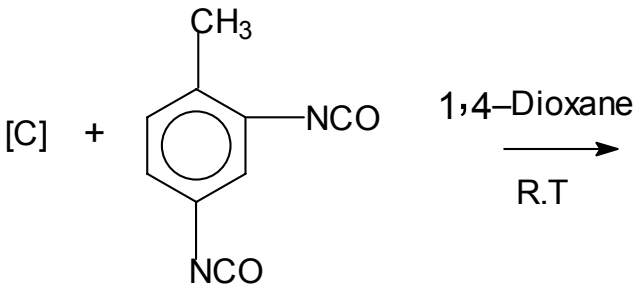
[C]
+
CH3
NCO
NCO
1,4–Dioxane
R.T

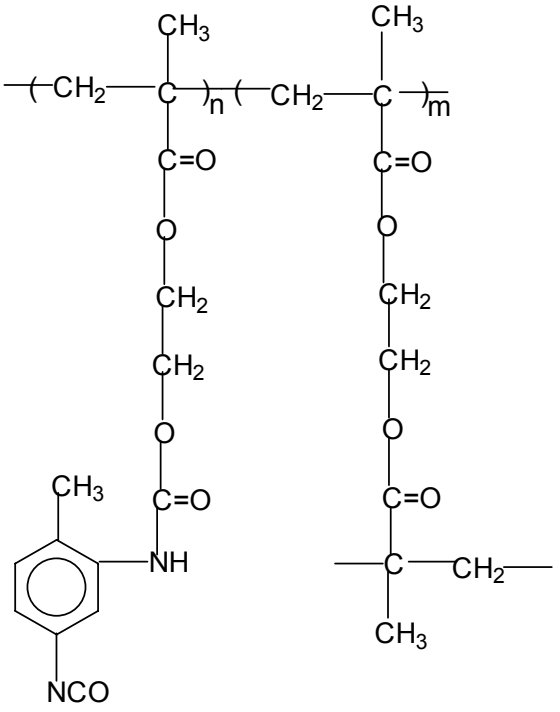
CH3
CH2
C
n
CH2
C
m
C=O
O
CH2
CH2
O
C=O
CH3
NH
NCO
CH3
C=O
O
CH2
CH2
O
C=O
C
CH2
CH3

[D]

Step 3

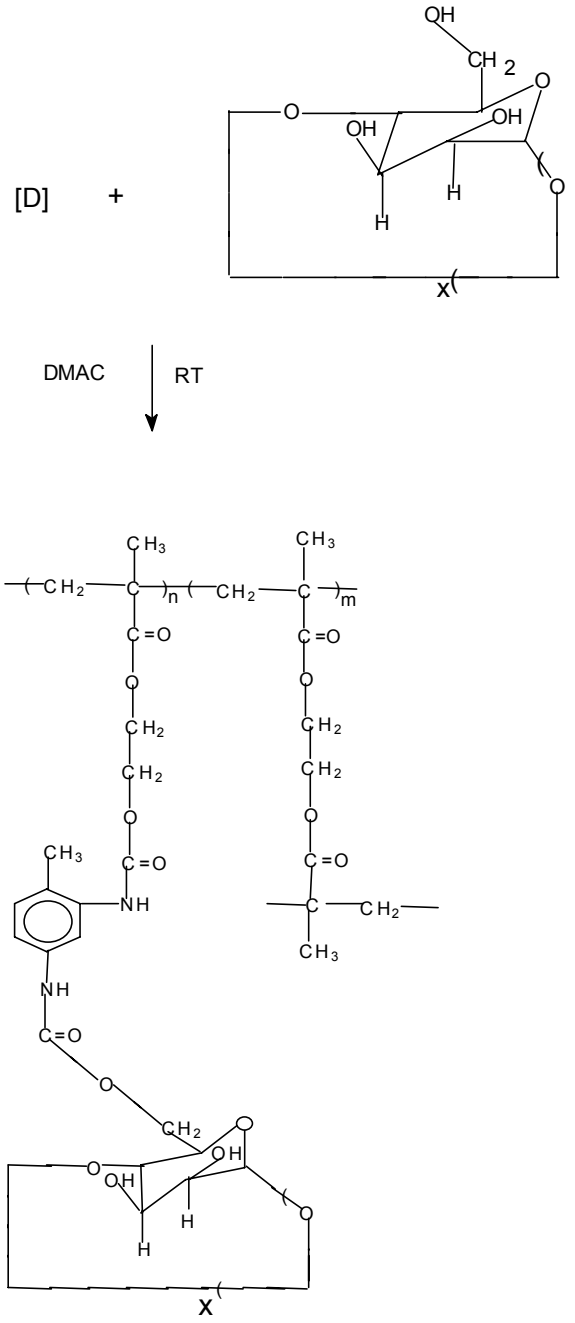

Here x = 6 (alpha-cyclodextrin); x = 7 (beta-cyclodextrin); x = 8 (gamma -cyclodextrin).

3.3 Characterisation

Bead yield was estimated as in Section 2.1.2.6, particle size measurement was as in Section 2.1.2.3, porosity was estimated as presented in Section 2.1.2.1, surface area measurement was as presented in Section 2.1.2.2, SEM is presented in Section 2.1.2.4 and IR spectra is presented in Section 2.1.2.5.

3.3.1 Elemental analysis

The nitrogen content was determined with an elemental analysis device (CHNS-O, EA 1108 elemental analyser) from Carlo Erba Instruments.

3.3.2 Solid state NMR

CP MAS ^{13}C NMR spectra (cross-polarisation and magic-angle spinning) were recorded on a Bruker DRX 500 spectrometer, operating at 500.13 and 125.75 MHz for ^{13}C, respectively. The sample spinning rate was 10 kHz. The cross-polarisation contact time was 1.0 ms, with 3-4 s recycle delays between successive scans.

3.3.3 Estimation of α, β and γ-cyclodextrin bound to polymer

The synthesised α, β and γ-cyclodextrin affinity matrices were assayed spectrophotometrically by using methyl orange, phenolphthalein and bromocresol green methods, respectively [25-27]. The amount of cyclodextrin was calculated from the difference between test and control values.

3.3.3.1 Estimation of α-cyclodextrin

Poly(hydroxyethyl methacrylate-ethylene dimethacrylate) (HE) was used as control. Required amount of base HE matrix and α-cyclodextrin bound HE matrices were taken in test tubes. The matrices were gradually added to solution comprised of 2 mL (18.32 mg/L) methyl orange solution, 0.1 mL 1 N hydrochloric acid and 1.1 mL (0.05 M) phosphate buffer. The test tubes were shaken, centrifuged and the optical

density (absorbance) was measured at 507 nm. α-CD was determined at 507 nm on the basis of its ability to form a stable colourless inclusion complex with methyl orange, which would depress the absorbance relative to that in the absence of the affinity (ligand) polymer.

3.3.3.2 Estimation of β-cyclodextrin

Required amount of base HE and β-cyclodextrin bound HE matrices were taken in test tubes. The matrices were gradually added to solution comprised of 4 mL (12.76 mg/L) phenolphthalein, 0.1 mL 1 N sodium hydroxide and 1.1 mL (0.05 M) tris buffer. The test tubes were shaken, centrifuged and the absorbance was measured at 540 nm. β-CD was determined at 540 nm on the basis of its ability to form a stable colourless inclusion complex with phenolphthalein, which depresses the absorbance relative to that noted for the identical polymer without β-CD bound to it.

3.3.3.3 Estimation of γ-cyclodextrin

Required amount of base HE matrix and γ-cyclodextrin bound HE matrices were taken in test tubes. The matrices were gradually added to solution comprised of 0.1 mL (3.49 g/L) bromocresol green, 0.1 mL 0.5 N hydrochloric acid, 1.1 mL (0.01 M) tris buffer and 2 mL (0.2 M) citrate buffer solution. The test tubes were shaken, centrifuged and the absorbance was measured at 630 nm. γ-CD was determined by measuring the change in the intensity of colour at 630 nm due to the formation of inclusion complex with bromocresol green.

3.3.4 Estimation of cholesterol by high performance liquid chromatography

Cholesterol uptake by the affinity matrix was determined by high performance liquid chromatography (HPLC). The HPLC system, consisting of a LDC analytical CM 4000 pump and UV-Visible detector (SM 4000), was used for the chromatographic

studies. Mobile phase consisted of the mixture of isopropanol and methanol (10:90 v/v). The chromatography analyses were performed at ambient temperature at a flow rate of 1 mL per minute.

Affinity matrices HE10a, HE10b and HE10c were used to investigate cholesterol binding. Required amount of affinity matrix were weighed into 8 mL capacity screw cap vials fitted with HDPE lined caps. Solution of cholesterol in methanol was added to each vial and the solutions were incubated overnight in a shaker at room temperature. The solutions were filtered into HPLC vials using disposable syringes. Cholesterol concentration remaining in the supernatant was determined by HPLC. A μ-bondapack C_{18} column in conjunction with 10% isopropanol in methanol was used as mobile phase at a flow rate 1 mL per minute for the chromatographic estimation.

The difference in peak height observed at 206 nm between the standard and the supernatant was used for estimating the extent of uptake of cholesterol by the affinity matrices.

3.4 Results and Discussion

Poly(HEMA-EGDM) beads were produced by suspension polymerisation. This methodology resulted in spherical beads in the size range 0.1-1 mm. Typical particle size distribution of poly(HEMA-EGDM) beads, as determined by particle size analyser, is presented in Figure 3.1. Figures 3.2 and 3.3 show SEM micrograph after grinding of poly(HEMA-EGDM) [HE10] and poly(HE-TDI-CD) [HE10b] matrices.

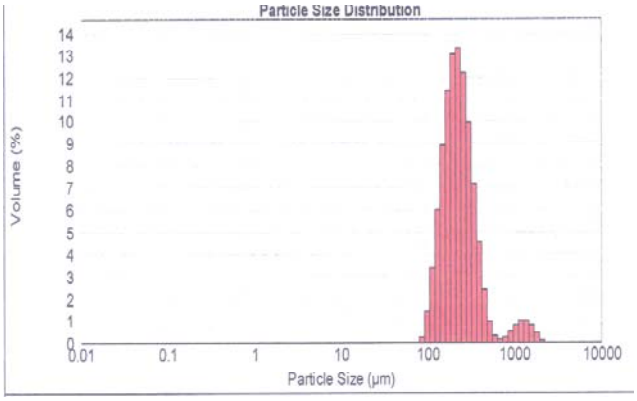

Figure 3.1: Particle size distribution in polymer HE11 with 150% crosslink density

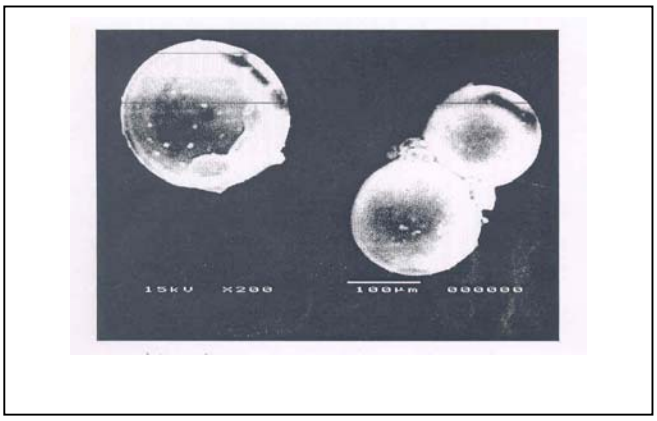

Figure 3.2: Surface morphology of polymer HE10

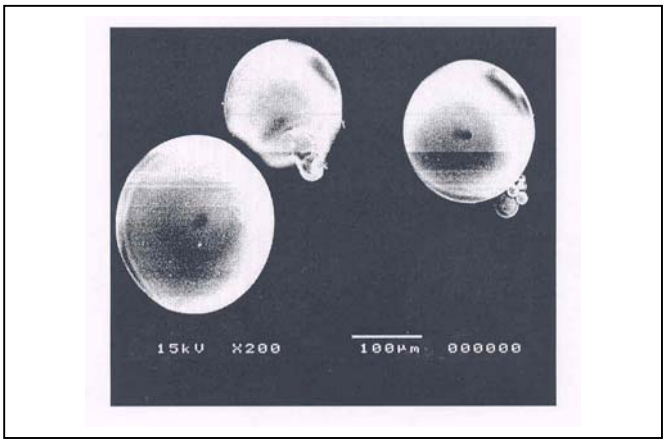

Figure 3.3: Surface morphology of polymer HE10b

As clearly shown, the poly(HEMA-EGDM) have a spherical form and rough surface. The cyclodextrin modified poly(HEMA-EGDM) have also a spherical form.

Mercury porosimetry provides good estimates of pore size and pore size (radii) distribution in the range < 5 to > 300 nm. Copolymers prepared from monomer feed ratios low in the crosslinking comonomer (EGDM) have low pore volume and surface area because a large number of nuclei are formed which tend to grow through each other. The data of pore volume and surface area for poly(HEMA-EGDM) are presented in Table 3.5.

Table 3.5: Effect of crosslink density on pore volume and surface area of poly(HEMA-EGDM)

Polymer No.	CLD %	Pore volume [mL/g]	Surface area [m^2/g]
HE7	25	0.03	7.24
HE8	50	0.05	10.07
HE9	75	0.23	83.35
HE10	100	0.26	66.94
HE11	150	0.41	77.70
HE12	200	0.67	112.94

Table 3.5 shows that the inner pore volume is low at lower crosslink density and increases with increase in crosslink density, from 0.03 to 0.67 mL/g (25 to 200%), due to increase in the number of pores. As the crosslink density increases, the pore volume increases rapidly. This indicates separation of cyclohexanol out of the network phase (gel phase). It is also seen that the surface area increases with increase in crosslink density, but no regular trend is noted, due to concomitant decrease in the size of the microsphere. Surface area also increases from 7.24 to 112.94 m^2/g with increase in crosslink density from 25 to 200%, due to decrease in the size of the microsphere. The pore size distribution of poly(hydroxyethyl methacrylate-ethylene dimethacrylate) are given in Table 3.6.

Table 3.6: **Variance in pore size distribution of poly(HEMA-EGDM) beads with crosslink density at constant monomer to porogen ratio (1:1.61, v/v)**

Polymer No.	CLD (%)	Pore size distribution (vol%), radius in nm								
		<5	5 -10	10-15	15-20	20-30	30-50	50-100	100-300	>300
HE7	25	44.99	42.49	2.50	0.00	0.00	0.00	0.00	0.00	10.00
HE8	50	22.53	24.25	24.28	6.24	2.45	0.00	4.34	3.16	6.98
HE9	75	5.90	32.31	24.41	13.64	9.62	7.12	1.97	1.25	0.59
HE10	100	15.69	40.45	17.58	8.13	8.51	3.97	2.65	0.94	0.19
HE11	150	45.53	44.26	9.57	0.00	0.00	0.00	0.00	0.00	0.00
HE12	200	7.64	21.29	15.65	13.51	19.43	12.24	6.53	1.93	0.00

Table 3.6 represents pore size distribution in poly(HEMA-EGDM) beads of differing crosslink densities prepared with cyclohexanol at 1:1.61 (v/v ratio). Pores are present over the entire range except for polymer HE11 (150% CLD), which is an artifact. The median pores are dependent on copolymer composition. On comparing HE10 and HE12, it is seen that the pore size widens with increase in crosslink density from 100 to 200%. These changes brought forth by increasing crosslink density, are mainly due to an increase in the volume of large pores (> 50 nm) and a concomitant decrease in volume of pores with size less than 50 nm (Table 3.6).

Nayak et al. [28] evaluated a number of diisocyanates for their suitability as spacers. They reported that the maximum amount of cyclodextrin binding was observed on poly(hydroxyethyl methacrylate-ethylene dimethacrylate) with TDI as spacer while phenylene methylene diisocyanate (PMDI), 1,6-hexamethylene diisocyanate (HMDI) and IPDI (isophorone diisocyanate) were inferior. Hence, in this study of binding cyclodextrins on to the poly(HEMA-EGDM) beads, TDI was chosen as spacer arm. For a particular crosslink density (25%), Nayak et al. reported that the amount of α-cyclodextrin bound to the poly(HEMA-EGDM) matrix is 83.5 mg per gram of polymer. In our investigation the amount of α-cyclodextrin bound is 106 mg per gram of

poly(HEMA-EGDM) matrix at fixed CLD (25%) which is 1.26 times higher [28]. The amount of cyclodextrin bound to the HE matrices are given in Tables 3.7, 3.8 and 3.9.

Table 3.7: α-Cyclodextrin bound (mg) on to the affinity matrices

Polymer No.	CLD (%)	α-cyclodextrin bound (mg/g)
HE7a	25	106
HE8a	50	165
HE9a	75	247
HE10a	100	434
HE11a	150	412
HE12a	200	603

Table 3.8: β-Cyclodextrin bound (mg) on to the affinity matrices

Polymer No.	CLD (%)	β-cyclodextrin bound (mg/g)
HE7b	25	83
HE8b	50	167
HE9b	75	319
HE10b	100	570
HE11b	150	473
HE12b	200	819

Table 3.9: γ-Cyclodextrin bound (mg) on to the affinity matrices

Polymer No.	CLD (%)	γ-cyclodextrin bound (mg/g)
HE7c	25	43
HE8c	50	141
HE9c	75	83
HE10c	100	370
HE11c	150	386
HE12c	200	396

From Table 3.7, it is seen that the amount of α-cyclodextrin bound to the HE matrix increases with crosslink density. A maximum of 603 mg of α-cyclodextrin was bound to the HE12 polymer with 200% crosslink density, which is 5.7 times over that on HE7 polymer with 25% crosslink density. From Table 3.8, it is seen that the amount of β-cyclodextrin bound to the HE matrix increases with crosslink density. A maximum of 819 mg of β-cyclodextrin was bound per gram of HE12 polymer with 200%

crosslink density, which is 9.8 times over that on HE7 polymer with 25% crosslink density. From Table 3.9, it is seen that the amount of γ-cyclodextrin bound to the HE matrix also increases with crosslink density. A maximum of 396 mg of γ-cyclodextrin was bound per gram of HE12 polymer with 200% crosslink density, which is 9.3 times over that on HE7 polymer with 25% crosslink density.

The cross-polarisation (CP), magic-angle spinning (MAS) ^{13}C NMR spectrum of poly(HEMA-EGDM) is presented in Figure 3.4. The structure of poly(HEMA-EGDM) is given in reaction Scheme (step 1). The assignment of the CP MAS ^{13}C NMR data of poly(HEMA-EGDM) are (in ppm): 17.85 {CH_3 carbon (f)}; 44.88 {quaternary carbon (d)}; 53.71 {-CH_2 carbon (e}; 59.50 and 66.02 {glycol region (b and c)} and 176.65 {C=O(O) of ester (a)}.

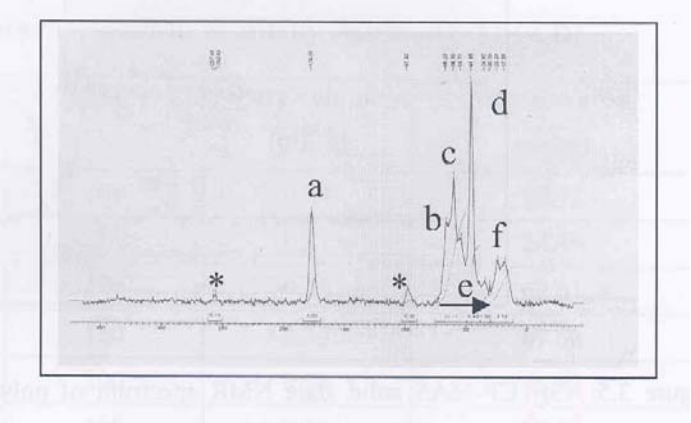

Figure 3.4: ^{13}C CP-MAS solid state NMR spectrum of poly(HEMA-EGDM), (a) C=O(O) of ester (b and c) –OCH_2CH_2O– of glycol (d) quaternary carbon (e) – CH_2 carbon (f) – CH_3 carbon and (*) spinning side band (SSB)

The cross-polarisation (CP), magic-angle spinning (MAS) ^{13}C NMR spectrum of poly(HEMA-EGDM)–TDI—β-CD is presented in Figure 3.5. The structure of poly(HEMA-EGDM)-TDI-β-CD is given in reaction Scheme (step 3). The assignment of CP MAS ^{13}C NMR data of poly(HEMA-EGDM)–TDI–CD are (in ppm): 17.56 {CH_3 carbon, (f)}; 44.54 {quaternary carbon (e)}; 65.26 to 59.76 {cyclodextrin + glycol

region (d)}; 136.96 to 124.34 {phenyl group (c)}; 153.28{ NH–C=O(O) of urethane (b)}; 176.55 {C=O(O) of ester (a)} and * spinning side band and one of the cyclodextrin carbon (C_1) appear at ~ 100 ppm.

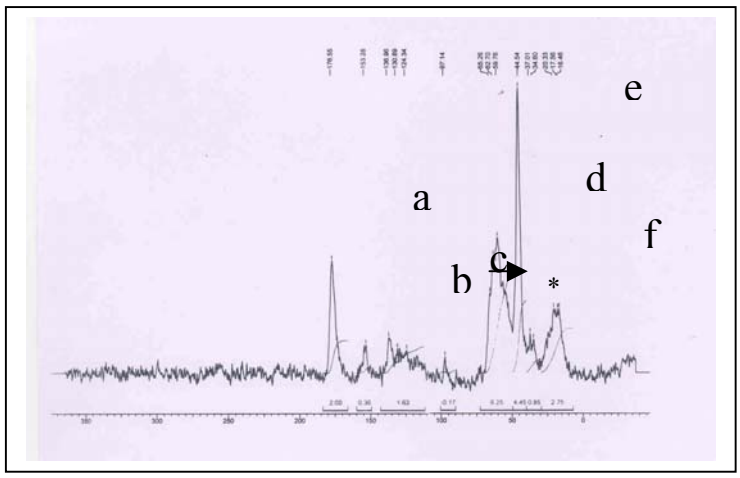

Figure 3.5: ^{13}C CP-MAS solid state NMR spectrum of poly(HEMA-EGDM)-TDI-β-CD, (a) C=O(O) of ester (b) –NH–C=O(O)– of urethane (c) phenyl carbon (d) cyclodextrin and glycol region (e) quaternary carbon (f) – CH_3 carbon and * spinning side band + cyclodextrin (C_1)

Poly(hydroxyethyl methacrylate-ethylene dimethacrylate) should possess specific pore size, pore size distribution, pore volume, surface area and concentration of reactive groups to be effective for the covalent binding of the ligands. The pore surface should possess functional groups, which can react efficiently to the ligand. Since hydroxyethyl methacrylate has one hydroxyl (-OH) group, where as ethylene dimethacrylate does not have OH group, an increase in % CLD decreases the number of reactive functional groups (-OH) per gram of macroporous polymer. The pore surface area is an important parameter for coupling of the ligand to the reactive functional group of the copolymeric matrix, and the decreasing trend of -OH groups with an increase in percentage of crosslink density are not sufficient data to explain the irregular coupling of cyclodextrin. This trend of increasing cyclodextrin binding in copolymer

with decreasing surface OH group indicates that pore size and its distribution are more important to prevent diffusional constraints on bulky cyclodextrin units within the pores. The pore volume and surface area of cyclodextrin modified poly(HEMA-EGDM) are given in Table 3.10.

Table 3.10: Pore characteristic of affinity matrix (HE-TDI-CD)

Polymer No.	CLD (%)	Pore volume (mL/g)	Surface area (m^2/g)
HE10a	100	0.34	90.73
HE7b	25	0.21	24.15
HE10b	100	0.35	69.61
HE11b	150	0.33	69.62
HE12b	200	0.28	56.87
HE10c	100	0.27	76.28

* a, b and c indicates that poly(HEMA-EGDM) bead are modified by α, β and γ cyclodextrin.

The pore volume goes through a maxima, from 0.21 mL/g (25% CLD) to 0.35 mL/g (100% CLD) and decreasing to 0.33 mL/g (150% CLD), 0.28 mL/g (200% CLD). Pore size distribution of cyclodextrin modified poly(hydroxyethyl methacrylate-ethylene dimethacrylate) are presented in Table 3.11.

Table 3.11: Pore size distribution of poly(HEMA-EGDM) coupled to α, β and γ-cyclodextrins

Polymer No.	CLD (%)	Pore size distribution (vol%), radius in nm								
		<5	5 - 10	10-15	15-20	20-30	30-50	50-100	100-300	>300
HE7b	25	0.00	21.99	16.69	11.08	13.00	8.12	9.75	13.20	6.13
HE10b	100	7.65	42.16	16.11	9.81	5.77	3.60	2.18	2.16	10.52
HE11b	150	16.06	40.94	18.10	7.35	1.58	0.00	8.05	6.54	1.34
HE12b	200	18.25	47.23	15.35	5.57	2.89	1.95	1.60	6.33	0.79
HE10a	100	21.27	43.10	15.63	5.54	5.78	4.11	2.37	1.95	0.25
HE10c	100	26.79	40.47	10.62	5.17	7.63	2.95	1.97	1.30	1.45

a, b and c indicates that poly(HEMA-EGDM) bead are modified by α, β and γ cyclodextrin

Table 3.11 represents pore size distribution of poly(HEMA-EGDM) bead coupled to cyclodextrins. It is seen in Table 3.11 that pores are present over the entire range. The

median pores are dependent on copolymer composition. It was observed that the volume percentage of pore >50nm in β-cyclodextrin modified poly(HEMA-EGDM) {HE7b = 29.08%, HE10b = 14.86%, HE11b = 15.93% and HE12b = 8.72) decreases as crosslink density increases, except at HE11b.

The IR spectra of poly(HEMA-EGDM), poly(HEMA-EGDM)-TDI-CD and CD, are given in Table 3.12, 3.13 and 3.14.

Table 3.12: IR spectrum of poly(HEMA-EGDM)

Peak position (cm^{-1})	Assignment
3500	-OH stretching
1715	-C=O stretching

Table 3.13: IR spectrum of poly(HEMA-EGDM)-TDI-CD

Peak position. (cm^{-1})	Assignment
3300	-NH stretching
1700	-C=O stretching
2200	absent
1020	acetal linkage

Table 3.14: IR spectrum of cyclodextrin

Peak position. (cm^{-1})	Assignment
3500	-OH stretching
1020	acetal linkage

From Tables 3.12 and 3.13, it is noted that the peak corresponding to the -OH group in HE polymer is nearly disappeared in the HE-TDI-CD and simultaneously a peak appears around 3300 cm^{-1}, which is due to the formation of –NH group between –OH and –NCO groups. The absence of a peak centered 2200 cm^{-1} indicates the formation of –NH group between –OH and –NCO groups. On the basis of Table 3.14, it can be said that the strong peaks centered 3500 and 1020 cm^{-1} can be assigned to the –OH group and the acetal type linkage of cyclodextrin.

From elemental analysis, it is seen that nitrogen content in poly(HEMA-EGDM) is nil. The nitrogen content was observed in cyclodextrin modified poly(HEMA-

EGDM). The nitrogen content of unmodified and modified poly(HEMA-EGDM) are presented in Table 3.15. The presence of nitrogen in modified poly(HEMA-EGDM) indicates the formation of urethane linkage in the reaction of poly(HEMA-EGDM) with cyclodextrin using toluene diisocyanate as spacer arm.

Table 3.15: Nitrogen content in underivatised and cyclodextrin derivatised HE matrix

Polymer No.	CLD (%)	Nitrogen content (%)
HE10	100	Nil
HE10a	100	4.17
HE10b	100	4.05
HE10c	100	6.03

3.4.1 Cholesterol binding

Affinity matrices (HE10a, HE10b and HE 10c) with 100% crosslink density were evaluated for cholesterol binding. The required amount of affinity matrix (0.05 g) was weighted into 8 mL screw cap vials fitted with HDPE caps. A solution of cholesterol (100 ppm) in methanol (5 mL) was added to each vial, and the vial was sealed and placed in a shaker overnight at room temperature and filtered. Filtrate was then analysed by high performance liquid chromatography to determine the concentration of cholesterol remaining in the supernatant.

Cyclodextrin are well known to form complexes with several components including steroid [29]. The factors mainly responsible for guest molecule binding are hydrophobic interaction between the guest molecule and cyclodextrin cavity, hydrogen bonding between the polar functional groups of guest molecules and the hydroxyl groups of cyclodextrin with the release of enthalpy rich water molecules from the cavity.

Table 3.17 summarises the extent of uptake of cholesterol by the cyclodextrin modified poly(HEMA-EGDM) matrix from methanol. Polymer HE10c absorbs a higher amount of cholesterol rather than HE10a and HE10c from methanol, indicating the strong influence of the medium on the interaction. Cholesterol is a hydrophobic steroid with a relatively planar structure and with one polar hydroxyl substituent in the ring [30]. Being a hydrophobic molecule, the solubility of cholesterol is low in methanol. This low solubility may be the driving factor for cholesterol adsorption.

Sreenivasan prepared methyl β-cyclodextrin based polymer by coupling of 2-hydroxyethyl methacrylate with methyl β-cyclodextrin using hexamethylene diisocyanate as coupling agent and studied cholesterol binding. Irregularly shaped particles were obtained by grinding. The amount of cholesterol adsorption by these particles varied between 5 to 7 mg per 100 mg of methyl β-cyclodextrin polymer [31]. Sreenivasan also prepared cyclodextrin based polymer for cholesterol adsorption by coupling of 2-hydroxyethyl methacrylate with β-cyclodextrin using hexamethylene diisocyanate as spacer arm, copolymerised with ethylene dimethacrylate and used for cholesterol binding. This polymer also was ground to irregularly shaped particles. The amount of cholesterol adsorption was 14.5 mg per 100 mg for this polymer [32]. In this present investigation of cholesterol binding, the beaded polymer (HE10a, HE10b and HE10c) used is suited to chromatographic application and cholesterol adsorption were 5.7, 14.6 and 19.7 mg per 100 mg of HE10a, HE10b and HE10c polymer, respectively.

The peak height and peak area of standard cholesterol solutions and supernatant of standard cholesterol solution, after keeping in polymer HE10a, HE10b and HE10c are presented in Table 3.16.

Table 3.16: Peak height and area of standard and supernatant cholesterol solutions

Solution No	Peak height	Peak area
1	9201	1012149
2	6591	725441
3	3749	229804
4	3261	140659

Solution 1 is the standard cholesterol solution while 2, 3 and 4 are the supernatant of cholesterol solution kept in HE10a, HE10b and HE10c polymers.

Table 3.17: Extent of adsorption of cholesterol by the affinity matrix

Affinity matrix	Cholesterol adsorbed (mg)/g	Adsorption %
HE10c	197	19.7
HE10b	146	14.6
HE10a	57	5.7

HE10a, HE10b and HE10c are the affinity matrix modified by α, β and γ-cyclodextrin, respectively.

A typical chromatogram of standard cholesterol solution and supernatant of cholesterol solution after keeping in polymers HE10a, HE10b and HE10 matrices are given in Figures 3.6-3.9.

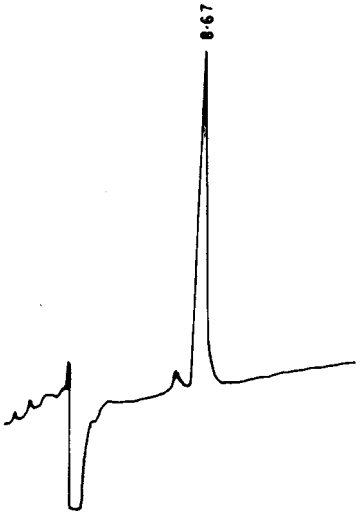

Figure 3.6: Chromatogram of standard cholesterol solution

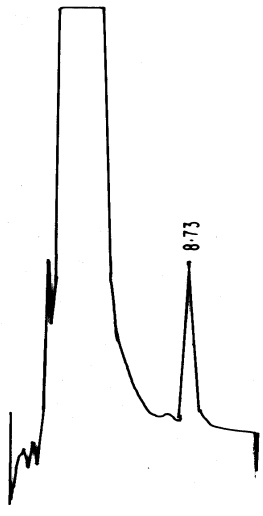

Figure 3.7: Chromatogram of supernatant of cholesterol solution after keeping in polymer HE10a

Figure 3.8: Chromatogram of supernatant of cholesterol solution after keeping in polymer HE10b

Figure 3.9: Chromatogram of supernatant of cholesterol solution after keeping in polymer HE10c

The difference in peak area between solution 1 and 2, 1 and 3, 1 and 4 are 286708, 782345 and 871490, respectively. The area decreases from 2 to 4 relative to standard cholesterol solution 1 but the difference in peak area between 1 and 2, 1 and 3, 1 and 4 increases indicating that HE10c polymer adsorbs more cholesterol relative to HE10a and HE10b. The cavity size of α, β and γ-cyclodextrin are 4.5-6 A^o, 6-8 A^o and 8.0-10 A^o, respectively. The end to end distance of cholesterol is 15 A^o. Hence a cholesterol molecule fits very snugly in the cavity of γ-cyclodextrin rather than α and β-cyclodextrin modified polymer.

3.5 References

1. J. Szejtli, Chem. Rev., **1998**, *98*, 1743.
2. J. Szejtli, Cyclodextrins and Their Inclusion Complexes, Akademiai Kiaso, Budapest, **1982**.
3. J. L. Atwood, J. E. D. Davies and D. Macniole, Inclusion Compounds, Academic Press, London, **1984**, Vol. 3.
4. M. L. Bender and M. Komi Yama, Cyclodextrin Chemistry, Springer-Verlag, New York, **1978**.
5. R. Breslow, Adv. Chem. Ser., **1980**, *191*, 1.
6. A. Zornoza, C. Martin, M. Sanchez, I. Velaz and A. Piquer, Int. J. Pharmaceutics, **1998**, *169*, 239.
7. C. A. Georgiou, S. G. skoulika and M. G. Polissiou, J. Inclusion Phenomena Macrocyclic Chem., **1999**, *34*, 85.
8. J. R. Moyano, M. J. Arias, J. M. Gines, J. I. Perez-Martinez, P. Munoz and F. Giordano, J. Thermal Analysis, **1998**, *51*, 1001.
9. Cs. Novak, M. Fodor, G. Pokol, V. Izvekov, J. Sztatisz, M. J. Arias and J. M. Gines, J. Thermal Analysis, **1998**, *51*, 1039.
10. E. Aicart and E. Junquera, J. Pharmaceutical Sci., **1999**, *88*, 1039.
11. L. Garefa-Rfo and J. R. Leis, J. Phys. Chem., **1997**, *101*, 7383.
12. K. Sreenivasan, J. Appl. Polym. Sci., **1996**, *60*, 2245.
13. P. J. A. Riberiro, A. M. Amado and J. J. C. Teixeira-Dias, J. Raman Spectrosc., **1996**, *29*, 155.
14. B. Szafran and J. Pawlaczyk, J. Inc. Phenom., **1999**, *34*, 131.
15. S. M. Han, Biomed. Chromatogr., **1997**, *13*, 25.
16. J. E. G. J. Wijnhoven and W. L. Vos, Science, **1998**, *281*, 802.
17. P. T. Tanev, M. Chibwe and T. J. Pinnavaia, Nature, **1994**, *368*, 321.
18. V. Maquet and R. Jerome, Mater. Sci. Forum, **1997**, *250*, 15.
19. S. Bancel and W. S. Hu, Biotechnol. Prog., **1996**, *12*, 398.
20. J. Pitha, S. M. Harman and M. E. Michel, J. Pharm. Sci., **1986**, *75*, 165.
21. J. Pitha, A. Gerloczy and A. Olivi, J. Pharm. Sci., **1984**, *83*, 833.
22. T. Loftsson, B. J. Olafsdottir and N. Bodor, Eur. J. Pharm. Biopharm., **1991**, *37*, 30.
23. D. P. Nayak, S. Ponrathnam, C. R. Rajan, A. Patkar, O. S. Yemul, Indian Patent filed, **2000**.
24. D. P. Nayak, S. Ponrathnam and C. R. Rajan, J. Chromat., A, **2001**, *922,* 63.

25. A. Lejuene, K. Sakaguchi and T. Imanaka., Anal. Biochem., **1989**, *181*, 6.

26. T. Kenako, T. Kato, N. Nakamura and K. J. Horikoshi, Jpn. Soc. Starch Sci., **1987**, *34*, 45.

27. K. Kato and H. Horikoshi, Anal. Chem., **1984**, *56*, 1738.

28. D. P. Nayak, A. M. Kotha, O. S. Yemul, S. Ponrathnam and C. R. Rajan, Biomacromolecules, **2001**, *2*, 1116.

29. L. Song and W. C. Purdy, Chem. Rev., **1992**, *82*, 1457.

30. B. Sellergren, J. Wieschemeyer, K. Boos and D. Seidel, Chem. Mater., **1998**, *10*, 4037.

31. K. Sreenivasan, J. Appl. Polym. Sci., **1998**, *68*, 1857.

32. K. Sreenivasan, Polymer International, **1997**, *42*, 22.

Chapter 4

Study of Metal-ion Binding with Modified Macroporous GMA-EGDM Copolymers

4.1 Introduction

Metal ions are the most perilous water pollutants due to poignant toxicity and carcinogenicity [1-3]. Some of the metal ions are cumulative poisons capable of being adsorbed and assimilated in the tissues of the organisms and causing noticeable adverse physiological effects [4]. Hence, removal of such metal ion are necessary, even at very low concentrations [5]. The necessity of removal of metal ions has led to an increasing interest in sorbents [6,7]. It is known that toxicity of a metal differs with its oxidation state, since these have differing physico-chemical and biological activities [8]. Pollution by arsenic in natural and industrial wastewater has been monitored and controlled to avoid its high toxicity to living things. Arsenic (As) exists in natural systems in a variety of chemical forms, including inorganic arsenic (III) and arsenic (V), and as several mono-, di- and tri -methylated arsenic compounds. Both elemental arsenic and arsenic (V) are markedly less toxic than arsenic (III). The toxicity of such compounds decreases in the order: arsine > arsenite > arsenate > alkyl arsenic acids > arsonium compounds and metallic arsenic. Mobility of arsenic in water is highest for arsenite, so it is the most important species in fresh water where arsenate is also dominant. Arsenic is an accumulative, potent and protoplasmic poison. Chronic poisoning by arsenic compounds leads to loss of appetite and weight, diarrhea alternating with constipation, gastrointestinal problems, peripheral neuritis, conjunctivitis, dermatitis and sometimes skin cancer. Arsenic have been reported as acute toxic element at lower concentrations [9]. The toxicity of As (III) is greater than the toxicity of As (V) [10]. So the speciation of metal ions is of great importance.

The adsorption on polymer sorbents is the best method for the removal of metal ions at ppm levels [11]. Now-a-days specific sorbents, consisting of a ligand (e.g. chelating agents) bound to a polymer, that interacts specifically with the metal ion [12-14], is considered as perhaps the most promising technique. Polymeric macrobeads have attracted attention as adsorbents as these can easily be produced and modified into specific sorbents by the introduction of metal chelating groups.

Macroporous polymeric beads, with large surface area and average diameter exceeding 200 μm, are generally used. The surface area of the polymeric sorbents range from 20 to 120 m^2/g. One of the most critical points in the use of porous sorbents is their pore structure, since the pore diffusion and the surface area in the pores determines adsorption rate and capacity, respectively. Sorbents with highly open pore structures are needed for high adsorption rates. However, the high active surface area of the porous sorbents is mainly due to the fine pores in the matrix, which are not available for a large molecule. In other words, large molecules can not penetrate into these pores and therefore can not use the active surface area, which therefore means low adsorption capacity for large molecule. So far it can be said that optimisation of pore structure of the carrier matrices is very important to achieve high adsorption rate and capacity.

One such carrier matrix is glycidyl methacrylate copolymers with epoxide pendent groups, which can be easily derivatised with amine to form the chelant. The reaction of epoxide group with amines is a nucleophilic addition, in which the nitrogen atom attacks as a rule the least protected carbon atom of the epoxide ring [15]. Macroporous poly(GMA-EGDM) reacts with a rich variety of amino compounds to impart new properties to the carrier matrix, thus indicating its enormous application as

immobilization carrier for enzyme, selective chelating agent and so on. Polyethylenimine (PEI) attached adsorbents have been reported in a series of recent publications for heavy metal removal [16-19]. The idea of using PEI chains stems from the fact that PEI is a very reactive with different chemicals, including metal ions. PEI was also utilised primarily to increase the number of sites for coordination and thus increase the capacity for the adsorbent [20]. The higher flexibility and durability of PEI as well as significantly lower material and manufacturing costs are also very important. In this study, polyethylenimine modified poly(GMA-EGDM) macrobeads were prepared and the metal chelating properties for arsenic (III) were determined. The effect of pore volume and specific surface area of copolymer beads on the adsorption of arsenic (III) ion were investigated.

4.2 Experimental

4.2.1 Materials

Polyethylenimine: Molecular weight: 1300; Density: 1.06 g/cm^3; Physical state: viscous liquid. The details of glycidyl methacrylate and other material are presented in Section 2.1.1.1. Polyethylenimine (PEI) was obtained as a gift from BASF. *Sodium arsenite*: ($NaAsO_2$) was from Aldrich.

4.2.2 Synthesis of GMA-EGDM copolymer of differing crosslink densities

The detailed synthesis procedure is presented in Section 2.1.1.2.

Table 4.1 Synthesis of poly(GMA-EGDM) beads, using cyclohexanol as porogen

Expt. No.	CLD (%)	GMA (mol)	EGDM (mol)	Monomer: porogen (v/v)
GE7	25	0.0447	0.0111	1:1.61
GE8	50	0.0352	0.0180	1:1.61
GE9	75	0.0293	0.0223	1:1.61
GE10	100	0.0249	0.0255	1:1.61
GE11	150	0.0198	0.0292	1:1.61
GE12	200	0.0161	0.0318	1:1.61

CLD = crosslink density

4.2.3 Modification of poly(GMA-EGDM) with polyethylenimine

The following procedure was used for the covalent attachment of PEI onto the poly(GMA-EGDM) beads. Dry poly(GMA-EGDM) beads (2.5 g) of differing crosslink densities were added into aqueous solution containing polyethylenimine (5 mL water, 3.13 mL PEI for polymer with 25% CLD) and kept in plastic bottles. The medium was shaken for 7 days at room temperature.

Table 4.2: Modification of poly(GMA-EGDM) bead by polyethylenimine (PEI)

Expt. No.	CLD (%)	Polymer (g)	PEI (mL)
GE7P	25	2.5	3.13
GE8P	50	2.5	2.53
GE9P	75	2.5	2.07
GE10P	100	2.5	1.81
GE11P	150	2.5	1.37
GE12P	200	2.5	1.11

PEI-attached poly(GMA-EGDM) beads were washed several times with distilled water to remove any physically adsorbed PEI from the beads. The modified polymer was dried at room temperature under reduced pressure. The PEI binding capacities were calculated based on the amount of PEI covalently attached per gram of poly(GMA-EGDM) beads. The amount of polyethylenimine attached to the poly(GMA-EGDM) bead was also determined using elemental analysis. Modification of poly(GMA-EGDM) by PEI are given in Table 4.2.

4.3 Characterisation of PEI derivatised poly(GMA-EGDM)

Bead yield was estimated as presented in Section 2.1.2.6, particle size measurement is presented in Section 2.1.2.3, porosity was estimated as presented in Section 2.1.2.1, Surface area measurement was as presented in Section 2.1.2.2, SEM was as presented in Section 2.1.2.4, IR spectra was as presented in Section 2.1.2.5 and elemental analysis was as presented in Section 3.3.1.

4.3.1 Elemental analysis of PEI modified poly(GMA-EGDM) beads

For the determination of amount of PEI attached to the poly(GMA-EGDM) beads, carbon, hydrogen and nitrogen content of derivatised beads were determined by an elemental analyser (CHNS-O, EA 1108-elemental analyser, Carlo Erba Instruments). The amount of PEI attached to the bead was determined from the percentage of nitrogen content.

4.4 Results and Discussion

As indicated in Chapter 2, poly(GMA-EGDM) beads were synthesised by suspension polymerisation to generate spherical beads in the size range 0.1-1 mm. Typical particle size distribution of poly(GMA-EGDM) beads as determined by particle size analyser is presented in Figure 4.1.

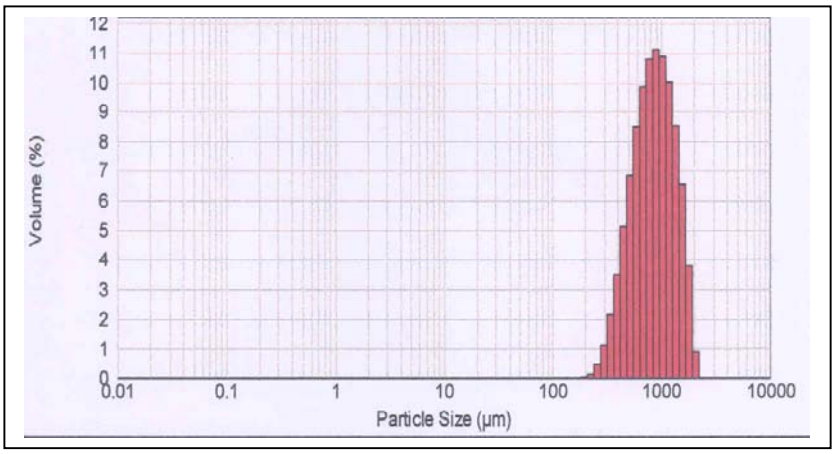

Figure 4.1: Particle size distribution of GE11 with 150% crosslink density

Figures 4.2 and 4.3 show SEM micrographs of poly(GMA-EGDM) and PEI attached poly(GMA-EGDM). The spherical form and rough surface of the poly(GMA-EGDM) macrosphere favour better adsorption of arsenic ion because of large surface area. The PEI derivatisation of poly(GMA-EGDM) does not affect its spherical form.

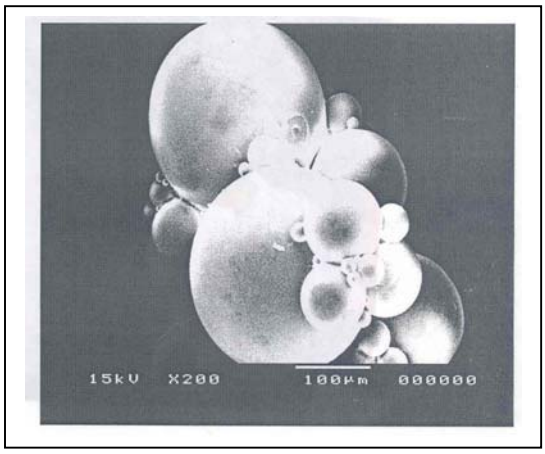

Figure 4.2: Surface morphology of poly(GMA-EGDM) (GE10)

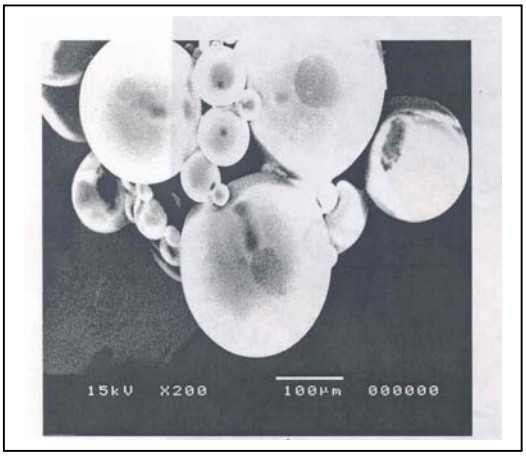

Figure 4.3: Surface morphology of PEI coupled poly(GMA-EGDM) (GE10P)

The macroporous poly(GMA-EGDM) beads may be visualised as crosslinked hydrogel. They do not dissolve in aqueous medium, but do swell, depending on crosslink density (i.e., percent EGDM). The degree of swelling decreases with increase in crosslink density. The dry beads are opaque (white in colour), which is an indication of the porosity in the matrix, as a result of the pore generating solvent (i.e., cyclohexanol) used in the polymerisation. However, the opacity of the beads are significantly decreased when the beads are swollen in water. After the polyethylenimine (PEI) derivatisation, the colour of the beads changes, which is a clear indication of the

incorporation of the polyethylenimine into the structure of the beads. It should be noted that these beads are quite rigid and strong, due to very high crosslink density.

Polyethylenimine is a highly branched polymer with 50%, 25% and 25% of secondary, primary and tertiary amino groups, respectively. Polyethylenimine was covalently attached to the macrobeads via nucleophilic addition between epoxy group of poly(GMA-EGDM) and primary amino group of polyethylenimine, under basic condition (pH=10.6). For the confirmation of PEI attachment to the poly(GMA-EGDM) beads, elemental analysis of the underivatised and PEI derivatised poly(GMA-EGDM) were obtained. The covalent attachment of PEI on to the poly(GMA-EGDM) bead was also determined by the potentiometric titration of a sample withdrawn from the medium after the adsorption, with 0.1 M standard hydrochloric acid solution. The amount of polyethylenimine attached to the macrobeads were in the range 47-79%. The data of PEI bound to the poly(GMA-EGDM) are given in Table 4.3.

Table 4.3: Effect of crosslink density on PEI binding to poly(GMA-EGDM)

Expt. No.	CLD %	Nitrogen content (%)	PEI (%)
GE7P	25	8.53	78.90
GE8P	50	6.61	61.20
GE9P	75	5.46	50.50
GE10P	100	5.34	49.39
GE11P	150	5.19	48.01
GE12P	200	5.10	47.17

It is seen in Table 4.3 that as the crosslink density increases, the percentage of PEI attached to the poly(GMA-EGDM) bead decreases, due to decrease in epoxy content with increase in crosslink density. Polyethylenimine leakage during metal ion adsorption experiment was also investigated. The absence of PEI leakage was

confirmed by elemental analysis. For this purpose, metal ion solution was kept in a plastic vial containing PEI derivatised poly(GMA-EGDM) beads. The metal ion solution was filtered and filtrate was collected for elemental analysis. The nitrogen content in filtrate was nil, after adsorption of metal ion solution onto to the PEI derivatised poly(GMA-EGDM) beads. This shows that washing procedure was sufficient to removal of physically adsorbed PEI molecules from the polymer matrix.

To explain the nature of the interaction between polyethylenimine and poly(GMA-EGDM), FTIR spectra of underivatised poly(GMA-EGDM) and PEI derivatised poly(GMA-EGDM) were obtained. FTIR spectra of poly(GMA-EGDM) shows peaks at 1722 and 1196 cm^{-1} due to stretching vibrations of C=O of ester group and C-O-C of epoxy group, respectively. The band at 1196 cm^{-1} due to stretching vibration of C-O-C of epoxy group disappears in PEI derivatised poly(GMA-EGDM), due to reaction of epoxy group of poly(GMA-EGDM) with primary amino group of polyethylenimine (PEI) and a peak at 3450 cm^{-1}, due to stretching vibration of OH, was observed in PEI derivatised poly(GMA-EGDM). The presence of peak at 3450 cm^{-1} indicates the formation of -OH group after the reaction of polyethylenimine with poly(GMA-EGDM). The peak at 3300 cm^{-1} indicates the stretching vibration of -NH group.

Table 4.4 represents the effect of crosslink density on pore volume and surface area of Poly(GMA-EGDM) beads. It shows that a decrease in crosslink density from 200 to 25% results in a decrease in the pore volume from 0.85 to 0.11 mL/g, due to decrease in the number of pores. Surface area also decreases from 110.57 to 22.07 m^2/g with

decrease in crosslink density from 200 to 25%, due to increase in the size of the microsphere.

Table 4.5 represents the effect of crosslink density on pore volume and surface area of PEI derivatised poly(GMA-EGDM). A decrease in crosslink density from 200 to 25% results in a decrease in the pore volume from 0.72 to 0.12 mL/g, due to decrease in the number of pores. Surface area also decreases from 137.50 to 36.97 m^2/g with decrease in crosslink density from 200 to 25%, due to increase in the size of the microsphere. On comparing it is seen that the pore volume of GE7P (0.72 mL/g) is less than GE7 (0.85 mL/g) because PEI enters into the pores of poly(GMA-EGDM) beads.

Table 4.4: Pore volume and surface area of poly(GMA-EGDM) beads

Expt. No.	CLD (%)	Pore volume (mL/g)	Surface area (m^2/g)
GE7	25	0.11	22.07
GE8	50	0.56	85.06
GE9	75	0.59	105.78
GE10	100	0.72	100.69
GE11	150	0.74	110.25
GE12	200	0.85	110.57

Table 4.5: Pore volume and surface area of PEI derivatised poly(GMA-EGDM)

Expt. No.	CLD (%)	Pore vol. (mL/g)	Surface area (m^2/g)
GE7P	25	0.12	36.97
GE8P	50	0.39	51.19
GE9P	75	0.43	48.34
GE10P	100	0.47	69.61
GE11P	150	0.63	78.11
GE12P	200	0.72	137.50

Table 4.6 represents pore size distribution of poly(GMA-EGDM) beads. It is seen that pores are present over the entire range. The median pores are dependent on copolymer composition. The pore size distribution shifted towards smaller pores as the crosslink density decreases from 200 to 25%. The changes in these characteristics, which are obtained upon decreasing the percentage of crosslink density in the

polymerisation mixture, are mainly due to a decrease in the volume of large pores (> 50 nm) and a parallel increase in volume of pores with size less than 50 nm.

Table 4.6: **Pore size distribution of poly(GMA-EGDM) beads**

Expt.	CLD	Pore size distribution (vol%), radius in nm								
No	(%)	<5	5-10	10-15	15-20	20-30	30-50	50-100	100-300	>300
GE7	25	0.00	39.53	39.90	0.25	0.43	1.78	3.36	13.72	0.94
GE8	50	5.61	18.74	16.39	13.65	23.32	17.85	4.01	0.02	0.41
GE9	75	9.12	21.69	17.21	16.18	18.75	11.72	4.50	0.00	0.00
GE10	100	5.95	20.00	10.28	12.73	13.95	18.61	11.53	4.08	2.19
GE11	150	4.56	18.29	13.72	11.68	16.88	19.53	12.53	2.12	0.00
GE12	200	2.65	16.85	12.14	8.40	14.06	18.81	18.82	6.22	0.28

CLD: crosslink density

Table 4.7: Pore size distribution of PEI derivatised poly(GMA-EGDM) beads

Expt.	CLD	Pore size distribution (vol%), radius in nm								
No	(%)	<5	5-10	10-15	15-20	20-30	30-50	50-100	100-300	>300
GE7P	25	29.14	33.15	16.57	0.00	0.00	10.28	1.79	7.83	1.24
GE8P	50	4.33	10.15	11.93	12.91	46.83	4.43	7.28	1.41	0.35
GE9P	75	0.00	0.00	36.69	16.92	24.34	2.45	18.44	1.02	0.14
GE10P	100	9.66	13.40	13.30	16.14	32.32	3.16	0.00	0.00	7.30
GE11P	150	3.27	13.97	21.86	17.08	22.78	5.32	0.00	13.59	2.09
GE12P	200	0.00	55.08	3.39	12.27	12.60	0.93	12.28	3.33	0.12

Table 4.7 represents pore size distribution of PEI derivatised poly(GMA-EGDM) beads. Pores over the entire range are retained. The volume percentage of pores (>50 nm) in GE12P is 15.73%, which is less compared to volume percentage of pores (>50 nm) in GE12 (25.32%), resulting in a decrease in pore volume from 0.85 to 0.72 mL/g (GE12 to GE12P). Similarly volume percentage of pores (>50 nm) in GE10P is 7.30%, which is less compared to volume percentage of pores (>50 nm) in GE10 (17.8%), resulting a decrease in pore volume from 0.72 to 0.47 mL/g (GE10 to GE10P) and so on.

4.4.1 Effect of porosity on the adsorption capacity for metal ion

The effect of porosity of the modified beaded polymers with different crosslink density on the adsorption of arsenic ion was investigated. The adsorption capacity for arsenic (III) ion by the affinity matrices, in relation to the crosslinker (EGDM), is given in Table 4.8.

Table 4.8: Effect of crosslinking on the adsorption of metal ion (As^{+++}) on the PEI derivatised poly(GMA-EGDM) beads

Expt. No.	CLD (%)	Metal ion adsorbed (μmol/g of polymer)
GE7P	25	0.069
GE8P	50	0.162
GE9P	75	0.177
GE10P	100	0.232
GE11P	150	0.254
GE12P	200	0.331

Polymer (GE12P) shows highest affinity for arsenic ion where as polymer (GE7P) which had insufficient porosity and surface area, had a poor affinity for arsenic ion compared to the polymer (GE12P). Adsorption is the accumulation of materials at an interface, the liquid/solid boundary layer. It is a mass transfer process where a substance is transferred from the liquid phase to the surface of the solid and becomes bound by chemical forces. Since adsorption is a surface phenomenon, the greater the surface of the medium, the greater its capacity to accumulate the material. So it clearly indicates that the adsorption capacity of these polymers for arsenic ion is greatly affected by their porosity. The binding of arsenic (III) ion with the secondary amine and hydroxyl group of the PEI modified poly(GMA-EGDM) may be interpreted on the basis of Pearson's concept of hard and soft acids and bases.

4.5 References:

1. R. E. Clement, G. A. Eiceman and C. J. Koester, Anal. Chem., **1995**, *67*, 221.
2. A. Imran and A. Y. Hassan, Chemosphere, **2002**, *48*, 275.
3. P. MacCarthy, R. W. Klusman, S. W. Cowling and J. A. Rice, Anal. Chem., **1995**, *67*, 525.
4. J. W. Moore and S. Ramamoorthy, Applied Monitoring and Impact Assessment, Springer, New York, NY, **1984.**
5. C. S. Luo and S. Huang, Sep. Sci. Technol., **1993**, *28*, 1253.
6. D. A. Harkins and G. K. Schweitzer, Sep. Sci. Technol., **1991**, *26*, 345.
7. A. Sugii, N. Ogawa and H. Hashizume, Talanta, **1980***, 27*, 627.
8. M. Stoepler, Hazardous Metals in the Environment, Elsevier, Amsterdam, **1992**.
9. C. K. Jain and I. Ali, Water Res., **2000**, *34*, 4304.
10. L. Lin, J. Wang and J. Caruso, J. Chromatogr. Sci., **1995**, *33*, 177.
11. M. Weltrowski, B. Martel and M. Morceller, J. Appl. Polym. Sci., **1996**, *59*, 647.
12. D. Adil, K. Kemal, S. Bekir, S. Serap and P. Erhan, J. Appl. Polym. Sci., **1991**, *71*, 1397.
13. D. C. Hwang and S. Damodaran, J. Appl. Polym. Sci., **1997**, *64*, 891.
14. C. Kantipuly, S. Katragadda, A. Chow and H. D. Goser, Talanta, **1990**, *37*, 491.
15. F. Svec, H. Hrudkuva, D. Horak and J. Kalal, Reactive Polymers, **1977**, *63*, 26.
16. M. J. Hudson and Z. Matejka, Sep. Sci. Technol., **1990**, *23*, 1417.
17. E. Duru, S. Bektas, O. Genc, S. Patir and A. Denizli, J. Appl. Polym. Sci., **2001**, *81*, 197.
18. R. R. Navarro, K. Sumi, N. Fujii and M. Matsumara, Wat. Res., **1996**, *30*, 2488.
19. A. Bahrimi, A. S. Bassi and E. Yanful, Can. J. Chem. Eng., **1999**, *77*, 931.
20. R. R. Navarro, K. Sumi and M. Matsumara, Wat. Sci. Tech., **1998**, *38*, 195.

Chapter 5

Summary and Conclusions

5.1 Summary and Conclusion

Chapter 1 is a general introduction to macroporous polymers, cyclodextrin and toxicity of metal ions. Macroporous, crosslinked polymers are efficient materials for many separation processes and are widely used as ion exchange resins and specific sorbents. Suspension polymerisation technique is used for the preparation of macroporous copolymer networks in the form of beads. The chapter also briefly describes cyclodextrins which form inclusion complexes (host-guest complexes) with various compounds, including steroids by molecular complexation. Finally, the chapter describes the use of macroporous polymer modified with amino compounds (act as chelating agent) for metal ion adsorption.

Chapter 2 describes the synthesis of a large number of porous network structures based on copolymerisation of glycidyl methacrylate-ethylene dimethacrylate, glycidyl methacrylate-divinyl benzene, allyl glycidyl ether-ethylene dimethacrylate (with epoxy functional groups) and 2-hydroxyethyl methacrylate–ethylene dimethacrylate, hydroxyethyl methacrylate–divinylbenzene (having hydroxy functional groups), by suspension polymerisation and by varying a number of different synthesis parameters.

It can be summarised from Tables 2.4-2.10 that the porosity in network porous copolymers prepared from glycidyl methacrylate and ethylene dimethacrylate is defined by the presence of inert solvent which phase separates from the growing polymer network. It can also be summarised (Table 2.4) that polymers with a very wide range of porosity can be synthesised. Thus, the pore volume of GE30 (0.0155 mL/g) is 3.54, 10.70, 54.67 and 57.09 times less than GE24 (0.0550mL/g), GE18 (0.1660 mL/g), GE12 (0.8475 mL/g) and GE6 (0.8850 mL/g), due to change of monomer:porogen ratio

(v/v) from 1:0 to 1:2.43 (GE30 to GE6) at fixed composition (200% CLD). It was observed (Table 2.6) that in absence of porogen, the volume percentage of pore >50nm are absent while median pores are in the 5-10 nm range. The porosity of the copolymer beads is dependent on the copolymer composition and relative volumes of monomer mixture as well as porogen.

Subtle structural variances in the porogen (pore generating solvent) have profound effects on pore properties. In networked porous copolymers prepared from glycidyl methacrylate and divinyl benzene (Tables 2.14 and 2.15), at fixed monomer:porogen ratio (1:1.61), the pore volume (GV7), in presence of cyclohexanol as a porogen, is 0.75 mL/g, which is 1.96 and 1.81 times less than that generated by hexanol and octanol {GV(h)1 (1.47 mL/g) and GV(o)1 (1.36 mL/g)} as porogens at fixed composition (25% CLD). Similarly, the surface area (GV7) is 98.10m^2/g which is 4 and 8.38 times greater {GV(h)1 (24.50 m^2/g) and GV(o)1 (11.70 m^2/g)} indicating that the use of cyclohexanol generates nano and micro-pores while hexanol and octanol generate meso and macro-pores. Table 2.20 shows that the volume percentage of pores (>50nm) (GV7) is 15.85% which is 5.27 and 5.53 times less {GV(h)1 (83.56%) and GV(o)1 (87.71%)}. Among the three porogens studied, relatively uniform pores were obtained with hexanol.

The concentration of the functional groups at the surface of the pores is dependent on the hydrophilic/hydrophobic character of both functional and crosslinking comonomers. In copolymers prepared from allyl glycidyl ether and ethylene dimethacrylate, the porosity of copolymer beads is dependent on the copolymer composition. The pore volume AG1 (Table 2.25) is 0.83 mL/g which is 1.60 times less

than AG6 (1.33 mL/g), due to increase of crosslink density from 25 to 200% at fixed monomer:porogen ratio (1:1.61). The volume percentage of pores (>50nm) in AG1 is 23.13% (Table 2.26) which is 2.15 times less than AG6 (49.80%).

In copolymers prepared from 2-hydroxyethyl methacrylate and ethylene dimethacrylate, (Table 2.30 to 2.33) it is seen that crosslink density, ratio of monomer and porogen volume and porogen type, influence the pore size and porosity. Table 2.30 shows that the pore volume of HE30 (0.0130 mL/g) is 2.86, 13.69, 51.84 and 61.69 times less than HE24 (0.0373 mL/g), HE18 (0.1780 mL/g), HE12 (0.6740 mL/g) and HE6 (0.8020 mL/g), due to change of monomer:porogen ratio (v/v) from 1:0 to 1:2.43 (HE30 to HE6) at fixed composition (200% CLD). The pore volume of HE7 (0.03 mL/g) is 2.66, 32, 19 and 27.3 times less than HE31 (0.08 mL/g), HE37 (0.96 mL/g), HE43 (0.57 mL/g) and HE49 (0.87 mL/g) at fixed composition (25% CLD). It can also be summarised from Table 2.36 that the volume percentage of pores (>50nm) in HE1 is 50%, which is 1.48 times less than HE6 (74.01%) at fixed monomer: porogen ratio.

Similarly in the HV series, the pore volume of HV1 is 0.05 mL/g which is 20 times less than HV6 (1.01 mL/g), due to increase of crosslink density from 25 to 200% at fixed monomer:porogen ratio (1:1.61). Thus the porosity of the copolymer bead is dependent on the copolymer composition.

Thus, within a series of networked porous polymers, the pore properties such as surface area, pore size, its distribution and volume can be effectively controlled by a combination of relative mole ratios of the monomers, porogen type and its relative volume. The concentration of the functional groups at the surface of the pores is dictated by the hydrophilic/hydrophobic character of the comonomer (EGDM vs DVB).

Chapter 3 describes the modification of macroporous poly(HEMA-EGDM), having hydoxy functional group, by suitable ligands (cyclodextrins). The binding of cyclodextrin to the backbone of macroporous crosslinked beaded polymer offers a highly selective system for chromatographic separation. Cyclodextrins are well known for their ability to form inclusion complexes with a variety of components (e.g cholesterol). The separation potential of particular interesting molecule could be enhanced several fold by incorporating cyclodextrin in the pores of networked polymers. It is observed (Tables 3.7-3.9) that with the increase in crosslink density the amount of cyclodextrin bound to the poly(HEMA-EGDM) increases. It is seen (Table 3.17) that the amount of cholesterol adsorption are 197 mg, 146 mg and 57 mg per gm of γ, β and α-cyclodextrin modified poly(HEMA-EGDM). The γ-cyclodextrin based macroporous beaded affinity matrix, based on HEG using 2,4-toluene diisocyanate as a spacer shows more cholesterol adsorption rather than α and β, due to greater cavity size of γ-cyclodextrin.

Chapter 4 describes the modification of poly(GMA-EGDM) by polyethylenimine and investigation of arsenic binding. Macroporous poly(GMA-EGDM) having epoxy groups have been modified by suitable chelating ligands (polyethylenimine), which are useful for metal ion separation. It can be summarised (Table 4.6) that the volume percentage of pore (>50 nm) in GE7 is 18.02%, which is 1.40 times less than GE12 (25.32%) at fixed monomer: porogen ratio (1:1.61). It can also be stated that (Table 4.7) the volume percentage of pore (>50 nm) in GE7P is 10.86% which is 1.44 times less than GE12P (15.73%) at fixed monomer:porogen ratio (1:1.61). It is noted that (Tables 4.6 and 4.7) the volume percentage of pore (>50 nm) in

GE7P is 1.65 times less than GE7, due to PEI entering into the pore of poly(GMA-EGDM). Table 4.8 shows that the arsenic (III) adsorption depends on the copolymer composition (crosslink density). The adsorption of arsenic (III) ion also depends on the porosity and surface area of the copolymer bead, since adsorption is a surface phenomenon, the greater the surface of the medium, higher is the adsorption capacity. A number of experimental and structural parameters determine the adsorption rate, such as concentration, pH, swelling degree, the amount of sorbent, the ion properties (hydrated ionic radius and coordination complex number), the initial concentration of metal ions, the chelate forming rate between the complexing ligand and metal ions.

Future scope of work

Modification of GMA-EGDM copolymers using chitosan, chitosan dithiocarbamate, evaluation of the derivatised resins for selective chelation of arsenic.

Modification of GMA-EGDM copolymers using iminodiacetic acid, bis(2-picolyl amine), bis(3-picolyl amine) and evaluation of the derivatised resins with chromium and cobalt.

Modification of HEMA-EGDM copolymers with derivatised cyclodextrins (having hydroxylamine and amino groups), binding metal ions, complexing with chiral molecules, sulphur compounds, studying stability constants etc.

List of publications

1. Biocatalysis by Penicillin G Acylase Anchored on Beaded Macroreticular Glycidyl methacrylate-Divinyl benzene Polymers: Effect of Pore Structure on Catalytic activity.

G. Ingavle, T. S. Pathak, A. Kotha and S. Ponrathnam, **Bull. Catal. Soc. India**, 2 (2003) 75-81.

2. Frontal copolymerization of 2-hydroxyethyl methacrylate and ethylene glycol dimethacrylate without porogen: Comparison with suspension polymerization.

S. Mule, T. S. Pathak, A. Vishwakarma, S. Ponrathnam and N. Pujari, Polymer international (communicated).

3. Macroporous poly(2-hydroxyethyl methacrylate-co-ethylene dimethacrylate): Effect of crosslinking density and porogen on pore volume and specific surface area (to be communicated).

4. Macroporous poly(allyl glycidyl ether-co-ethylene dimethacrylate): Effect of crosslinking density on pore volume and specific surface area (to be communicated).

5. Macroporous copolymer matrix modified with γ-cyclodextrin as a better selective receptors of cholesterol rather than α and β cyclodextrin (to be communicated).

6. Metal chelating by polyethylenimine grafted on the macroporous poly(glycidyl methacrylate-co-ethylene dimethacrylate) bead (to be communicated).